IN VIVO FAST SCAN CYCLIC VOLTAMMETRY REVEALS DISTINCT DOMAINS OF DOPAMINE TERMINAL FUNCTION IN THE STRIATUM

by

Keith F. Moquin

B.S. Chemistry, The Pennsylvania State University, 2005

Submitted to the Graduate Faculty of

Arts and Sciences in partial fulfillment

Of the requirement for the degree of

Doctor of Philosophy

University of Pittsburgh

2011

UNIVERSITY OF PITTSBURGH

FACULTY OF ARTS AND SCIENCES

This dissertation was presented

by

Keith F. Moquin

It was defended on

June 28, 2011

And approved by

Shigeru Amemiya, Associate Professor, Chemistry Department

Renã A.S. Robinson, Assistant Professor, Chemistry Department

Gonzalo E. Torres, Associate Professor, Neurobiology Department

Dissertation Director: Adrian C. Michael, Professor, Chemistry Department

IN VIVO FAST SCAN CYCLIC VOLTAMMETRY REVEALS DISTINCT DOMAINS OF DOPAMINE TERMINAL FUNCTION IN THE STRIATUM

Keith F. Moquin Ph.D.

University of Pittsburgh, 2011

The striatal dopaminergic system regulates several brain functions; movement, cognition, motivation, and reward. As such, failures of this system lead to numerous diseases including Parkinson's disease, schizophrenia, and drug addiction. Dopaminergic neurons communicate with, and regulate the function of, target cells by controlling the extracellular dopamine concentration. Release of dopamine from neuron terminals elevates the extracellular concentration activating pre- and post-synaptic transmembrane receptor proteins. Clearance of dopamine via the dopamine transporter lowers the extracellular concentration, terminating dopamine receptor activation. This dissertation focuses on the role the pre-synaptic dopamine D2-receptor and the dopamine transporter play in the management of extracellular dopamine concentrations, i.e. dopamine signaling.

We employ carbon fiber electrodes in conjunction with fast scan cyclic voltammetry to detect changes in the extracellular dopamine concentration during and after electrical stimulation of dopamine neurons. Fast scan cyclic voltammetry is the ideal analytical method to detect dopamine signaling events because it has a high spatiotemporal resolution that can track sub-second changes in the extracellular dopamine concentration from small populations of terminals. Pharmacological drugs are used to determine the role of D2-receptor and dopamine transporter proteins in controlling the extracellular dopamine concentration.

Our results reveal that differences in dopamine transporter function alter D2-receptor activation, segmenting the striatum into two domains of dopamine terminals; fast and slow. Localized fast domains, which fit the classic model, release dopamine immediately upon stimulation and clear dopamine rapidly following the stimulus. In Slow domains, evoked release is initially inhibited but accelerates as stimulation continues. The rate of dopamine clearance from slow domains is significantly slower. Thus, we redefine the striatal dopamine system, once thought to be homogenous, as a pathway comprised of two distinct domains of dopamine function. These results reveal a previously undiscovered slow domain of dopaminergic activity; changing our understanding of how the striatal dopaminergic system regulations brain function, and providing new insights into the causes of, and therapies for, dopaminergic pathologies.

TABLE OF CONTENTS

LIST OF FIGURES

LIST OF EQUATIONS

PREFACE

I would like to take this opportunity to thank all of those who made my graduate career a successful and enjoyable experience. First, I would like to thank Dr. Adrian C. Michael who taught me that the best science requires skill, creativity, fearlessness, adaptability, and a bit of sailing. His patience and guidance has molded me into scientist and person I am today.

I would like to thank Dr. Shigeru Amemiya, Dr. Stephan Petoud, Dr. Renã A. S. Robinson, Dr. Sunil Saxena, Dr. Megan Spence, Dr. Gonzalo E. Torres, and Dr. Stephen Weber for their time serving on my committees and their counsel in my growth as a researcher. I would also like to thank the amazing support staff at the Chemistry department including the electronic shop staff, administrative staff, and machine shop staff. The countless hours they spend making every graduate student's life a little less difficult is noticed and greatly appreciated.

I have been fortunate enough to share a laboratory with a colorful cast of characters during my time in the Michael lab. Each of them has taught me something about myself, and I only hope that I did the same for them. I would especially like to acknowledge Laura Borland, Andrea Jaquins-Gerstl, Joe Mitala, Christina Mitala, Yuexiang Wang, and Bridget Willoughby. Without their efforts this story would not exist.

I would like to thank my family who supports my every decision, even the slightly crazy ones. Their constant encouragement makes difficult roads easy to travel. I would like to thank my dog, Smokey, who always knew when a long walk would assist the writing process. Finally, and most importantly, I would like to thank my wife, Emily. Her smile brightens even my worst days and her laughter keeps me sane. I would not be here today without her.

1.0 INTRODUCTION

1.1 ABSTRACT

The first time I hiked in a forest my dad stressed to me the importance of looking back the way you came. When I asked him why, he replied: “because the path you take often looks very different when viewed from the other direction. If you aren’t familiar with the surroundings you can get lost”. Looking back not only reveals where you have been, but it also provides the context for where you are and enlightens the path forward. Without this knowledge we are doomed to wander aimlessly amongst the trees.

This dissertation focuses on the mechanisms controlling the release and clearance of the neurotransmitter dopamine from the extracellular space. The rates of dopamine release and clearance determine the extracellular dopamine concentration, and thus the time course of neurotransmitter signaling. The following chapter provides an overview of the in vivo detection of dopamine neuron activity. Basic striatal dopaminergic neuron anatomy and function is explained. The advantages and limitations of the electrochemical method fast scan cyclic voltammetry in the detection of dopamine are discussed. Finally, the current model of striatal dopamine signaling is presented. Successes and knowledge gaps are highlighted, providing an orientation for this dissertation and the backdrop for its significance in the field.

1.2 THE NIGROSTRIATAL DOPAMINERGIC SYSTEM

The nigrostriatal dopamine pathway is one of four main dopamine pathways in the brain. Dopamine neurons originate in the substantia nigra. Each neuron extends an axon from the substantia nigra, through the medial forebrain bundle, into the striatum (Carr and White 1986; Horvitz 2000). There, they branch into millions of DA terminals that innervate the entire striatum with a 2 μm average distance of separation (Doucet *et al* 1988). Each DA terminal forms a synapse with a gamma-aminobutyric acid (GABA) neuron dendrite or spine, forming a synaptic junction. The two cell walls do not touch, leaving a 15 nm thick and 300 nm wide synaptic gap between the two cell walls (Garris *et al* 1994). The synaptic gap empties into a larger extracellular space, which comprises 20% of the striatum's total volume (Cserr *et al* 1991; Nicholson and Rice 1991; Cragg *et al* 2001). Cerebral spinal fluid, a buffer solution, fills the synaptic gap and the extracellular space, allowing small molecules: ions, neurotransmitters, oxygen, etc., to move freely between cells.

It is in this buffer solution that DA terminals convey their message to the GABA neuron cell body. This message is a vital component in the regulation of several functions including motion, cognition, motivation, and reward. A dysfunctional nigrostriatal dopamine pathway is linked to several disorders such as Parkinson's disease, attention deficit hyperactivity disorder, schizophrenia, and drug addiction (Grace 1991; Abi-Dargham *et al* 2000; Swanson *et al* 2000; Lotharius and Brundin 2002; Phillips *et al* 2003b; Salahpour *et al* 2008). It is necessary to learn how DA neurons communicate information in order to understand how the DA system regulates function and causes DA based disorders.

Because the GABA cell and DA terminal do not form a direct connection, they communicate via the interaction of the neurotransmitter dopamine with target receptor proteins.

This protein is a transmembrane g-protein coupled receptor that spans the cell wall (Clark and White 1987). The protein has two main components; the DA binding site in the extracellular space and a g-protein binding site in the intracellular space. DA binding to the receptor protein causes a conformational change to occur, altering the binding affinity of the receptor to the g-protein. The activated g-protein interacts with the adenylate cyclase enzyme, altering cyclic AMP production (Monsma *et al* 1990; Schinelli *et al* 2004). There are two types of DA receptor proteins; D1-like receptors that increase cyclic AMP production, and D2-like receptors that inhibit cyclic AMP production. GABA cells contain both D1- and D2-like receptors, DA terminals only have D2-receptors (D2R) (Delle-Donne *et al* 1997).

The DA binding constant to DA receptor proteins is 1-2 μM (Grigoriadis and Seeman 1985). Below this concentration threshold the GABA receptor cell does not receive a DA signal input. DA terminals regulate the extracellular DA concentration, controlling the time course of DA signaling at the GABA cell. DA terminals adjust the DA extracellular concentration by regulating the rate of DA release from, and clearance into, the terminal. The balance of release and clearance set the extracellular DA concentration, and thus the time course of DA signaling.

In the terminal, DA is contained in spherical lipid bilayers called vesicles (Greengard *et al* 1993; Sulzer *et al* 1995). A high frequency train of action potentials lasting several hundred milliseconds are sent from the cell body through the axon to the terminal. Here they open calcium ion channels, increasing the intracellular Ca^{2+} concentration. The influx of calcium causes vesicle fusion to the terminal cell wall, releasing dopamine into the synaptic gap. DA diffuses throughout the extracellular space binding to DA receptors, i.e. signaling. DA binding to the pre-synaptic D2R triggers an autoinhibitory effect, suppressing further DA release (Limberger *et al* 1991; Benoit-Marand *et al* 2001).

It is important to note that several lines of evidence suggest that DA signaling occurs in the extracellular space, not the synaptic gap. In the striatum, DA diffuses at a rate of 2.4×10^{-6} cm^2/s (Rice *et al* 1985; Nicholson and Rice 1991; Nicholson 1995). At this rate, DA diffuses out of the synaptic gap into the extracellular space (area: 4.5×10^{-11} cm^2) in approximately 2.0×10^{-5} s (Garris *et al* 1994). Also, DA receptors are located in the extracellular space, not the synaptic gap (Sesack *et al* 1994). Therefore it is the concentration of DA in the extracellular space that determines DA signaling events.

In order to terminate a signal, DA is cleared from the extracellular space back into the terminal by a transporter protein located only on the terminals (Ciliax *et al* 1995; Nirenberg *et al* 1996). The DA transporter (DAT) is a symporter that couples DA movement with the influx of two sodium ions (Torres *et al* 2003). DAT clears DA from the extracellular space quickly, with some studies reporting a DA clearance rate of 5 μM/s (Wu *et al* 2002). This rapid uptake process limits DA's distance of diffusion in the striatum to tens of microns (Garris *et al* 1994; Cragg and Rice 2004). Also, the DAT can transport DA from the cytoplasm into the extracellular space, a process called reverse transport (Sulzer *et al* 1995).

DA release, clearance, autoinhibition, diffusion, and reverse transport all contribute to the steady state extracellular DA concentration as well as the magnitude and duration of DA release events. Because these processes are rapid, monitoring DA signaling requires an analytical method that is selective to DA, has a high nM detection limit, and a subsecond temporal resolution. Further, this device must be small enough to minimize tissue damage during in vivo sampling (Rousche and Normann 1998; Szarowski *et al* 2003; Biran *et al* 2005; Jaquins-Gerstl and Michael 2009).

1.3 IN VIVO ELECTROCHEMISTRY AND DOPAMINE

In the spring of 1973, the first paper utilizing electrochemical analytical techniques to monitor changes in the concentration of the small neurotransmitter, dopamine, in living tissue was published in the journal of Brain Research (Kissinger *et al* 1973). This article marks the first time neurological events were monitored as they occurred in real time in a living system. Today, that publication has spawned an entire field of research, significantly increasing our understanding of neurological function. The following section explains the in vivo technique and its advantages and limitations in the detection of DA, while providing a brief history of early in vivo electrochemistry.

Electrochemistry applies voltage potentials to an electrode surface, a carbon fiber electrode (CFE) in this case, to drive oxidation and reduction processes, and then measures the current generated from these reactions. The potential required to run these redox reactions is analyte specific, and the magnitude of the generated current is proportional to the analyte concentration. Thus, electrochemistry can be used to identify and quantify electroactive species in a sample.

Typically, the applied voltages needed to complete the oxidation and reduction cycle are separated by $\frac{59\,mV}{n}$, where n is the number of electrons (Bard and Faulkner 2001). In order to detect both oxidation and reduction, cyclic voltammetry is performed. First, the applied potential is ramped at a constant rate from a rest potential to a potential greater than the oxidation potential, oxidizing the species. The scan is then reversed back to the rest potential, reducing the species. Typical cyclic voltammetry scan rates range from 1 mV/s to 1 V/s. A cyclic voltammogram plots the current change versus potential revealing the peak oxidation and

reduction potentials. The locations of these peaks are specific to the species and the experimental conditions. Thus the cyclic voltammogram acts as an analyte fingerprint.

DA is an electroactive catecholamine with two hydroxyl groups attached to the 3rd and 4th position of the benzene ring. The catechol group can be oxidized, removing two electrons and two protons, converting dopamine into dopamine-o-quinone (DAQ). This process is reversible, so DAQ can be reduced back to DA with the addition of two electrons and two protons.

DA, however, does not go through a typical redox reaction. The removal (oxidation) and addition (reduction) of the two electrons and two protons on each DA molecule occur as four separate events, not as one reaction (Deakin *et al* 1986; Wipf *et al* 1986). As such, there are six possible pathways for DA oxidation and DAQ reduction, known as the nine-member box (Larivon 1984). DA oxidation and DAQ reduction do not follow the same pathway, so the separation of oxidation and reduction potentials is larger than 29.5 mV. Even at 1 V/s, the time delay between scanning the oxidization and reduction potentials allows DAQ produced by DA oxidation to diffuse away from the microelectrode surface. The resulting cyclic voltammogram has a sigmoidal shape without a discernable reduction peak (Bard and Faulkner 2001).

In order to detect the reduction peak, and thus accurately identify DA, fast scan cyclic voltammetry (FSCV) is employed. FSCV is cyclic voltammetry at fast scan rates (400 V/s in our hands). At this scan rate, DA oxidizes at 650 mV and DAQ reduces at -250 mV (all potentials vs a Ag/AgCl reference electrode). Fast scan rates have two added bonuses in the in vivo detection of DA. First, at a sweep rate of 400 V/s, the 3 V scan takes 7.5 ms to complete. Therefore, DA scans can be repeated at 10 Hz, giving FSCV sub-second temporal resolution (Bath *et al* 2000; Robinson *et al* 2001). Second, the fast scan rate eliminates any interference from ascorbic acid, an anti-oxidant found in the brain at 200-400 μM concentrations (Gonon *et al* 1981). Ascorbic

acid has similar oxidation and reduction peaks, but the electrochemical redox reactions are slower than DA. At fast scan rates, the ascorbic acid redox reactions do not occur, and therefore do not contribute to the detected change in current. Another way to eliminate ascorbic acid signals is to coat the electrode surface with a Nafion polymer layer, which prevents anions, e.g. ascorbic acid, from reaching the electrode surface (Gerhardt *et al* 1984). However, this layer slows DA's migration to the electrode, creating a diffusional distortion that must be deconvoluted (Kawagoe *et al* 1992; Garris *et al* 1994; Garris and Wightman 1995).

The CFE used to detect DA has a diameter of 7 µm and can be cut to any length ranging from 1 mm to a disk. The electrode's size limits brain damage caused during implantation, enabling the electrode to monitor DAergic events from minimally altered neurons (Clapp-Lilly *et al* 1999; Peters *et al* 2004; Jaquins-Gerstl and Michael 2009). Also, the electrode's small surface area limits the number of terminals the electrode samples from. Thus, CFEs measure DA events from discrete terminal populations. Finally, the CFE is sensitive to changes in DA concentration and has a detection limit in the high nM range (Wightman *et al* 1978; Gonon *et al* 1984). Taken together, FSCV with a CFE is capable of detecting sub-second, high nM changes in DA concentration from small populations of neurons in vivo.

FSCV has one major limitation. The technique is not well-suited to measuring the baseline analyte concentration. Each FSCV scan generates a large current 2000-2500 nA in amplitude over the entire potential scan. The main source of this signal comes from the non-faradaic charging current caused by the fast scan rate. However, any faradaic current caused by oxidation and reduction reactions contributes as well. For example, high nM DA concentrations generate 1 -100 nA of current during a scan, representing less than 1 % of the total current. Further, the background current amplitude is unique to each experimental setup, electrode and

buffer solution. Therefore, it is impossible to detect or measure DA from a single fast scan cyclic voltammogram. (It is important to note that cyclic voltammetry does not have this issue. The slower scan rate produces a minimal non-faradaic current, enabling the detection of the faradaic current without interference.)

Because of the large non-faradaic current, FSCV is best-suited to measuring changes in the DA concentration, not absolute values. In order to measure DA, at least two voltammetric scans are required; a background scan before a DA concentration change and a scan following the concentration change. The current generated from the non-faradaic source and faradaic current generated from electroactive species at a constant concentration remains unchanged in both scans. Subtracting the two cyclic voltammograms leaves only the current change due to the change in DA concentration. This process is repeated for each cyclic voltammogram recorded during the experiment. Plotting the current change from background at the DA oxidation potential (~650 mV) at the time point of each scan reveals changes in DA concentration over time.

Cyclic voltammograms collected before the DA event have a similar current profile compared to the background voltammogram. Background Subtraction of these voltammograms yields a value of zero plus or minus noise. However, FSCV is a differential method, so the zero value represents the change in DA concentration, not the absolute value. In fact, the magnitude of change is independent of the baseline, or basal, DA concentration within the limits of detection. In other words, the signal generated by a 2 μM increase in the DA concentration will be identical in either a 1 nM or 1 μM basal DA concentration. For this reason FSCV is unable to measure the absolute concentration of DA. Despite this limitation, FSCV has proved a very powerful tool in the in vivo detection of DA signaling.

1.4 EVOKED DOPAMINE HETERGENEITY: THE FORK IN THE ROAD

One way to create a detectable change in the extracellular DA concentration is to evoke DA release by electrical stimulation. In order to stimulate the neurons a bipolar stimulating electrode is placed on the medial forebrain bundle, which contains DAergic nerve axons, and an alternating electrical current is applied (Ewing *et al* 1983; Kuhr *et al* 1984; Heien *et al* 2005). The applied current depolarizes axons, sending an action potential to the terminal. The frequency, amplitude, and duration of the electrical stimulation are all factors in the amount of DA released by the stimulation (Wightman *et al* 1988; May and Wightman 1989a; Kawagoe *et al* 1992; Wu *et al* 2002).

However, stimulus parameters do not appear to be the sole determinant of the evoked DA profile and amplitude detected by the CFE. Initial studies discovered that the electrode stimulation evokes a range of detected DA release profiles (May and Wightman 1989b; Kawagoe *et al* 1992). These disparate responses are accessed by moving the CFE into a new striatal location (Kawagoe *et al* 1992; Wightman *et al* 2007). Early papers published on this evoked DA heterogeneity hypothesized that diffusion was the main source of the differences in the rate of evoked DA release (May and Wightman 1989b). The theory states that a slow initial response was the result of a CFE placed some distance from DA terminals. During an electrical stimulation, DA is immediately released by terminals, but must diffuse to the electrode for detection causing a signal delay (Kawagoe *et al* 1992; Venton *et al* 2003). This hypothesis implies that these slow responses are caused by experimental error and are wrong. In order to correct for this error, the electrode location is optimized until the electrode detects an immediate evoked DA response. This fast response indicates that the CFE is immediately adjacent to the DA terminals (Venton *et al* 2003).

Despite the fact that the hypothesis was never proven, electrode optimization to find fast-type responses has become ubiquitous in striatal DA experiments (Cass and Gerhardt 1994; Garris *et al* 1994; Benoit-Marand *et al* 2001; Robinson *et al* 2001; Venton *et al* 2002; Avshalumov and Rice 2003; Garris *et al* 2003; Phillips *et al* 2003a; Phillips *et al* 2003b; Robinson *et al* 2003; Cheer *et al* 2005; Heien *et al* 2005; Kita *et al* 2007; Wightman *et al* 2007; Sombers *et al* 2009; Addy *et al* 2010; Herr *et al* 2010). The electrode is placed in the striatum and the evoked response is recorded. If the response is not rapid, 1 μM in 0.2 s, the electrode is dialed lower into the striatum and the stimulus is repeated (May and Wightman 1989a). This entire process continues until the desired fast-type evoked DA response is detected. At this point the experiment starts. This method removes slow-type responses from the experiment, and thus from the literature.

Due to electrode optimization, the past twenty five years of Striatal DA research in anesthetized and awake animals as well as in vitro tissue slices has focused almost exclusively on fast-type responses (Cragg *et al* 2001; Avshalumov and Rice 2003; Phillips *et al* 2003b; Cheer *et al* 2004; Heien *et al* 2005). The effects of DA receptor agonists and antagonists, and DAT inhibitors on both the basal DA concentration and profile of fast-type evoked DA has been thoroughly characterized (Sulzer *et al* 1995; Benoit-Marand *et al* 2001; Rougé-Pont *et al* 2002; Wu *et al* 2002; Greco and Garris 2003; Sevak *et al* 2007; Espana *et al* 2008). From these data a sophisticated model of DA neuron communication in the striatum has been formed.

Transient DA release events occur at 1 Hz intervals releasing high nM concentrations into the extracellular space (Wightman and Robinson 2002; Heien *et al* 2005). A rapid DAT mediated DA uptake process quickly clears this DA, maintaining a 2-10 nM basal DA concentration (Wightman *et al* 2007). DA receptor binding is minimal at low nM concentrations,

so there is limited DA signaling and no pre-synaptic autoinhibition of release (Grigoriadis and Seeman 1985). The DA terminals are primed and ready to fire.

Phasic action potentials sent to the terminals triggers vesicle fusion to the cell wall, releasing large concentrations of DA into the extracellular space. During this event the rate of vesicular release overwhelms the rate of DA uptake via DAT (Wightman *et al* 1988; Wu *et al* 2001). The result is a 1-2 μM increase in the DA concentration recorded by the CFE within 0.2 s of the onset of the action potential (Benoit-Marand *et al* 2001; Wu *et al* 2001; Robinson *et al* 2003). At this concentration, DA interacts with post-synaptic DA receptors on the GABA cell, i.e. DA signaling. The pre-synaptic D2R is also activated by this initial release process, triggering D2R mediated autoinhibition (Usiello *et al* 2000; Benoit-Marand *et al* 2001; Kita *et al* 2007). This autoinhibitory effect suppresses further DA release in the face of continued stimulation. At the end of the stimulus, DA release stops and extracellular DA is cleared from the extracellular space back into the terminal by DAT within a second (Wu *et al* 2001; Wu *et al* 2002). The extracellular concentration returns to the pre-stimulus 2-10 nM basal concentration. DA receptors are no longer bound by DA, so the neurological signal to the GABA cells and the autoinhibitory tone on the DA terminals is terminated.

In this model DA signaling is limited by two factors. First, the low nM basal DA concentration limits DA signaling to phasic release events. In between these phasic events the basal concentration is below DA receptor activation (Grigoriadis and Seeman 1985). Second, rapid DA clearance and D2R mediated autoinhibition limits the duration of phasic events. Thus, this model suggests that DA signaling in the striatum only occurs for brief periods of time during phasic events. The majority of the time DA terminals are not signaling.

While accurate, the 'fast-type' model cannot be used to explain every DA based disorder. There are several paradoxes suggesting that phasic signaling is not the sole component of the striatal DA system. For example, attention deficit hyperactivity disorder (ADHD) is characterized by attention problems and hyperactivity. Theories suggest that increased DA signaling is the root cause of this disorder. In the 'fast-type' model increased DA signaling could be cause by an increase in the basal DA concentration, or an increase in the amplitude and duration of phasic release. ADHD is successfully treated with the DAT inhibitor, methylphenidate, which slows DA clearance (Izenwasser *et al* 1990). Slowed clearance can increase basal DA concentrations and increase the duration of phasic events (Volkow *et al* 2001; Wu *et al* 2002; Heien *et al* 2005; Montgomery *et al* 2007). If ADHD is caused by an increase in DA activity, how does further increasing DA signaling mitigate symptoms?

Parkinson's disease presents another paradox to the 'fast-type' model. Parkinson's disease is highlighted by a 90% decrease in striatal DA terminal density (Bernheimer *et al* 1973; Robinson and Whishaw 1988). Striatal denervation leads to loss of motor control and dementia in the patient, implementing DA signaling in these functions (Albin *et al* 1989; Maneuf *et al* 1997). Parkinson's disease is successfully treated with L-3,4-dihydroxyphenylalanine (L-DOPA), a DA precursor. L-DOPA is converted into DA by the aromatic L-amino acid decarboxylase enzyme. This enzyme is found in several cell lines, so L-DOPA can be converted into DA even in the absence of DA terminals (Melamed *et al* 1980). The absence of DA terminals means that the DA produced from L-DOPA is not released by phasic events, nor cleared by DAT. Therefore, it is hypothesized that DA leaks into the extracellular space increasing the basal DA concentration, a tonic DA signaling event (Melamed *et al* 1980; Hefti *et*

al 1981; Keller *et al* 1988; Zigmond *et al* 1992). If tonic DA signaling does not occur during normal DAergic function, why is it necessary in the treatment of Parkinson's disease?

This dissertation re-examines the striatal DA system, focusing on the oft ignored slow-type responses. We discover that the slow-type response is not a product of diffusion caused by a lack of DA terminals in the vicinity of the CFE. Rather the slow-type response is caused by local DA terminals under a tonic DA signal. As such, we conclude that the striatal DAergic pathway is actually a dual pathway that signals on both short (phasic) and long (tonic) time scales. This discovery will revolutionize the way we view striatal DA function and pathologies.

2.0 TONIC AUTOINHIBITION CONTRIBUTES TO THE HETEROGENEITY OF EVOKED DOPAMINE RELEASE IN THE RAT STRIATUM

2.1 ABSTRACT

Electrically evoked dopamine release as measured by voltammetry in the rat striatum is heterogeneous in both amplitude and temporal profile. Previous studies have attributed this heterogeneity to variations in the proximity of the voltammetric electrode to DA terminals. We reach the alternate conclusion that local variations in autoinhibition is the major contributor to this phenomenon. We demonstrate that low-amplitude, slow evoked DA responses in the striatum occur even when recording electrodes are close to DA terminals. Moreover, the responses are affected by the D2 agonist and antagonist, quinpirole and raclopride, respectively, in a manner consistent with the known functions of presynaptic D2 autoreceptors. Whereas recent voltammetric studies have focused attention on high-speed DA transients, we find that autoinhibited responses are prevalent in the dorsal striatum. In these experiments, autoinhibition preceded the electrical stimulation, which is consistent with prior reports from our laboratory that the striatum contains a tonic pool of extracellular DA at basal concentrations sufficient to occupy D2 receptors. We conclude that the striatum contains DA terminals operating on multiple time courses due to spatial fluctuations in autoinhibitory tone. We provide direct, real-time observations of the functional consequence of tonic and phasic DAergic signaling in vivo.

2.2 INTRODUCTION

Central dopamine (DA) neurons exhibit a broad functional diversity that underlies their role in numerous pathologies, including substance abuse (Phillips *et al* 2003b), schizophrenia (Abi-Dargham *et al* 2000), and attention deficit hyperactivity disorders (Salahpour *et al* 2008). The mechanisms responsible for DA's diversity of function and dysfunction are a matter of longstanding interest. The anatomical compartmentalization into the nigrostriatal and mesolimbic DA systems is well known (Carli *et al* 1985; Carr and White 1986; Horvitz 2000). Furthermore, DA systems operate on multiple time scales to selectively encode function. Accordingly, rapid DA signaling encodes reward and learning whereas slower DA signaling appears more relevant to motor function (Schultz 2007). However, the literature does not contain direct observations of extracellular DA engaged in both rapid and slow signaling.

Fast-scan cyclic voltammetry (FSCV) has revealed a wealth of information on the role of rapid extracellular DA transients in reward and learning (Wightman and Robinson 2002). DA transients are produced by burst firing of DA neurons in response to salient stimuli (Schultz 1998). On the other hand, DA neurons also exhibit tonic firing (Grace 1991; Benoit-Marand *et al* 2001; Venton *et al* 2003). The low levels of DA release associated with tonic firing are challenging to detect (Venton *et al* 2003) and less amenable to direct investigation. In addition, the dopamine transporter (DAT) contributes to DA release (Lonart and Zigmond 1991; Falkenburger *et al* 2001). In our hands (Kulagina *et al* 2001; Borland and Michael 2004; Mitala *et al* 2008), FSCV shows that DAT-mediated release produces a tonic extracellular DA concentration in the rat striatum sufficient to occupy DA receptors (Grigoriadis and Seeman 1985), including the presynaptic D2 autoreceptors that affect DA release, synthesis, and uptake (Usiello *et al* 2000; Benoit-Marand *et al* 2001; Rougé-Pont *et al* 2002). This is a surprising

result, however, as existing literature suggests that DA terminals are not autoinhibited under basal conditions (Garris *et al* 1994; Garris and Wightman 1995; Benoit-Marand *et al* 2001).

For example, D2 antagonists increase evoked DA release upon prolonged electrical stimulation of the medial forebrain bundle (MFB) (May and Wightman 1989b; May and Wightman 1989a) but do not affect DA release evoked by brief (1- or 4-pulse) stimuli (Garris *et al* 1994; Garris and Wightman 1995). The absence of an effect on brief stimulus responses implies an absence of autoinhibition under basal conditions. Similarly, haloperidol modestly affects DA release evoked by 3-pulse stimuli unless the brief stimuli are delivered momentarily after a conditioning prestimulus (Benoit-Marand *et al* 2001). The prestimulus transiently evokes autoinhibition, implying again that autoinhibition is weak or absent under basal conditions.

However, evoked DA release is a highly heterogeneous phenomenon (May and Wightman 1989b; May and Wightman 1989a). Consequently, only a subset of optimized recording locations illustrate the point that DA terminals are not normally autoinhibited. Until now the heterogeneity of evoked DA release has been attributed to a variable DA innervation of terminal fields, such that some recording locations are close to DA terminals whereas others are not. Consequently, it has become common practice to adjust the position of recording electrodes to, presumably, locate DA terminals (Garris *et al* 1993). This practice, combined with other refinements of the FSCV technology, has produced detailed knowledge of both evoked and naturally occurring sub-second DA transients, fostering seminal insights into their physiological and functional significance(Robinson *et al* 2001; Phillips *et al* 2003b; Roitman *et al* 2004; Stuber *et al* 2005). On the other hand, relatively little attention has been paid to sites that do not exhibit transient DA release.

The literature suggests that recording sites that do not produce transient DA release are those where DA terminals are absent, such as the "non-DA" sites revealed by immunohistochemical studies (Venton *et al* 2003). Evoked responses in such locations exhibit low amplitudes and sluggish temporal features, which have been attributed to diffusional distortions of the DA signal evoked at terminals remote from the electrode (i.e. the electrode missed its intended target) (May and Wightman 1989b; Garris *et al* 1994). However, herein we provide two lines of evidence that such responses derive instead from autoinhibition of DA terminals. First, we show that several qualitative features of the responses are inconsistent with diffusional phenomena. Second, we show that the D2 drugs, raclopride and quinpirole, affect the responses in a manner consistent with the known functions of D2 autoreceptors (Usiello *et al* 2000; Benoit-Marand *et al* 2001; Rougé-Pont *et al* 2002). Our findings clearly show that the recording sites are not devoid of DA terminals. Instead, these are sites where DA terminals are powerfully autoinhibited even under basal conditions. Hence, our study provides direct voltammetric observations of DA terminals simultaneously engaged in both rapid and slow DA signaling depending, at least in part, on the strength of a spatially variable autoinhibitory tone. We hypothesize that the autoinhibitory tone derives from the tonic pool of extracellular DA in the striatum (Kulagina *et al* 2001; Borland and Michael 2004).

2.3 METHODS AND MATERIALS

2.3.1 Carbon fiber electrodes

Single 7-μm diameter carbon fibers (T650, Cytec Carbon Fibers LLC., Piedmont, SC) were placed inside borosilicate glass capillaries (dimensions prior to pulling 0.4 mm ID, 0.6 mm OD, A-M systems Inc., Sequim, WA). The capillaries were pulled to a fine tip with a vertical

micropipette puller (Narishige, Los Angeles, CA) and backfilled with low-viscosity epoxy (Spurr Epoxy, Polysciences Inc., Warrington, PA). The exposed carbon fibers were cut to a length of 400 μm and sonicated in reagent grade isopropyl alcohol (Sigma, St. Louis, MO) containing activated carbon (Fisher Scientific, Fair Lawn, NJ) for 30 minutes (Bath *et al* 2000). A droplet of mercury in the electrode barrel established electrical contact between the fiber and a nichrome contact wire (Goodfellow, Huntingdon, Cambridgeshire, UK).

2.3.2 Fast scan cyclic voltammetry

FSCV was conducted with an EI 400 high-speed potentiostat (originally constructed by Ensman Instruments but presently available from ESA Inc., Chelmsford, MA) and the program "CV Tar Heels v4.3" (courtesy of Dr. Michael Heien, Department of Chemistry, Pennsylvania State University). The resting potential was 0 V vs Ag/AgCl and the voltammetric waveform consisted of three linear potential sweeps to +1 V, -0.5 V, and back to 0 V at a sweep rate of 400 V/s. The scans were performed at 10 Hz. The DA oxidation current was recorded between 0.5 and 0.7 V during the first sweep. DA voltammograms were obtained by background subtraction.

2.3.3 Electrode calibration

Electrodes were pre- and post-calibrated in a flow cell with gravity fed artificial cerebral spinal fluid solution (aCSF: 1.2mM Ca^{2+}, 152mM Cl^{-}, 2.7mM K^{+}, 1.0mM Mg^{2+}, 145mM Na^{+}, pH 7.4). Electrodes with rapid DA response times were identified by pre-calibration: electrodes exceeded 85% of their steady-state DA signal in less than 300 ms, i.e. by the third measurement after a step change in DA concentration. Conversion of in vivo oxidation currents to DA concentrations was based on post-calibration results. Standards for calibration were prepared by dissolving dopamine HCl (Sigma Aldrich, St. Louis, MO) in aCSF.

2.3.4 Animals

Male Sprague-Dawley rats (250-350g) (Hilltop, Scottsdale, PA) were anesthetized with isoflurane (2% by vol.) and placed in a stereotax (David Kopf Instruments, Tujunga, CA) with the incisor bar raised 5 mm above the interaural line (Pellegrino *et al* 1979). A heating blanket (Harvard Apparatus, Holliston, MA) maintained body temperature at 37^{o}C. A twisted, bipolar, stainless steel stimulating electrode was placed over the medial forebrain bundle (MFB) (from bregma: 1.6 mm lateral, 2.2 mm posterior, 8.0 mm below dura). A carbon fiber microelectrode was placed in the ipsilateral striatum (from bregma: 2.5 mm lateral, 2.5 mm anterior, initially 4.5 mm below dura). The final position of the stimulating electrode was set by lowering it until evoked DA release was observed in the striatum: this is a well-established adopted protocol for locating the tip of the stimulating electrode so as to activate ascending DAergic fibers (Ewing *et al* 1983; Kuhr *et al* 1984; Heien *et al* 2005).

2.3.5 Electrical stimulation

The stimulus was an optically isolated, constant-current, biphasic waveform (frequency 60 Hz, pulse height 270 µA, pulse width 2 ms). Single train and multiple train stimuli were employed for this study. Single trains lasted between 0.2 s and 5 s in duration, as indicated below. During multiple train stimuli, four 1-s trains were delivered with 2-s or 4-s intervals between the trains. Stimuli were delivered before and 30 min after drug administration.

2.3.6 Drugs

Raclopride tartrate (Sigma Aldrich, St. Louis, MO) was administered at a dose of 2 mg/kg, i.p. dissolved in phosphate buffered saline (155mM Na^{+}, 155mM Cl^{-}, 100mM phosphate, pH 7.4).

(-)Quinpirole hydrochloride (Sigma Aldrich, St. Louis, MO) was administered at a dose of 1 mg/kg, i.p. dissolved in phosphate buffered saline.

2.3.7 Modeling

Evoked DA responses were simulated with Wightman's model, embodied in the following equation (Wightman *et al* 1988):

Equation 1:

$$\frac{d[DA]_{ex}}{dt} = f * [DA]_p - \frac{V_{\max} * [DA]_{ex}}{[DA]_{ex} + K_M}$$

where $[DA]_{ex}$ represents the extracellular DA concentration, f is the stimulus frequency, $[DA]_p$ is the concentration of DA released-per-pulse, V_{max} is the maximum velocity of DA uptake, and K_M is the DAT Michaelis constant. The effects of diffusion on $[DA]_{ex}$ were examined by convoluting the output of Equation 1 with Fick's second law of diffusion. The convolution was implemented by a finite element algorithm in Excel. We have described the use of finite element algorithms in several previous papers (Lu *et al* 1998; Yang *et al* 1998), so the details are omitted here. Finite element algorithms for solving diffusion equations are well known (Bard and Faulkner 2001).

2.3.8 Data analysis

Voltammetric currents recorded in vivo were converted to DA concentrations by post-calibration of the electrodes. During multi-train stimuli, the voltammetric signal occasionally did not return to baseline during the interval between trains. In these cases, voltammetric signals were re-zeroed at the start of each stimulus train. Pre- and post-drug response amplitudes during consecutive stimulus trains were analyzed by means of two-way ANOVA.

2.4 RESULTS

2.4.1 Heterogeneity of evoked dopamine release

As previously reported (May and Wightman 1989b; May and Wightman 1989a), electrical stimulation of DAergic fibers in the MFB evokes heterogeneous DA release in the ipsilateral striatum. The two stimulus responses in Fig 2.1 were recorded using identical voltammetric procedures in two different rats. The stimulus durations were 200 ms (12 pulses) and 1 s (60 pulses) in Figs 2.1A and 2.1B, respectively. In each case, a similar amplitude of DA release was evoked, ~1.7 μM in these examples, despite the 5-fold difference in stimulus duration. In some cases (Fig 2.1A) the evoked response rises rapidly when the stimulus begins and falls immediately when the stimulus ends. In other cases (Fig 2.1B) the response rate is slow initially (arrow 1) but increases as the stimulus continues (arrow 2). There is no sign of the response rate increasing in Fig 2.1A. Instead, the response rate decreases slightly, as the DA concentration after 200 ms of stimulation is less than double the concentration after 100 ms (diamond).

In the past, a temporal profile such as the one illustrated in Fig 2.1B (a slow initial rise followed by a faster subsequent rise) was attributed to diffusional phenomena, giving rise to the view that the electrode was not positioned near DA terminals. However, in this study we show that several other attributes of these evoked responses are inconsistent with this explanation. For example, in the event that the appearance of DA at the electrode is delayed by diffusion, then the disappearance of DA at the end of the stimulus should also be delayed (see also Fig 2.8, below). This is because, in the event the electrode is not close to DA terminals, DA molecules must undergo diffusion before encountering the dopamine transporter (DAT). In previous reports (Kawagoe *et al* 1992), a delay at the end of the stimulus has been called an "overshoot." However, there is no overshoot in the example of Fig 2.1B. Instead, the DA signal decreases on

the first post-stimulus measurement (arrow 3). The rapid onset of DA clearance indicates that the electrode is positioned near DA terminals, as DAT is only found on DA terminals.

2.4.2 Hybrid evoked responses

Variable response profiles also arise within individual animals (Fig 2.2). The example in Fig 2.2, which we refer to as a hybrid response, exhibits an initial rapid rise in ECS DA when the stimulus starts that ends after 200 ms. The response falls and then increases again but at a slower rate than before. Hybrid responses reveal the simultaneous detection of DA from terminals exhibiting heterogeneous behaviors within the recording site of a single electrode. The hybrid responses confirm that the heterogeneity of response profiles are not attributable to any instrumental factors, such as the response time or sensitivity of the voltammetric electrode.

The response reported in Fig 2.1A was from a site exhibiting a hybrid response: the stimulus was shortened to 200 ms to isolate the rapid signal component.

2.4.3 Classification of response profiles

For the sake of clarity, we seek an objective way to classify the heterogeneous response profiles. A convenient way to do this is based on whether or not the rate of evoked release increases during the stimulus, as in Fig 2.1B. We classify such responses as “slow-type” because the rate of release is initially slow. Responses that rise linearly, and that sometimes show a decrease in the rate of appearance of DA (Fig 2.1A), are classified as “fast-type”. Although it is generally true that, with a stimulus of similar frequency and duration, fast-type responses exhibit larger amplitudes than slow-type responses, this classification scheme is not based on the amplitude. Since it is easy to identify responses that exhibit an increase in the rate of evoked release during a stimulus, this classification scheme is objective.

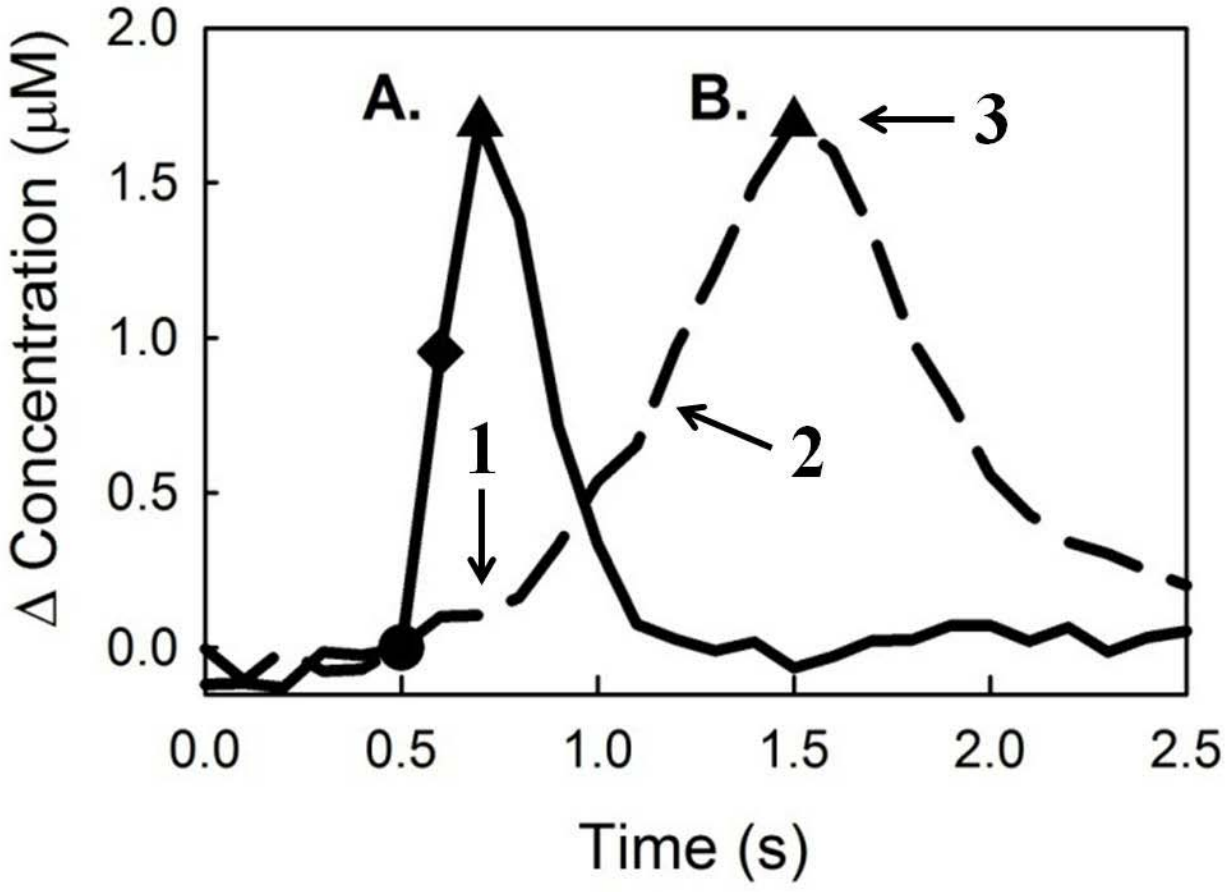

Figure 2.1 Kinetic heterogeneity of evoked DA release in the rat striatum.

The symbols mark the start (circles) and finish (triangles) of the stimuli. The evoked change in extracellular DA was recorded by FSCV with 400-mm long carbon fiber microelectrodes. (A) A fast-type response: DA increases rapidly during the stimulus and falls rapidly after the stimulus. The amount of DA evoked after the first 6 stimulus pulses (diamond) is more than half of the amount of DA evoked after 12 pulses (triangle), indicating that the rate of DA release is decelerating. (B) A slow-type response: evoked DA release begins slowly (arrow 1) and accelerates as the stimulus continues (arrow 2). At the end of stimulation the signal returns toward baseline immediately (arrow 3), showing no signs of overshoot.

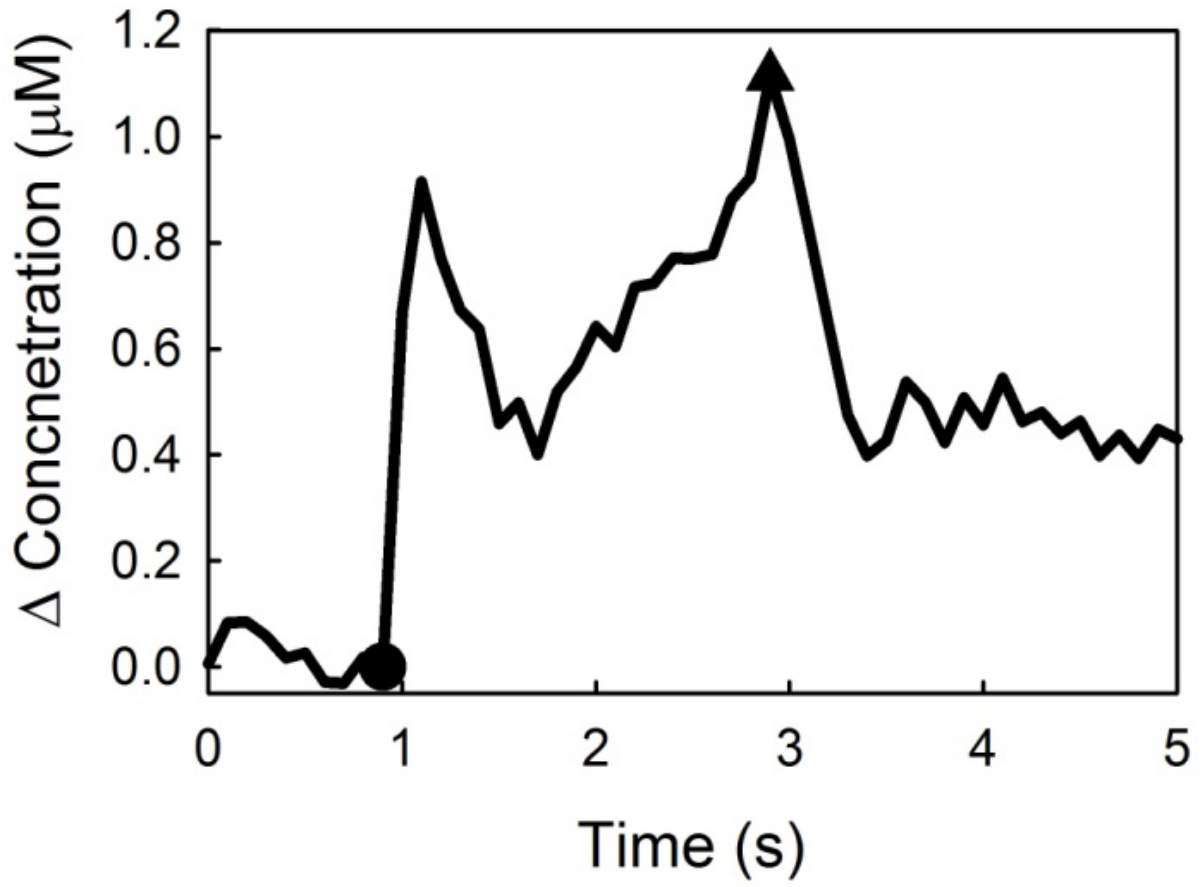

Figure 2.2 An electrode location exhibiting both fast-type and slow-type release.

This hybrid-type response has two peaks. The slope of the ascending part of the first peak is steeper than the second peak counterpart. The rapid rise of the first peak demonstrates a fast-type response, while the second peak has a slow-type response.

2.4.4 Evoked dopamine release during multiple stimulus trains

We characterized fast, slow, and hybrid responses using multiple trains of MFB stimulation (Figs 2.3-2.6). In these figures, circles and triangles mark the start and end, respectively, of each stimulus train. To compare the responses to individual trains, we re-zeroed each response at the beginning of each train (notice that the circle symbols denoting the start of each train all fall on the x-axes of the figures and there is a break in each trace 1 s before each train)

Most experiments involved 1-s stimulus trains separated by 2-s intervals. When the first train evoked a fast-type response (Fig 2.3A), subsequent trains evoked descending response amplitudes. These descending amplitudes highlight the tendency for the rate of evoked release to slow down when the initial rate is high. This slow-down phenomenon has been reported before and attributed to an exhaustion effect and/or autoinhibition resulting from the evoked increase in extracellular DA (Garris *et al* 1994; Benoit-Marand *et al* 2001).

On the other hand, when the first train evoked a slow-type response (Fig 2.3B), subsequent trains evoked ascending response amplitudes. In the example of Fig 2.3B, the rate of evoked release increased during the first train and each subsequent train evoked consecutively faster DA release. Hence, when the interval between trains is 2 s, the increase in the rate of evoked DA release carries over from one train to the next. This carry-over effect is short-lived, however, as it is almost abolished if the interval between trains is increased to 4 s (Fig 2.3C). The individual slow-type responses in Figs 2.3B and 2.3C are representative examples: Fig 2.3D summarizes normalized slow-type response amplitudes with 2-s and 4-s intervals from 13 animals (ANOVA; $F_{(1,96)} = 61.6$; n=13; $p<0.00001$). In these experiments, there was no need to reposition the electrodes to locate slow responses: in our hands, of the fast- and slow-type responses, the slow-type is the prevalent one in the rat striatum.

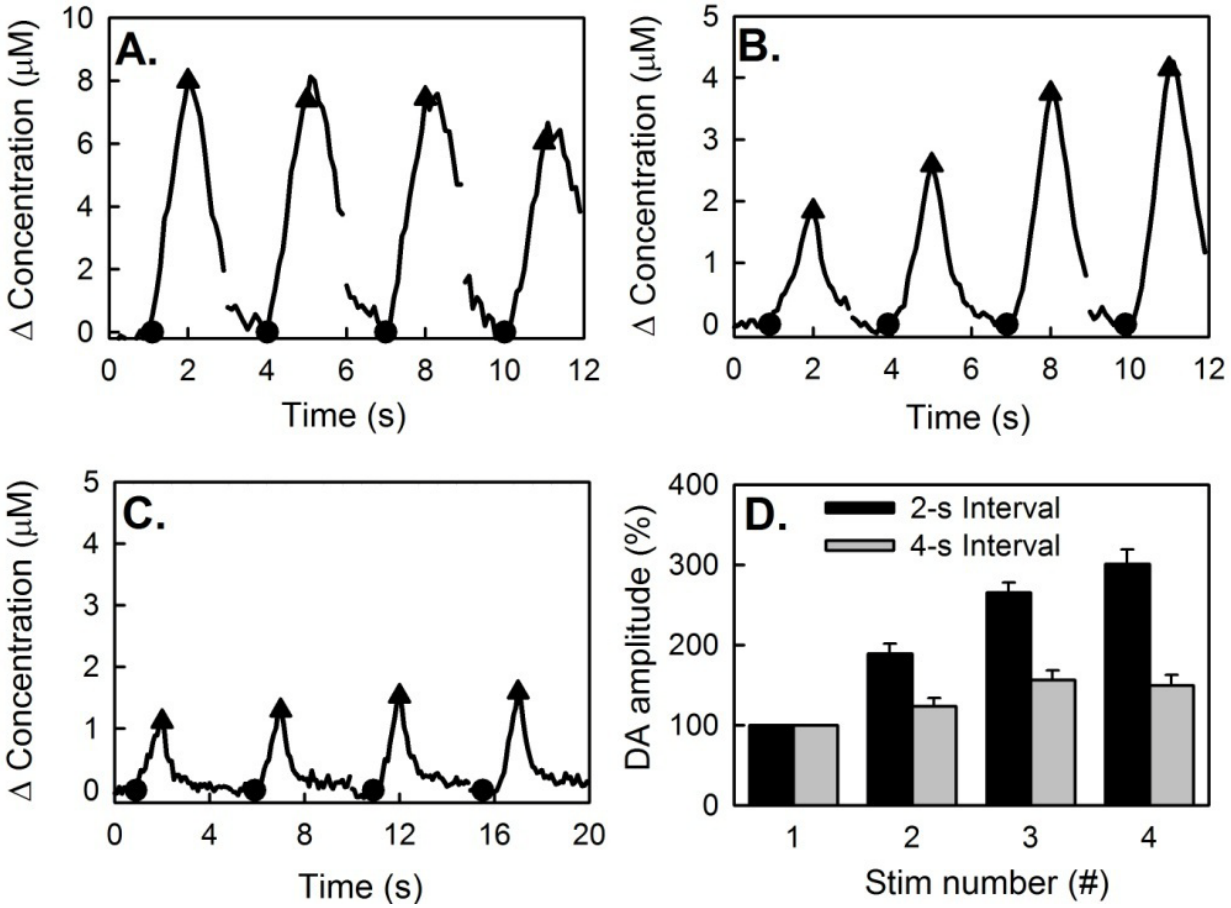

Figure 2.3 DA recordings by FSCV during consecutive trains of MFB stimulation.

(A) Fast-type response during 1-s trains at 2-s intervals. (B) Slow-type response during 1-s trains at 2-s intervals. (C) Slow-type response during 1-s trains at 4-s intervals. (D) Comparison of the normalized amplitudes of the slow-type responses at 2-s and 4-s intervals: the difference between the 2-s and 4-s groups is significant (ANOVA; $F_{(1,96)} = 61.6$; n=13; $p<0.00001$).

As mentioned, slow-type responses were previously attributed to diffusion. Here, however, we find that the increased response rate persists across a 2-s interval between the trains. This persistence cannot be explained by diffusion (see also Fig 2.8). Thus, the persistence, along with the absence of response overshoots, is inconsistent with the idea that the slow-type responses are caused by diffusion.

Multiple stimulus trains (1-s trains with 2-s intervals between the trains) were used at recording sites exhibiting hybrid responses (Fig 2.4). In the majority of these cases, a fast response appears as a leading shoulder superimposed on a subsequent slow response. The leading shoulder was most apparent during the first stimulus train. We used the evoked amplitude after the 12^{th} stimulus pulse (black diamonds in Fig 2.4A) to quantify the fast responses. The amplitude after the 12^{th} pulse decreased from train-to-train, consistent with the decrease in the rate of evoked release associated with fast-type responses. We also examined the response to 12-pulse stimulus trains (200-ms trains with 1.8-s intervals between the trains) and again observed a decrease in the rate of evoked release (Fig 2.4B). Figure 2.4C shows averaged DA amplitudes for three animals after the 12^{th} and 60^{th} pulse during a 1-s train, 2-s interval stimulation and a 0.2-s train, 1.8-s interval stimulation. The pattern of evoked release at the different time-points is significantly different (ANOVA; $F_{(2,24)} = 44.6$; $n=3$; $p<0.00001$). However, a Tukey post-hoc test reveals that the 12^{th} pulse and 0.2-s train responses are not significantly different, suggesting that the fast-type response functions independently of the slow-type response. In order to record these hybrid responses, it was necessary to optimize the placement of the recording location. Even with optimization, we were unable to locate hybrid responses in all animals. Thus, sites yielding hybrid responses are relatively rare compared to those that yield slow responses.

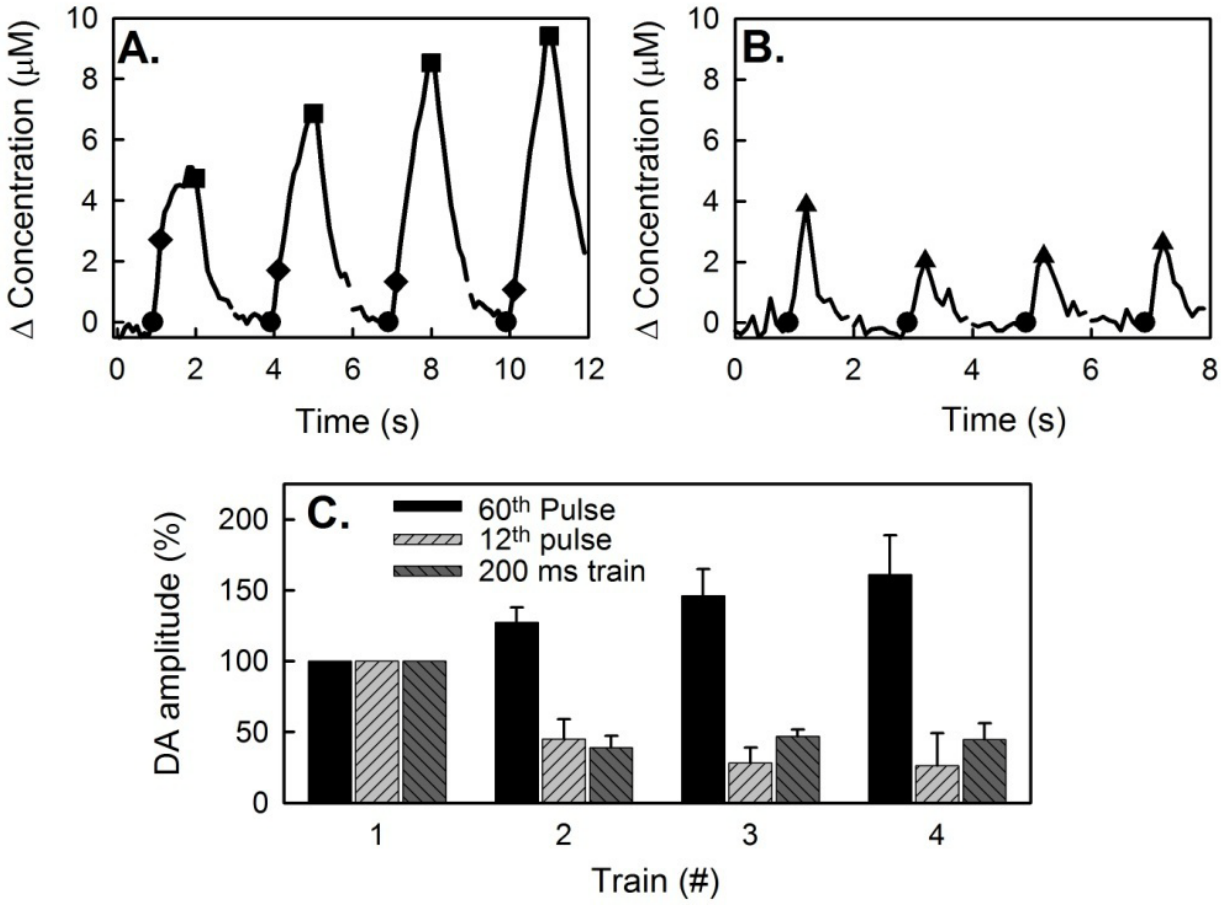

Figure 2.4 Kinetic hybrid responses during consecutive trains of MFB stimulation.

(A) During 1-s trains at 2-s intervals the fast-type signal component appears as a leading shoulder on the response. The signal recorded after 12 stimulus pulses (diamonds) was used to quantify the amplitude of the fast signal component. The signal recorded after 60 pulses (squares) was used to quantify the slow component. (B) DA during 200-ms (12-pulse) trains at 1.8-s intervals: these short trains isolate the fast signal component. (C) Normalized response amplitudes: according to ANOVA the group effect is significant (ANOVA; $F_{(2,24)} = 44.6$; n=3; $p<0.00001$); according to the Tukey post-hoc test, there is no difference between the responses after 12 pulses during 1-s trains and the responses evoked by 200-ms trains.

2.4.5 The role of the dopamine D2 receptor

The D2 receptor antagonist, raclopride (2 mg/kg i.p), converts slow-type responses to fast-type responses (Fig 2.5). In the example of Fig 2.5A, the pre-raclopride response (1-s trains with 2-s intervals between trains) is slow-type. However, the post-raclopride response in the same recording site is fast-type. Raclopride eliminated the initial period of slow release and later trains evoked responses with descending amplitudes. In multiple animals (n=5), raclopride consistently and substantially increased the amplitude of the response to the first stimulus train and abolished the increase in the response amplitude during subsequent trains (Fig 2.5B).

In every case involving slow-type responses, raclopride increased the amplitude of the DA measurement from the very beginning of the first stimulus train, i.e. after 12 stimulus pulses. Pre-raclopride, evoked DA release was often not detectable after the first 12 stimulus pulses. Hence, the effect of raclopride is not dependent upon the evoked release of DA. In this important regard, our results are different from the 1-to-4 pulse results of Wightman and Gonon (Garris *et al* 1994; Benoit-Marand *et al* 2001). To quantify this effect, we measured the slope of the evoked response between 100 and 300 ms (6-18 pulses) after the start of each stimulus train (Fig 2.5C). In five animals raclopride consistently and significantly increased the initial slope of the DA signal compared to the pre-drug response (ANOVA; $F_{(1,32)} = 21.9$; n=5; $p<0.0001$). These observations carry two important meanings. First, they show that the slow responses, when they occur, are a consequence of autoinhibition that occurs due to a preexisting tone of DA on D2 receptors, i.e. basal DA as opposed to evoked DA. Second, they show that the electrode is positioned near DA terminals as, within the temporal resolution of these experiments (100 ms), there is no delay in the arrival of DA at the electrode post-raclopride. The delay observed pre-raclopride, therefore, is logically attributable to the electrode being positioned close to autoinhibited DA terminals.

Raclopride affects both DA release and clearance (Greco *et al* 2006). So, we wished to establish whether the effect of raclopride is due to a change in DA release or DA clearance. For this purpose, we adjusted the stimulus duration to establish similar evoked amplitudes pre- and post-raclopride and then aligned the responses at the end-point of the stimuli (Fig 2.5D). This procedure revealed no consistent effect of raclopride on DA clearance, suggesting the effects reported here are derived from alterations in evoked release.

The D2R agonist, quinpirole (1 mg/kg i.p.), consistently and significantly extended the initial period of slow evoked release (Fig 2.6): evoked release was not detected during the first stimulus train (Fig 2.6A). This clearly shows that a delay in the evoked response can be due to the activation of inhibitory receptors rather than an absence of DA terminals. Later stimulus trains produced ascending response amplitudes, as before. The post-quinpirole amplitudes were significantly lower than the pre-drug amplitudes (Fig 2.6B; ANOVA; $F_{(1,32)} = 29.1$; n=5; $p<0.0001$). As before, we adjusted the stimulus durations to match the pre- and post-quinpirole amplitudes and aligned the responses at their end-points (Fig 2.6C). Quinpirole had no systematic effect on DA clearance. Interestingly, aligning the responses in this way produced similar temporal profiles of evoked release. Thus, quinpirole extended the initial slow phase of evoked release but did not thereafter alter the time course of the subsequent response.

Quinpirole (1 mg/kg i.p.) abolishes the fast component of hybrid responses (Fig 2.7A). The fast component of hybrid responses was isolated with a short 200 ms stimulus (12 pulses). Quinpirole (1 mg/kg i.p.) abolished all 12-pulse stimulus responses (Fig 2.7B and 2.7C). After quinpirole, even when the stimulus duration was extended, only slow-type evoked responses (slow initial responses rates and subsequent facilitation, Fig 2.7A) are observed. These results confirm that activation of D2 receptors abolishes the fast component of these responses.

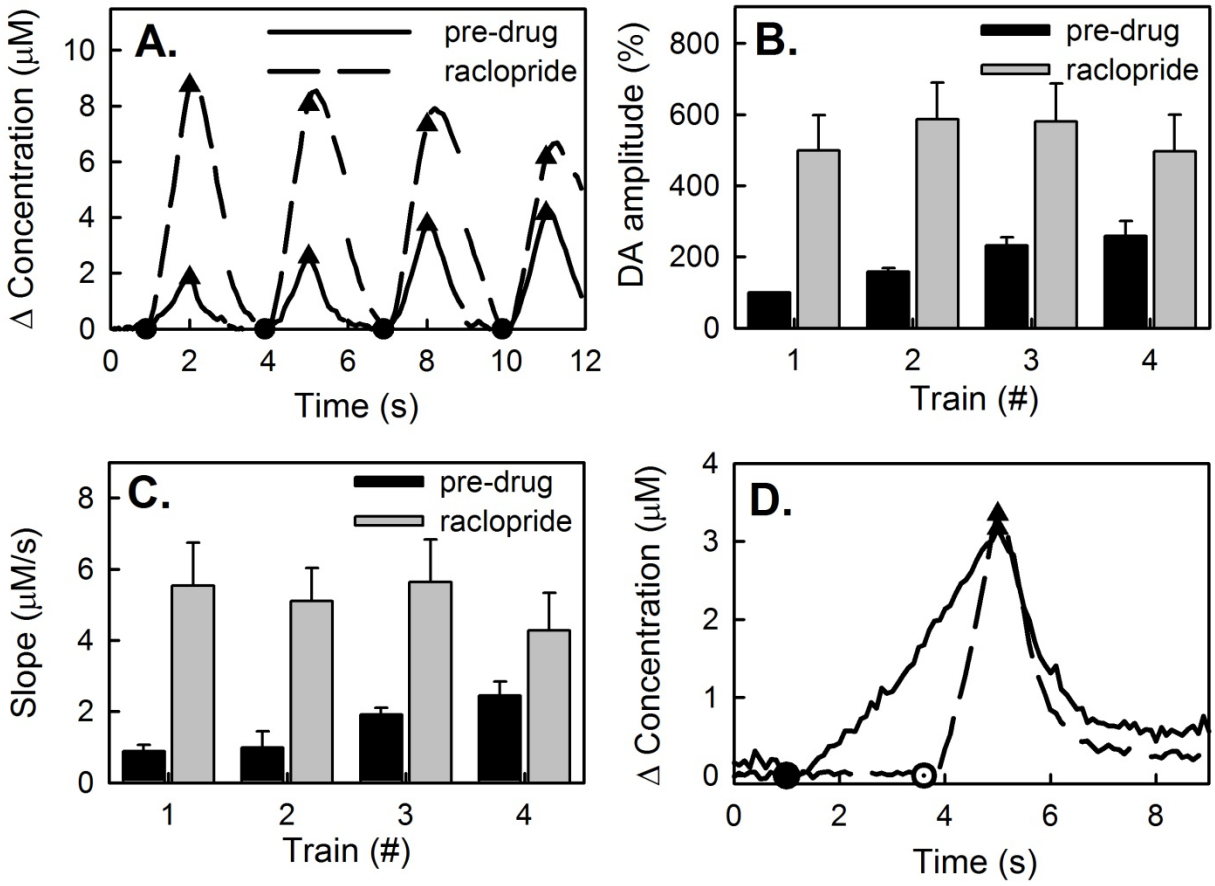

Figure 2.5 Raclopride accelerates DA release.

(A) Raclopride (2 mg/kg i.p.) converts slow-type responses (pre-drug, solid line) to fast-type responses (post-drug, dashed line). (B) The effect of raclopride is significant (ANOVA; $F(1,32) = 52.86$; $p<0.00001$). Pre-drug there was a significant difference between the responses to the consecutive trains, but raclopride abolished this difference (ANOVA; $F(3,32) = 0.88$; $n=5$; $p>0.5$). (C) The effect of raclopride on the initial rise of the DA signal is also significant (ANOVA; $F(1,32) = 21.9$; $n=5$; $p<0.0001$). Raclopride removed the delay present in the pre-drug signal, causing DA signals that increased immediately upon stimulation. (D) The duration of pre- and post-drug stimuli were adjusted to produce a similar maximal amplitude. Then the responses were aligned at the end of the stimulus to permit a comparison of the clearance kinetics. Raclopride had no consistent effect on DA clearance, suggesting that the effects of raclopride noted in this figure are due to changes in the velocity of evoked DA release.

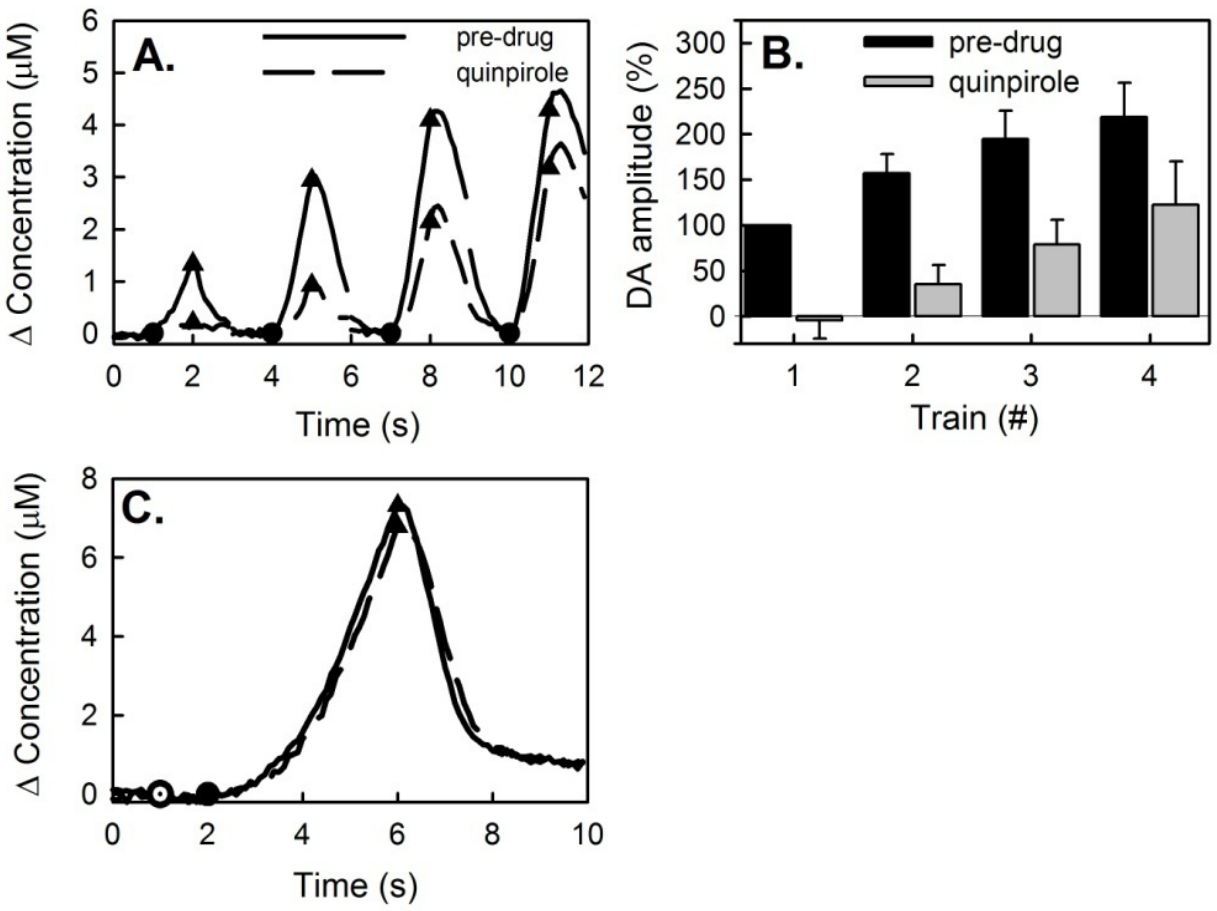

Figure 2.6 Quinpirole further delays slow-type evoked DA release.

(A) Quinpirole decreased the response amplitudes during 1-s trains at 2-s intervals. However, quinpirole did not prevent the acceleration of evoked DA release. (B) The effect of quinpirole on the normalized response amplitudes is significant (ANOVA; $F_{(1,32)} = 29.1$; n=5; $p<0.0001$). Quinpirole did not remove the significant difference between the response amplitudes to consecutive trains (ANOVA; $F_{(3,32)} = 6.8$; n=5; $p<0.002$). (C) The duration of pre- and post-drug stimulus responses were adjusted in order to evoke similar response amplitudes, thus the start of stimulation pre-drug (closed circle) and quinpirole (open circle) were staggered. Quinpirole delayed the onset of evoked release but thereafter did not alter the kinetics of evoked DA release or the kinetics of DA clearance after the stimulus.

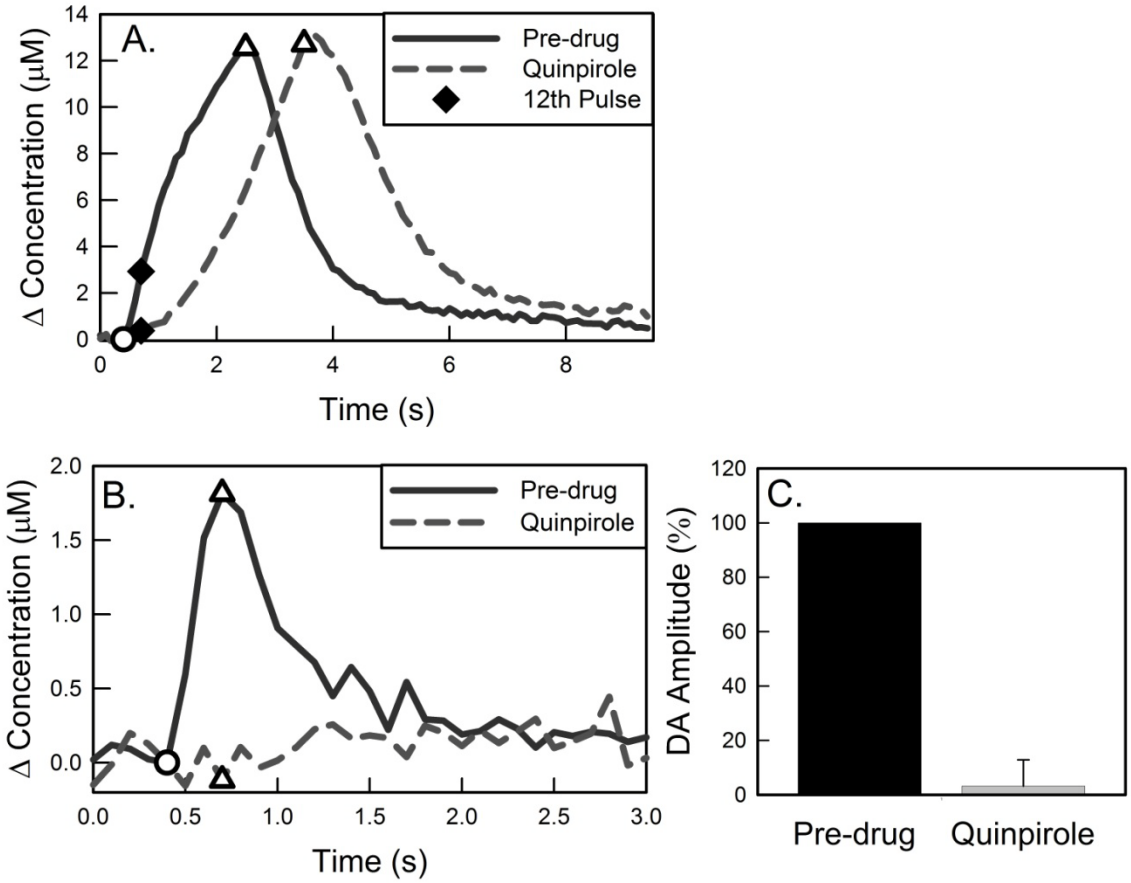

Figure 2.7 Quinpirole converts hybrid responses to slow-type responses.

(A) Before quinpirole, evoked release begins without delay after the onset of stimulation (60 Hz). Quinpirole delays the onset of evoked release and diminishes the amplitude of release evoked by the first 12 stim pulses (solid diamonds). (B) Quinpirole abolishes 12-pulse stim responses. (C) The decrease in DA release evoked by 12 stim pulses after quinpirole is significant (ANOVA: $F(1,3) = 100.8$; $n = 3$; $p<0.001$).

2.4.6 Insights from Wightman's model of evoked release

At several points during this paper, we have relied on the concept that the slow-type responses exhibit features inconsistent with diffusion. Here, we explain this point in more detail.

The simplest form of Wightman's model, i.e. equation 1 with constant parameters ($[DA]_p$, V_{max}, and K_M), is incapable of reproducing responses with a slow initial rate that later increases (as in Fig 2.1B). The modeled responses all slow down as the stimulus proceeds (Fig 2.8A). The examples of Fig 2.8A were generated with standard parameter values from the literature. This behavior has a very simple origin: the release term, $f * [DA]_p$, is constant but the uptake term, $\frac{V_{max}*[DA]_{ex}}{[DA]_{ex}+K_M}$, increases as $[DA]_{ex}$ increases. Thus, as the stimulus proceeds, $[DA]_{ex}$ increases but so does the rate of uptake, so the response has to slow down.

When the simulated responses are convoluted with diffusion, they do speed-up (Fig 2.8B). In the example of figure 2.8B, a simple response is convolved with diffusion over a distance of 15 μm using the DA diffusion coefficient measured in the rat striatum (Nicholson and Rice 1991). Indeed, the convolution produces a slow initial response that speeds up as the stimulus proceeds (arrow 1). Qualitatively, there is a good match between the convoluted responses and the slow-type voltammetric responses recorded in vivo (e.g. Fig 2.1B). However, the convoluted simulated response exhibits an obvious overshoot at the end of the stimulus (arrow 2), which is absent in our in vivo recordings.

During this study, we made no attempt to fit the convoluted simulations to our in vivo results because we do not agree that diffusion causes the slow-type responses. For the same reason, we have made no attempt to use deconvolution to remove diffusional effects from our in vivo results. In past work, deconvolution was employed to remove the effects of diffusion through Nafion layers on electrodes (Kawagoe *et al* 1992). We did not employ Nafion layers in

the present work. Furthermore, we have here reported examples of fast-type responses, which demonstrate that the slow-type responses are not caused by slow electrodes or other instrumental factors. Therefore, we have no justification to apply deconvolution to our results.

Diffusion also does not explain the train-to-train increases in evoked release characteristic of slow-type responses. In the example of figure 2.8C, the simple model was used to simulate a response to four 1-s trains with 2-s intervals between the trains with and without convolution (same distance and diffusion coefficient as in Fig 2.8B). The simple model, with or without convolution, does not reproduce the changes in temporal profile and amplitude observed in vivo (Fig 2.3B), so we conclude that these observations are not caused by diffusional phenomena.

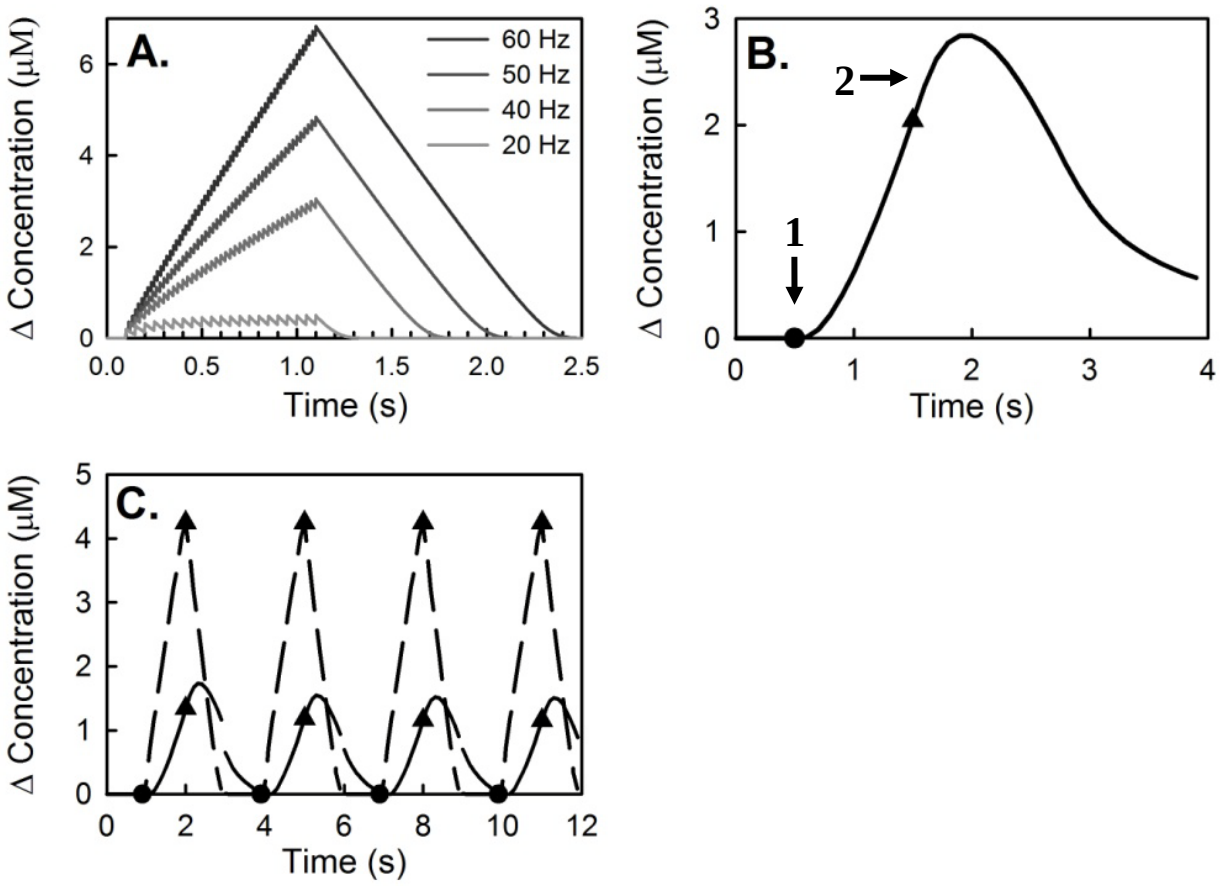

Figure 2.8 The Wightman model of dopamine release and diffusion

(A) Theoretical evoked DA curves using the Wightman model (V_{max} = 6 mM/s, K_M = 200 nM, $[DA]_P$ = 200 nM). The modeled curve rises without delay at all stimulus frequencies. (B) The effects of a 15 μm diffusion gap on the Wightman model curve (60 Hz). Diffusion causes an initial delay in the DA signal (arrow 1), and an overshoot of signal after the end of stimulation (arrow 2). (C) Modeling 1-s trains, 2-s interval stimulations. The Wightman model predicts four equal evoked curves (dashed lines). Diffusion of four identical evoked curves produces four signals with similar delays and amplitudes.

2.5 DISCUSSION

The findings of the present study support the conclusion that the slow-type evoked responses arise when DA terminals proximal to the recording electrode are autoinhibited by basal extracellular DA. Direct evidence to support this conclusion stems from the ability of the D2 antagonist, raclopride, to eliminate the slow initial phase of evoked DA release and the ability of the D2 agonist, quinpirole, to extend it. We consider this a tonic, rather than phasic, effect because autoinhibition was present prior to the onset of electrical stimulation. This is consistent with our prior reports that the striatal extracellular space contains a tonic pool of DA at concentrations sufficient to activate DA receptors (Kulagina *et al* 2001; Borland and Michael 2004; Mitala *et al* 2008). Our study provides direct, real-time recordings of DA functioning in vivo on multiple time scales determined, at least in part, by the efficacy of a local autoinhibitory tone.

2.5.1 Diffusion or complex release kinetics?

May and Wightman (May and Wightman 1989b; May and Wightman 1989a) reported the tendency of evoked responses to begin slowly and to speed up with continued stimulations, as we have also reported here (Fig 2.1B). Although May and Wightman speculated that this feature might be due to an increase in the rate of evoked release, they attributed it instead to diffusional phenomena arising when the recording electrode is remote from DA terminals (May and Wightman 1989b). Other authors have suggested that diffusional phenomena might arise when the electrode is surrounded by a zone of dead tissue (Benoit-Marand *et al* 2007), although our electron microscopy study shows that any that any dead zone is too small to create severe diffusional distortion (Peters *et al* 2004). As we have mentioned, however, other features of the

slow type responses speak against the diffusion-based explanation. First, the responses do not exhibit the expected overshoots at the end of the stimulus trains (Fig 2.1B and 2.8B), which shows that the electrode is close to DAT and, therefore, DA terminals. Second, diffusion does not explain the persistence of increased rates of evoked release across the intervals between trains (compare Fig 2.3B with Fig 2.8C). Third, the initial slow phase of release was abolished by raclopride (Fig 2.5) and extended by quinpirole (Fig 2.6) and thus stems from a D2R-mediated control of evoked release. There is no evidence to suggest that diffusion is sensitive to D2 receptors.

2.5.2 Other methodological considerations

Immunohistochemical studies have demonstrated that DA terminal fields contain non-DA sites (Venton *et al* 2003), i.e. sites that lack DA terminals. However, the electrodes employed for this study were 400 μm long, which is very long compared to the dimensions of the non-DA sites (less than 10 μm) identified by Venton *et al.* (2003). Thus, it is not possible that our DA measurements were confined to non-DA sites. Likewise, the slow DA responses were not limited by the performance attributes of the voltammetric electrodes. Slow initial responses gave way to more rapid responses, at the same electrode, by virtue of continued electrical stimulation or by the administration of raclopride. On the same grounds, we eliminate the possibility that the slow responses stem from poor placement of the stimulating electrode.

2.5.3 Slow type responses are prevalent in the striatum

Using 400-μm long electrodes, the recording of slow type responses in the striatum is routine. For this reason, we consider the slow type responses to be the prevalent striatal response.

Furthermore, since many of the responses recorded during this study were exclusively of the slow type, we conclude that these responses occur with a domain size commensurate with the length of the electrode. We did also occasionally observe hybrid responses with a fast type response component, but we had to search for these sites. This portrays the fast sites as the comparatively rare DAergic behavior in the striatum and associated with a spatial domain size smaller than that of the slow type responses.

Hence, it is our point of view that the prevalence of the slow type responses in the striatum indicates that a majority of DAergic terminals in this brain structure exist under a state of tonic autoinhibition. This point has been overlooked in the previous literature, in part due to the attribution of slow type responses to diffusional phenomena. In an attempt to avoid the perceived diffusional distortion of responses, many users of voltammetry optimize the placement of their recording electrodes so as to concentrate their studies on fast-type responses. An important insight from our study is that the search for optimized recording sites likely constitutes a search for sites were DA terminals are free of autoinhibition. This explains the contrast between our conclusions and those of Wightman (Garris *et al* 1994) and Gonon (Benoit-Marand *et al* 2001). On the basis of very brief electrical stimuli (1 to 4 pulses), these authors concluded that DA terminals normally experience little or no autoinhibition in the absence of MFB stimulation. However, their studies were performed in fast sites found by optimizing the placement of the electrodes, as evidenced by the fact that brief responses were detectable (both authors mention that the brief stimuli do not always produce detectable responses). The fact that autoinhibition has been overlooked as a contributing factor in the heterogeneity of the striatal DA system can be attributed to the decision to focus attention on fast responses.

2.5.4 A comment on stimulus-induced acceleration of evoked DA release

While autoinhibition provides a clear explanation for the slow initial rate of evoked release, our study does not provide an explanation for the acceleration of evoked release that occurs with continued stimulation. While stimulus-induced acceleration of neurotransmitter release is an interesting and known phenomenon (Greengard *et al* 1993), it was not the main focus of the present study. The stimulation frequency we used (60 Hz) is clearly supraphysiological, as DA neurons burst around 20 Hz and tonically fire at 1-2 Hz (Grace and Bunney 1984; Benoit-Marand *et al* 2001; Hyland *et al* 2002). Thus, the details of the release evoked by 60 Hz stimuli are not likely to be of direct physiological relevance. The value of this supraphysiological stimulus is its ability to reveal the existence of pre-stimulus autoinhibition, which is the main focus of our study. Since the autoinhibition we describe here is derived from endogenous DA present in the extracellular space, we presume that the autoinhibition is physiologically relevant.

2.5.5 The role of autoreceptors

Our results show that the slow type responses are a consequence of autoinhibition triggered by basal DA present in the extracellular space prior to the onset of electrical stimulation. It is important to emphasize that the D2R drugs did not simply alter the magnitude of the slow-type responses but also rather dramatically altered their time course. The D2R antagonist, raclopride, caused the DA signal to appear before the onset of pre-raclopride slow-type evoked release (Fig 2.5). The D2R agonist, quinpirole, delayed the appearance of the DA signal without substantially altering the subsequent dynamics of release or clearance (Fig 2.6). Thus, we conclude that the slow-type kinetics arise when DA terminals are under an autoinhibitory tone prior to the initiation of the stimulus.

The impact of D2Rs on fast-type evoked DA release has been thoroughly characterized by other laboratories in several experimental models (Limberger *et al* 1991; Kennedy *et al* 1992; Benoit-Marand *et al* 2001; Phillips *et al* 2002; Avshalumov and Rice 2003; Kita *et al* 2007). A main conclusion of those prior studies is that autoinhibition of fast type responses begins only after the stimulus itself delivers DA to the extracellular space. These results are confirmed by the ability of the D2R agonist, quinpirole, to convert fast type responses into slow type responses (Fig 2.7). Thus, there is a clear contrast in the manner by which autoinhibition affects slow- and fast-type behaviors. However, this contrast is related to differences in D2R expression, since both the slow- and fast-type responses are sensitive to D2R agonists and antagonists, although in different ways.

2.5.6 The origin of pre-stimulus autoinhibition

We conclude that the kinetic status of striatal DA terminals, i.e. whether they exhibit fast or slow evoked responses, is at least partially determined by the absence or presence, respectively, of autoinhibitory tone. Recently, our laboratory presented FSCV-based evidence for the presence in striatal extracellular space of micromolar concentrations of non-evoked DA (Kulagina *et al* 2001; Borland and Michael 2004; Mitala *et al* 2008). Such DA concentrations are sufficient to tonically activate D2R autoreceptors (Grigoriadis and Seeman 1985). The micromolar concentration of DA we reported exceed the low-nanomolar basal DA levels reported by microdialysis. However, several studies have explained that the combined effects of tissue damage and DA uptake cause microdialysis to underestimate actual in vivo DA concentrations, even when no-net-flux or extrapolation to zero-flow is used (Clapp-Lilly *et al* 1999; Peters *et al* 2000; Bungay *et al* 2003; Borland *et al* 2005; Mitala *et al* 2008). While our prior studies demonstrated the presence of a tonic extracellular DA pool in the striatum, the present study

demonstrates the functional significance of that tonic DA pool. Sites within the striatum previously identified as non-DAergic, due to the absence of DA transients, are now reinterpreted as sites where tonic DA signaling is taking place.

3.0 USING SEGMENTED FLOW TO CONTROL DRUG LEAKAGE FROM THE TIP OF DUAL-FUNCTION DOUBLE BARREL PICOSPRTIZER ELECTRODES

3.1 ABSTRACT

Recent studies using fast scan cyclic voltammetry in conjunction with carbon fiber electrodes identify unique domains of dopamine terminal function within the striatum. Further exploration of these domains requires a device capable of electrode location optimization and temporally controlled analyte delivery at the recording site. In this study we use a dual function double barrel picospritzer electrode, where the open tip of the picospritzer barrel is immediately adjacent to the carbon fiber electrode. This system can deliver controlled volumes of analyte solution at optimized recording sites. However, while monitoring current change during both baseline and evoked dopamine release at the adjacent carbon fiber electrode we discover that physiologically relevant concentrations of analyte leak from the tip of the picospritzer barrel. In order to gain temporal control of analyte release we use segmented flow. An air bubble separates the buffer solution at the tip of the electrode from the analyte solution in the barrel, preventing analyte leakage from the tip. Initial picospritzer ejections compress the air bubble allowing the analyte solution to mix into the tip solution. Once the analyte is in the tip solution further picospritzer ejections deliver the analyte into the extracellular space. This method prevents the untimed delivery of analytes to the extracellular space.

3.2 INTRODUCTION

The Nigrostriatal dopamine pathway is comprised of a relatively small number of dopamine (DA) neurons. These cells originate in the substantia nigra, their axons run along the medial forebrain bundle, and their terminals innervate the striatum. This singular physiology suggests a system of dopaminergic cells with a singular function. Yet the striatum has a broad functional diversity including; substance abuse, schizophrenia, and attention deficit hyperactivity disorder (Abi-Dargham *et al* 2000; Phillips *et al* 2003b; Salahpour *et al* 2008).

Recent studies of the striatal dopamine system using carbon fiber electrodes in conjunction with fast scan cyclic voltammetry reveal significant heterogeneity in dopamine terminals response to stimulation and drugs (Kita *et al* 2007; Zachek *et al* 2010). This heterogeneity is linked to the time course of dopamine-2 receptor (D2R) activation via regulation of basal DA concentrations by the dopamine transporter (DAT) (Benoit-Marand *et al* 2001; Moquin and Michael 2009; Wang *et al* 2010; Moquin and Michael 2011). These unique populations of terminals co-exist within the striatum, and are accessed by manipulating the electrode location, termed 'electrode optimization' (Garris *et al* 1993). Further understanding of these domains and their functional relevance will shed new light on the striatal dopamine sytem and its disorders.

A dual function picospritzer electrode system that is mobile and capable of highly localized analyte delivery would be a valued tool in the continued study of dopamine sub-populations. The ability to locally deliver analytes to the detection location will enable isolated studies of the effects drugs have on sub-populations of terminals (Kehr *et al* 1972; Grace and Bunney 1985; Kalivas 1993). Also, analyte delivery devices are required for the administration of drugs that do not cross the blood brain barrier (Reese and Karnovsky 1967; Nagy *et al* 1984).

Therefore it is vital to develop an analyte delivery and detection system that is mobile within brain tissue, such that sub-populations can be located, identified, and manipulated.

A picospritzer system is able to deliver sub-second bursts of compressed air (0-100 psi) into the back of a pulled glass capillary. The applied pressure forces controlled volumes of fluid through the capillary tip. This analyte delivery device has been used in conjunction with a separate detection electrode in in vivo and in vitro setups (Cass *et al* 1993; Cragg *et al* 2001; Daws and Toney 2007; Makos *et al* 2009). In order to minimize the distance separating the two devices, the picospritzer and detection electrode are placed into the sample at an angle with respect to each other. This enables picospritzer placement 100 µm from the detection electrode.

This setup has two problems. First, the orientation of the picospritzer and electrode does not allow for electrode optimization. The picospritzer and detection electrode are not parallel so electrode optimization changes the distance separating the delivery device and the detection electrode. Second, even at distances of 100-300 µm, there is significant spherical diffusion of the analyte from the picospritzer to the tissue at the detection electrode (Bard and Faulkner 2001; Daws and Toney 2007). Thus, a large volume of solution must be delivered into the extracellular space in order for a small concentration of analyte to reach the detection electrode (Cass *et al* 1993).

In order to overcome these issues, we utilize a double barreled pulled glass capillary whose barrel tips are immediately adjacent to each other. One barrel contains a carbon fiber detection electrode protruding from the tip and the other barrel ends in an open hole at the tip for delivery of an analyte solution. In this study we employ a picospritzer to deliver the analyte solution via short bursts of compressed air. Others have used this double barrel system in conjunction with iontophoresis (Herr *et al* 2008). Regardless of the analyte delivery method,

placing the delivery device and detection electrode together solves the above issues. First, the detector and delivery system move in tandem allowing for electrode optimization. Second, the detection electrode is at the site of analyte delivery, enabling detectable analyte delivery that is highly localized without diffusional distortions.

The co-localization of the picospritzer and detection electrode enables accurate comparisons of endogenous and exogenous DA clearance kinetics. Prior experiments using separated delivery and detection devices measured significantly different rates of exogenous DA clearance compared to evoked DA clearance (Cass *et al* 1993; Cass and Gerhardt 1994; Kiyatkin *et al* 2000; Sabeti *et al* 2002). The picospritzer electrode resolves this controversy by delivering highly localized bursts of exogenous DA at optimized electrode locations. When recorded from the same slow-type striatal location, evoked and exogenous DA clear the extracellular space at the same rate (Moquin and Michael 2011).

However, when placed immediately adjacent to the picospritzer tip, the carbon fiber electrode baseline signal detects solution leaking from the picospritzer tip into the extracellular space. Further, analytes in the tip solution leak into the extracellular space at physiologically relevant concentrations. Uncontrolled picospritzer leakage prevents temporal control of analyte delivery. We solve this issue by using segmented flow to separate the buffer solution at the tip of the electrode from the buffer solution containing drugs in the barrel. Several priming ejections compress the air bubble separating the two solutions, allowing them to mix. Once loaded into the tip solution, the analyte is delivered into the extracellular space by another picospritzer ejection. While this method does not resolve the leak, it enables the current system to release drugs of interest in a controlled, time-dependant manner.

3.3 METHODS

3.3.1 Double barrel picospritzer electrode system

Double barrel borosilicate glass capillaries (dimensions prior to pulling 0.68 mm ID, 1.2 mm OD, A-M systems Inc., Sequim, WA) were altered by breaking off approximately one inch of one of the barrels using a straight edged tungsten carbide glass scoring knife (Wale apparatus Co., Hellertown, PA). The single barrel portion of the longer capillary was connected to the Picospritzer apparatus. The shorter barrel housed the carbon fiber electrode.

Carbon fiber electrodes were made by placing a single 7-μm diameter carbon fibers (T650, Cytec Carbon Fibers LLC., Piedmont, SC) were placed inside the shorter borosilicate glass capillary. The double barrel capillaries were pulled to a fine tip with a vertical micropipette puller (Narishige, Los Angeles, CA). The tips of the pulled barrels stayed together forming a single point. The pulled glass formed a seal around the carbon fiber and left an open hole at the tip of the picospritzer barrel (Fig 1). The electrode barrel was backfilled with low-viscosity epoxy (Spurr Epoxy, Polysciences Inc., Warrington, PA). The exposed carbon fibers were cut to a length of 400 μm. A droplet of mercury in the electrode barrel established electrical contact between the fiber and a nichrome contact wire (Goodfellow, Huntingdon, Cambridgeshire, UK). Picospritzer barrels were prepped for drug delivery by placing the tip of the double barrel device into a beaker of artificial cerebral spinal fluid solution (aCSF: 1.2mM Ca^{2+}, 152mM Cl^{-}, 2.7mM K^{+}, 1.0mM Mg^{2+}, 145mM Na^{+}, pH 7.4). Capillary action pulled the solution up the open tip of the picosprtizer barrel. A drug solution (either DA or raclopride in aCSF) was backfilled into the picospritzer barrel. Initial experiments mixed the aCSF and drug solutions in the barrel such that they became one solution. Later experiments (when noted) separated the two solutions with an air bubble 1-1.5 mm in length.

3.3.2 Fast scan cyclic voltammetry

FSCV was conducted with an EI 400 high-speed potentiostat (originally constructed by Ensman Instruments but presently available from ESA Inc., Chelmsford, MA) and the program "CV Tar Heels v4.3" (courtesy of Dr. Michael Heien, Department of Chemistry, University of Arizona). The rest potential was 0 V vs Ag/AgCl and the voltammetric waveform consisted of three linear potential sweeps to +1 V, -0.5 V, and back to 0 V at a sweep rate of 400 V/s. The scans were performed at 10 Hz. The DA oxidation current was recorded between 0.5 and 0.7 V during the first sweep. DA voltammograms were obtained by background subtraction.

3.3.3 Exogenous analyte delivery

Analyte solutions were prepared by dissolving the analyte in aCSF. Dopamine HCl or raclopride tartrate (Sigma Aldrich, St. Louis, MO) were dissolved at concentrations of 25 mM or 2 mM respectively. The analyte solution was delivered from the picospritzer tip using a picospritzer III system (Parker Hannifin, Fairfield, NJ). The picospritzer was attached to the single barrel portion of the longer capillary. Solutions were ejected from the tip of the picospritzer barrel using high pressure nitrogen (10-30 psi). Pressure ejection lasted 0.2 s to 30 s. Injections of DA were monitored using FSCV and the adjacent carbon fiber electrode.

3.3.4 In beaker experiments

The picospritzer barrel was filled with an aCSF solution in the tip, and an aCSF and DA solution in the barrel. The Picospritzer electrodes were connected to the picospritzer and electrochemical systems and placed in a beaker filled with phosphate buffered saline (PBS: 155mM Na^+, 155mM Cl^-, 100mM phosphate, pH 7.4). The fast scan cyclic voltammetry was used to monitor current changes at the carbon fiber electrode during 30 s picospritzer ejections at 30 psi.

3.3.5 In vivo experiments

Male Sprague-Dawley rats (250-350 g) (Hilltop, Scottsdale, PA) were anesthetized with isoflurane (2% by vol.) and placed in a stereotax (David Kopf Instruments, Tujunga, CA) with the incisor bar raised 5 mm above the interaural line (Pellegrino *et al* 1979). A heating blanket (Harvard Apparatus, Holliston, MA) maintained body temperature at 37^{o}C. A twisted, bipolar, stainless steel stimulating electrode was placed over the medial forebrain bundle (MFB) (from bregma: 1.6 mm lateral, 2.2 mm posterior, 8.0 mm below dura). A picospritzer electrode was placed in the ipsilateral striatum (from bregma: 2.5 mm lateral, 2.5 mm anterior, initially 4.5 mm below dura). The final position of the stimulating electrode was set by lowering it until evoked DA release was observed in the striatum: this is a well-established adopted protocol for locating the tip of the stimulating electrode so as to activate ascending DAergic fibers (Ewing *et al* 1983; Kuhr *et al* 1984; Heien *et al* 2005).

3.3.6 Electrical stimulation

The stimulus was an optically isolated, constant-current, biphasic waveform (frequency 60 Hz, pulse height 270 µA, pulse width 2 ms). Single trains lasting 3s in duration were used to determine the rate of dopamine release at each electrode location.

3.3.7 Electrode calibration

Electrodes were post-calibrated in a flow cell with gravity fed aCSF. Conversion of in vivo oxidation currents to DA concentrations was based on post-calibration results. Standards for calibration were prepared by dissolving dopamine HCl (Sigma Aldrich, St. Louis, MO) in aCSF.

3.3.8 Data analysis

Voltammetric currents recorded in vivo were converted to DA concentrations by post-calibration of the electrodes. The maximum amplitudes of evoked or exogenous DA were measured using the DA oxidation potential (~650 mV) at the end of each event. The ejection of aCSF was measured at a non-DA redox potential (200 mV). ANOVA was used to determine the statistical significance of maximum peak amplitudes.

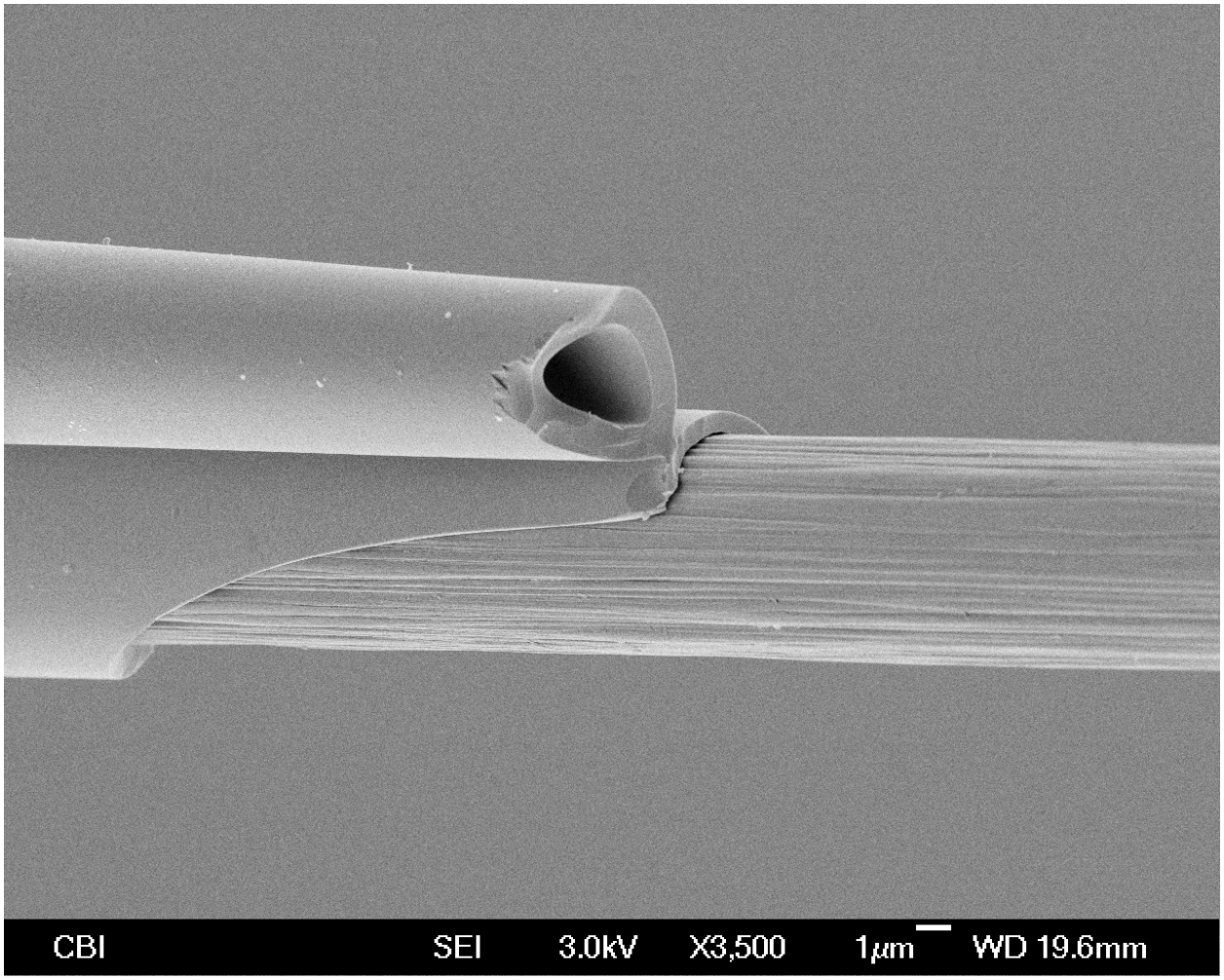

Figure 3.1 Scanning electron microscope image of the picospritzer electrode tip

The bottom barrel contains the carbon fiber microelectrode. The top barrel ends in an open tip. Analytes are delivered from the tip directly at the recording site by means of the Picospritzer III pressure ejection system.

3.4 RESULTS

3.4.1 Picospritzer destabilizes electrode baseline

Using fast scan cyclic voltammetry, a carbon fiber electrode detects fluctuations in current caused by chemical changes on the electrode surface and concentration changes of electroactive species in solution. A stable baseline indicates that both the electrode surface and analyte concentrations are unchanged. Consistent with previous studies, single barrel carbon fiber electrodes placed into the striatum of an anestitized rat quickly equilibrate, achieving a steady baseline signal (Phillips *et al* 2003a; Robinson *et al* 2003; Borland and Michael 2004; Heien *et al* 2005; Wightman *et al* 2007). In our hands baseline recordings from single barrel electrodes are stable on the order of minutes and contain signal fluctuations on the order of 0.1- 0.2 µM from baseline DA (Fig 2A). This result demonstrates the stability of the recording electrode and the constancy of the striatal extracellular fluid that the electrode samples.

When the same experiment is repeated with a picospritzer electrode containing an aCSF solution at the picospritzer tip, the baseline signal is not stable. These electrodes record extreme signal fluctuations vacillating more than 1 µM from baseline in a matter of seconds (Fig 3.2A). Cyclic voltammograms do not correspond to any identifiable redox species, e.g. dopamine (data not shown). Fluctuations in current are detected in all double barrel electrodes, but the timing and amplitude of fluctuation is not consistent, and thus smoothed by averaging (Fig 3.2A – black). These fluctuations suggest that either the carbon fiber or the extracellular concentration of electroactive species in the extracellular space is rapidly changing. However, the single barrel experiments demonstrate that the electrode and extracellular solution are stable. The only difference between the single and double barrel experimental setup is the presence of the picospritzer tip filled with aCSF at the site of the electrode in the double barrel experiment.

Therefore these data suggest that ions freely flow from the picospritzer tip into the extracellular solution, altering the extracellular fluid.

3.4.2 Exogenous drugs and evoked dopamine

A picospritzer tip filled with an aCSF solution containing either dopamine or raclopride was placed into the rat striatum. Once the stimulus electrode was placed over the medial forebrain bundle, the picospritzer electrode was lowered into a new recording location 0.5 mm below its previous location and the dopamine signal from a 3 s evoked stimulation was recorded. After 5 minutes a picospritzer ejection delivered the analyte solution into the extracellular space and the stimulation was repeated in order to assess the effect of locally administered drugs on evoked DA release.

The administration of exogenous DA in aCSF has no effect on the slow-type evoked response profile collected 30 s after the picospritzer ejection. This result is consistent with the finding that slow domain short term potentiation is lost when increases in extracellular DA are separated by at least 4 s (Fig 2.3C) (Moquin and Michael 2009). Also, these data demonstrate that aCSF has no effect on evoked DA. Raclopride ejected from the picospritzer increased the rate and magnitude of evoked DA, consistent with raclopride's action as a D2R antagonist (Fig 2.5A) (May and Wightman 1989a; Benoit-Marand *et al* 2007; Moquin and Michael 2009). Further, this result is consistent with reports implicating local D2R activation in evoked DA autoinhibition (Herr *et al* 2010).

3.4.3 Picospritzer leak alters evoked dopamine

In order to determine if the picospritzer leaks a physiologically relevant concentration of analyte the prior experiment was repeated sans the picospritzer ejection. A picospritzer electrode with

raclopride in the tip solution was lowered into a new striatal location and a 3 s stimulation evoked dopamine release. After 5 minutes the stimulation was repeated. At no point in the experiment was raclopride delivered into the extracellular space by a picospritzer ejection.

The second stimulus evoked a larger magnitude of dopamine, consistent with the profile of evoked release from uninhibited terminals (Fig 3.2D). The change in evoked dopamine is statistically identical to the change caused by the picospritzer ejection of raclopride (Fig 3.2E). These results clearly demonstrate that a physiologically relevant concentration of raclopride leaked from the picospritzer tip within 5 minutes, blocking D2R mediated autoinhibition (see figure legend of ANOVA details).

3.4.4 Segmented flow

In order to gain temporal control of analyte delivery, the analyte solution was separated from the tip solution by a segment of air (Fig 3A). While the tip solution still leaked, the air segment prevented the analyte from reaching the tip and leaking into the extracellular space. Picospritzer ejections compress the air bubble, allowing the analyte solution to mix into the tip solution (Fig 3B). After several ejections, the tip solution was primed with a high concentration of analyte (Fig 3C). Further picospritzer ejections delivered the analyte into the extracellular space.

Note that the air bubble remains in place in the picospritzer barrel and is not ejected into the brain. This is important because ejecting air onto the electrode surface breaks the electrochemical connection.

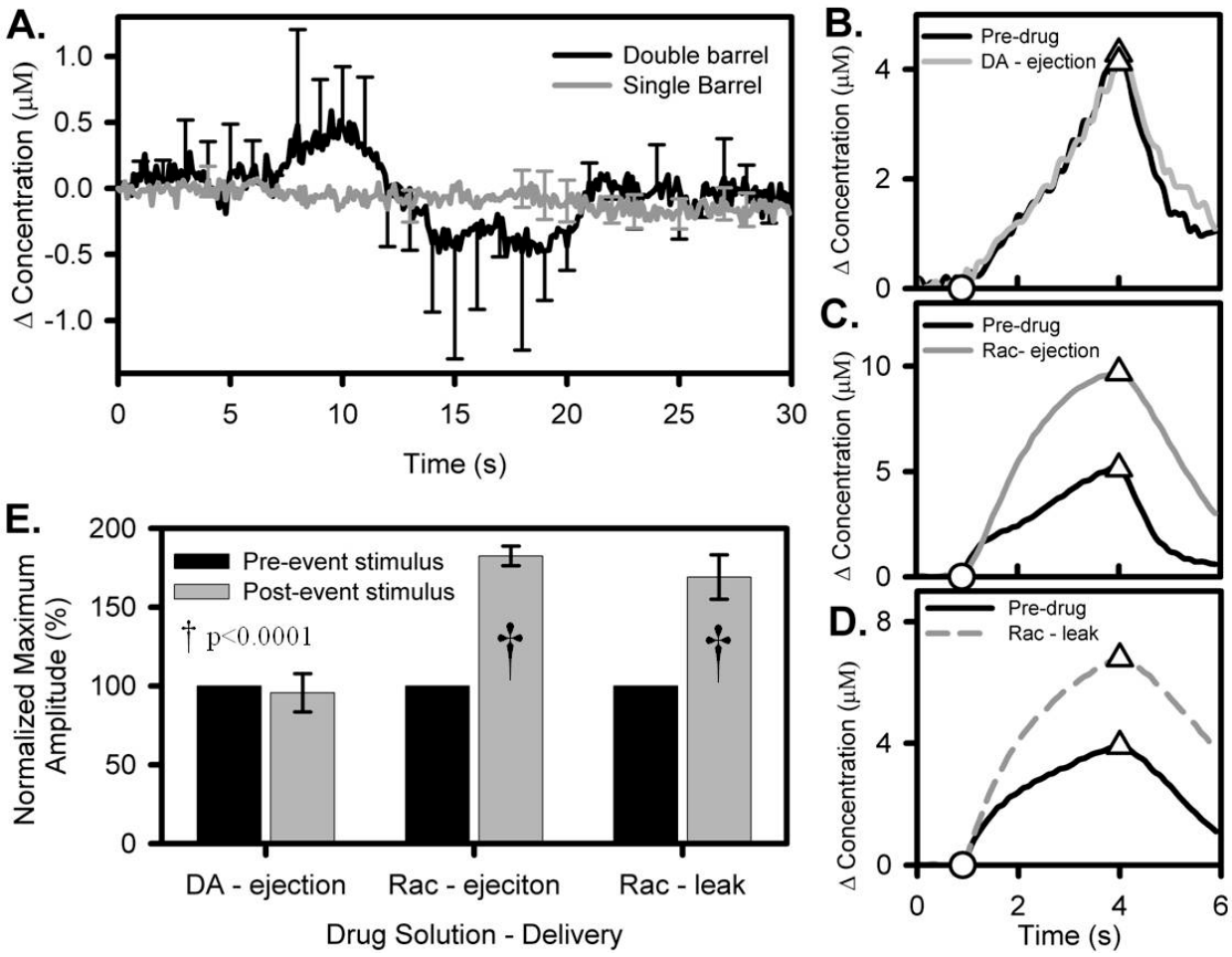

Figure 3.2 The picospritzer tip leaks.

(A) Averaged in vivo baseline recordings from single barrel carbon fiber electrodes and double barrel picospritzer electrodes containing an aCSF solution (n = 3). Standard deviations at 1 second intervals are plotted (vertical bars). Standard deviations less than 0.1 μM were not plotted for clarity. The baseline signal from a single barrel electrode is stable. The picospritzer electrode baseline is not stable. (B-C) 3 s evoked DA profiles five minutes before and 30 s after a picospritzer ejections. Circles and triangles represent the start and end of stimulation respectively. (B) Exogenous DA did not alter the profile of evoked release. (C) Locally delivered raclopride removed autoinhibition, consistent with its function as a D2R antagonist. (D) Raclopride alters the evoked response profile even if a picospritzer ejection is not performed. The picospritzer electrode containing raclopride is lowered into a new recording location immediately followed by a 3 s stimulation (black line). After five minutes the 3 s stimulation is repeated (grey dashed line). (E) The normalized change in maximum evoked amplitude of ejected and non-ejected (i.e. leaked) raclopride are nearly identical and statistically different than the effect of exogenous dopamine (n=3, one-way ANOVA, tukey post-hoc, $F_{(5,12)}= 31.4$, † $p < 0.001$).

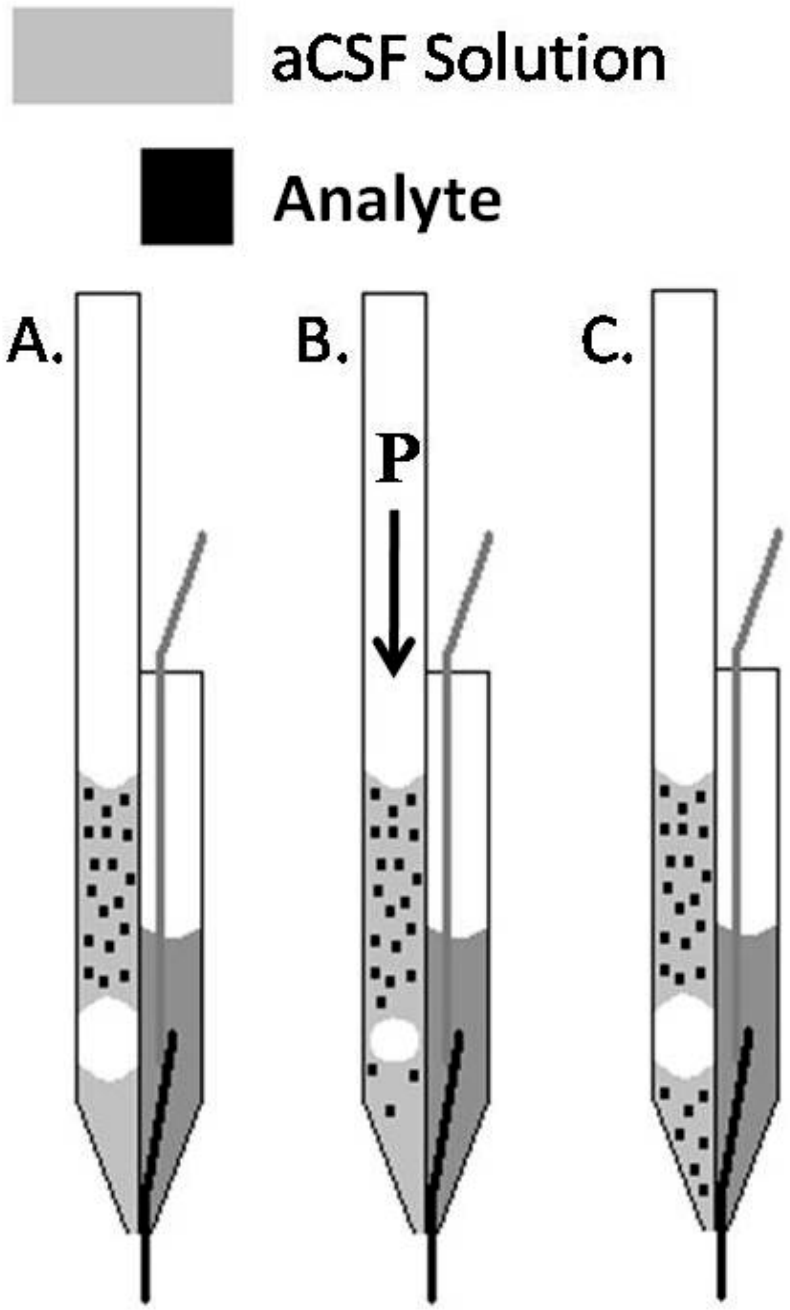

Figure 3.3 Schematic of a picospritzer electrode utilizing segmented flow.

(A) The picospritzer barrel was filled with two separate solutions; an aCSF solution (grey) at the tip, and an analyte solution (grey with black squares) backfilled into the barrel. An air buble (~1mm in length) separated the two solutions. (B) Air pressure from the Picospritzer compresses the air bubble allowing the analyte solution to mix with the aCSF solution. (C) Following several ejections the tip solution is loaded with the analyte. Further picospritzer ejections will deliver the analyte along with aCSF.

3.4.5 Temporal control of picospritzer ejections

A solution of aCSF was front filled into the picospritzer tip via capillary action. An analyte solution of DA and aCSF was backfilled into the picospritzer barrel, leaving an air bubble to segment the two solutions. The electrode was placed in a beaker of PBS. Using fast scan cyclic voltammetry, the carbon fiber electrode monitored changes in current during a series of picospritzer ejections (30 psi, 0.5 s). The change in current over time is plotted at two potentials in each experiment; a non-DA redox potential (Fig 3.4A), and DA's maximum oxidation potential (Fig 3.4B). The start of each picospritzer ejection is marked by a black circle.

Differences in ionic concentrations of the aCSF solution in the barrel and the PBS solution in the beaker generate a change in current at the electrode surface during all picospritzer ejections (Fig 3.4A). Every picospritzer ejection caused a similar increase in current at the non-DA redox potential, indicating that each picospritzer ejection expels a similar amount of solution into the beaker. These current changes did not occur at DA's oxidation or reduction potential, and thus are not associated with the delivery of DA into the beaker.

At the DA oxidative potential (~650 mV) the current did not increase during the first three ejections (Fig 3.4B). As a change in the non-DA redox potential was recorded, initial picospritzer ejections deliver aCSF, but not DA, into the beaker. DA is detected during latter picospritzer ejections (Fig 3.4B). The DA oxidation current continues to rise with each ejection, demonstrating that the DA solution continues to mix into the tip solution increasing the DA concentration at the tip.

Background subtracted cyclic voltammograms from the 2^{nd} and 6^{th} picospritzer ejections confirm that DA is delivered during the latter, but not initial, ejections (Fig 3.4C and D). While there are notable fluctuations in the background subtracted voltammotram at the 2^{nd} ejection, the voltammogram lacks discernable DA oxidation or reduction peaks (Fig 3.4C). These current

changes are associated with differences in the ionic concentrations of the two buffer solutions. The background subtracted cyclic voltammogram from the 6th ejection has prominent DA oxidation and DA-o-quinone reduction peaks (Fig 3.4D). These data indicate that several picospritzer ejections are required to load DA into the tip solution. Prior to mixing DA is separated from the tip solution, and thus not ejectable. It should also be noted that the 6th cyclic voltammogram also contains the characteristic features associated with the ejection of aCSF into PBS. Note the peak at 250 mV during the forward sweep and the rise in current during the potential return from -500 to 0 mV. These features can be removed by background subtracting the 2nd voltammogram from the 6th.

These results are reproducible across several different electrodes (Fig 3.4E). All electrodes utilizing segmented flow require several Picospritzer ejections before the analyte reaches the picospritzer tip solution (see figure legend of ANOVA details). The DA oxidation current consistently increases during continued ejections as the concentrated DA solution continues to mix into the tip solution. The DA current levels off as the concentration of DA in the tip solution approached the analyte solution concentration (data not shown).

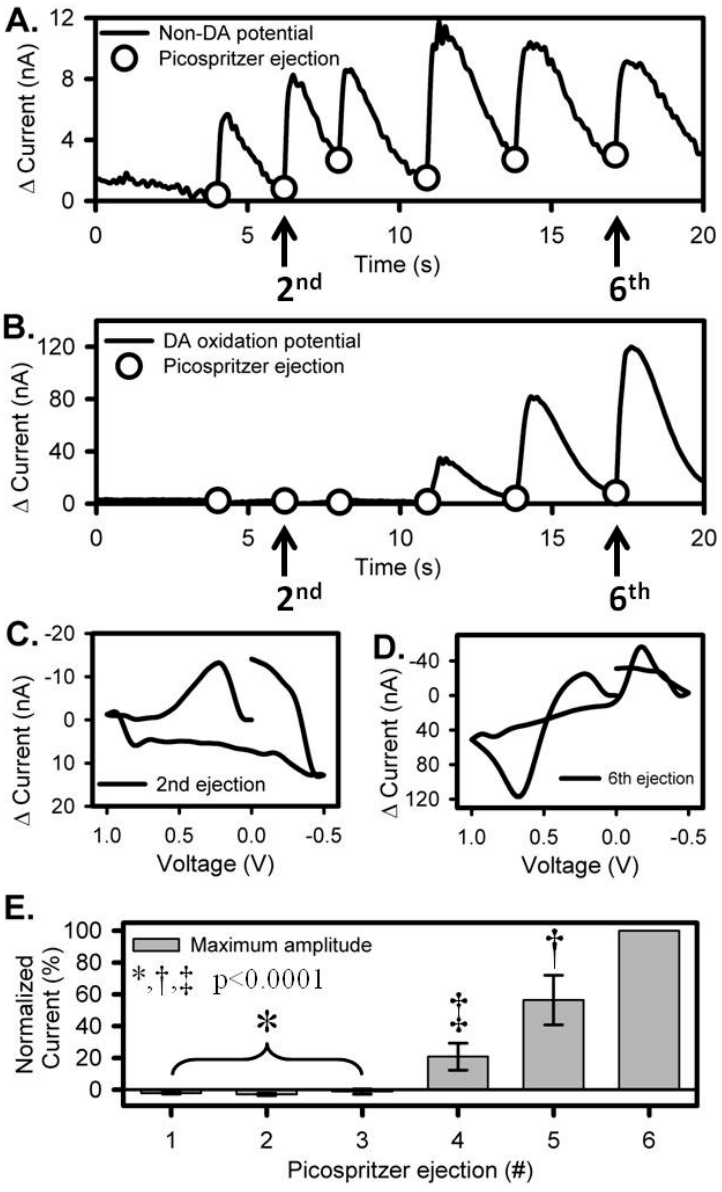

Figure 3.4 Controlled drug release from the picospritzer using segmented flow.

A picospritzer electrode containing a solution of aCSF and DA is placed into a beaker of PBS. (A) The current change at an aCSF/PBS-sensitive, DA-insensitive potential (250 mV in this example) verify ejections of aCSF solution into the beaker during each picospritzer event (circles). (B) Current change at DA's oxidative potential show that DA was not in the aCSF solution ejected during the first three picospritzer events, but did mix into the tip solution during latter ejections. (C, D) Cyclic voltammograms recorded during the 2nd and 6th picospritzer ejection respectively. The 2nd voltammogram has a noticeable peak at 250 mV (due to differences in the PBS and aCSF solution), but does not have any discernable DA oxidation or reduction peak. The 6th voltammogram has classic DA redox peaks. Notice that the aCSF/PBS peak at 250 mV remains. (E) The delayed release of DA from a picospritzer utilizing segmented flow is reproducible (n=3, one-way ANOVA, tukey post-hoc, $F_{(5,12)}$= 98.9, *,†.‡ $p < 0.001$).

3.4.6 Segmented flow in vivo

In vivo, temporal control of analyte delivery is obtained using the picospritzer electrode and segmented flow. In this example the tip was filled with aCSF and the barrel was backfilled with an aCSF solution containing DA. The two solutions were separated by an air bubble. The picospritzer electrode was place in the striatum of an anesthetized rat and the DA oxidation current was monitored during picospritzer ejections (20 psi, 0.5 s).

A current change at the DA oxidation potential is noticed from the first picospritzer ejection (Fig 5). However, cyclic voltammograms recorded during these ejections did not have discernable DA oxidation or reduction peaks (Fig 5 inset). Thus, this current increase is associated with differences in the ionic concentration of the extracellular space and aCSF solution and not with the ejection of DA.

Several picospritzer ejections are required to expel DA into the extracellular space (Fig 5). This result demonstrates that segmented flow works in vivo. In this case, electrode post-calibration revealed that an extremely large DA concentration (~ 100 μM) was ejected into the striatum. This increase in concentration is quite large compared to physiological fluctuations in DA concentration (Garris *et al* 1994; Benoit-Marand *et al* 2001; Phillips *et al* 2003b; Robinson *et al* 2003; Heien *et al* 2005). The concentration of DA, the ejection time, and ejection pressure can be adjusted in order to deliver smaller, physiologically relevant concentrations of DA.

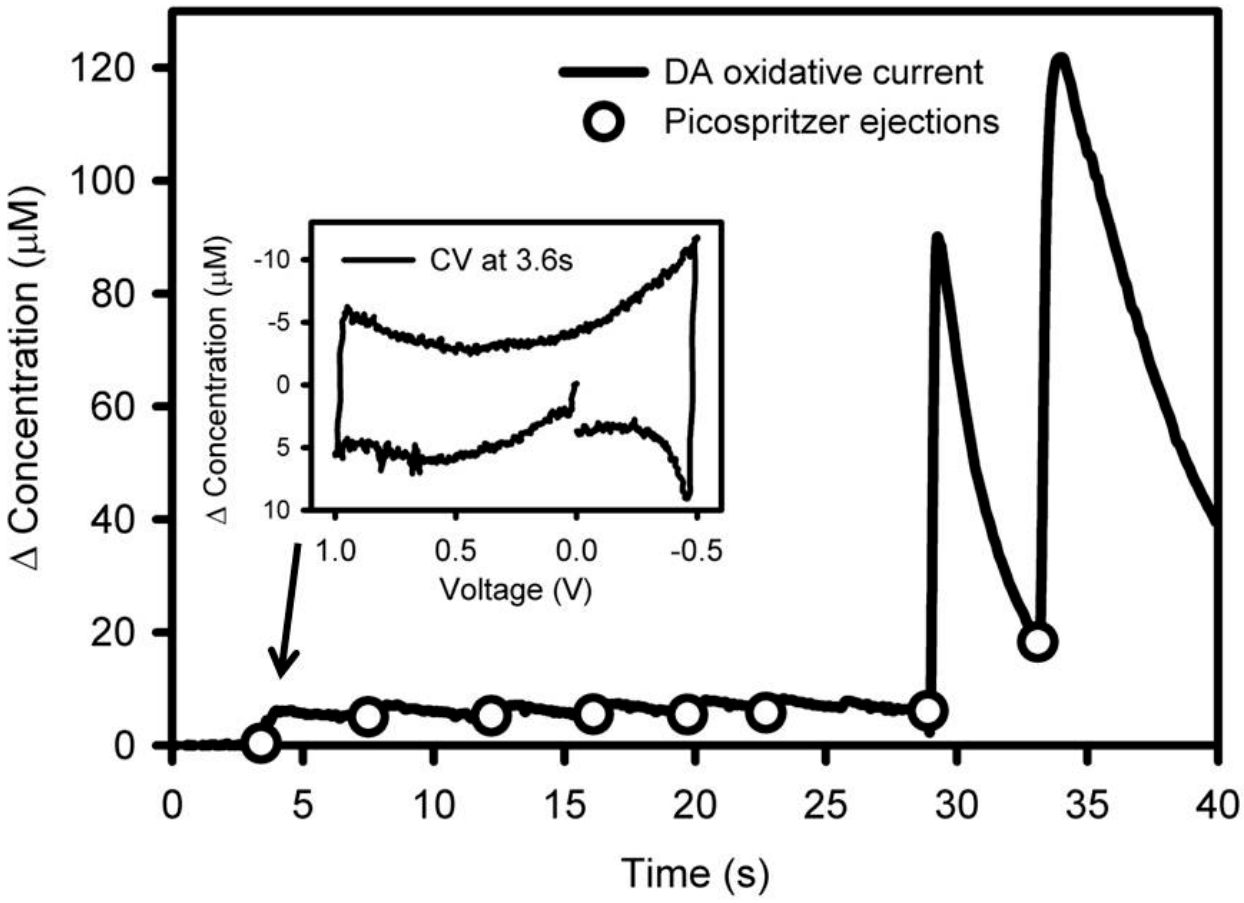

Figure 3.5 Segmented flow controls DA release in vivo.

Current change at DA's oxidative potential show that several picospritzer ejections (circles) are required to load DA into the tip solution before it can be ejected into the extracellular space. There is an increase in current during each picospritzer ejection at this potential. However, a cyclic voltammogram from the first ejection (inset) shows that this increase does not correspond to DA.

3.5 DISCUSSION

In this study we discover that the tip of picospritzer leaks buffer solution and analytes. This issue was discovered during the implementation of a dual function picospritzer electrode device capable of delivering analytes of interest and electrochemical detection in the same location. This device places the detection electrode at the site of analyte delivery, which allows for electrode optimization, and minimizes diffusional distortion of the analyte. This issue was previously not identified because other experimental setups place the detection electrode 100 to 300 µm away from the picospritzer tip (Cass *et al* 1993; Cragg *et al* 2001; Daws and Toney 2007; Makos *et al* 2009).

The uncontrolled release of analyte into the extracellular space is resolved using segmented flow. The analyte solution is separated from the tip solution with an air bubble. Initial picospritzer ejections compress the air bubble separating the two solutions allowing the analyte to mix into the tip solution. Once in the tip solution the analyte is delivered during further picospritzer ejections. While segmented flow does not prevent the picospritzer tip from leaking, it does control the time course of analyte delivery.

3.5.1 Qualifying the picospritzer leak

In this study we demonstrate picospritzer tip leakage two ways. First we monitor in vivo baseline signals from signal barrel electrodes and double barrel picospritzer electrodes filled with aCSF (Fig 3.2A). The baseline signal from the picospritzer electrode is clearly less stable than the single barrel electrode. The baseline signal instability of the picospritzer electrode indicates that either the electrode or the extracellular environment is not stable. Single barrel electrodes in both this and other experiments have stable baselines on the minute time scale (Sabeti *et al* 2002;

Borland and Michael 2004; Wang *et al* 2010). The stability of the single barrel electrode indicates that both the electrode surface and the ionic concentration of the extracellular fluid are constant during the experimental procedure. Figure 3.5 demonstrates that the aCSF solution, while an accurate mimic of extracellular brain fluid, is not an exact match. Picospritzer ejections of aCSF in vivo create a large current change due to variations in the ionic concentration of the two solutions. Thus, the unstable baseline detected by the picospritzer electrode appears to be an artifact of aCSF solution leaking from the tip.

The second way we detect leaking from the picospritzer tip is through the actions of the D2R antagonist raclopride. The D2R is an autoinhibitory receptor that suppresses DA release upon activation (Garris *et al* 1993; Benoit-Marand *et al* 2001; Kita *et al* 2007; Moquin and Michael 2009). Systemic intraperitoneal injections of raclopride block D2R function, removing the delayed onset of evoked release in slow domains (Fig 2.5A)(Moquin and Michael 2009) and the short term depression of evoked release in hybrid responses (Fig 4.1C) (Moquin and Michael 2011). These results are reproducible when raclopride is locally administered via picospritzer ejections (Fig 3.2C) or iontophoresis (Herr *et al* 2008), implicating pre-synaptic D2Rs in autoinhibition. The effect of raclopride on evoked DA is identical even when raclopride is not ejected from the picospritzer tip (Fig 3.2D). This result demonstrates that a physiologically relevant concentration of raclopride leaks from the electrode tip, blocking D2R activity. Thus the picospritzer does not have temporal control of analyte release, making the assessment of the effects of drugs on the dopamine system impossible.

3.5.2 Controlling analyte release with segmented flow

Figure 3.3 schematically describes how segmented flow controls the time course of analyte reaching the picospritzer tip. Briefly, the analyte is separated from the tip solution by an air

bubble. The picospritzer tip still leaks, but the analyte is not in the tip solution so only aCSF buffer enters the extracellular space. The ejection of aCSF does not change the profile of evoked DA release (Fig 3.2B). Also, aCSF does not change the DA clearance rate in slow domains (Moquin and Michael 2011). In fact the clearance rate of evoked DA and exogenous DA is identical in slow domains (Fig 4.2E). Thus, aCSF leaking does not alter the function of DA neurons.

Cyclic voltammograms recorded during initial picospritzer ejection confirm that the analyte, DA in this example, is not in the tip solution (Fig 3.4B and 3.5). These initial ejections also serve to compress the air bubble separating the two solutions. The ejection of analyte into the extracellular space during latter ejections confirms that the compressed air bubble allows the analyte solution to mix into the tip solution (Fig 3.4B and 3.5).

The addition of segmented flow allows the picospritzer electrode to temporally control analyte release, adding a new tool to the in vivo study of dopaminergic activity. Previously, experimental designs were limited by the inability to move both the picospritzer tip and detection electrode while maintaining the same distance of separation (Sabeti *et al* 2002; Wang *et al* 2010). This limitation made local administration of both permeable and non-permeable analytes following electrode optimization near impossible. Optimization increases the distance between the electrode and picospritzer tip, which in turn magnifies spherical diffusion. If the electrode is optimized then only permeable analytes can be administered by intraperitoneal or intravenous injections. The double barrel picospritzer electrode moves both components in tandem so distance between the electrode and picospritzer tip remains the same during electrode optimization. Further, segmented flow prevents the analyte from reaching the tip during optimization. Thus this device can be optimized into the desired DA domain, the pre-drug

response recorded, the analyte delivered into local environment, and the analyte effect on the local DA system measured.

3.5.3 Diffusion

Experimental setups using separate analyte delivery and detection electrode devices leave a 100 to 300 µm gap between the two devices (Cass *et al* 1993; Cragg *et al* 2001; Sabeti *et al* 2002; Daws and Toney 2007; Wang *et al* 2010). At this distance analytes reach the electrode via diffusion. Diffusionally distorted signals are initially delayed, then accelerate, and overshoot after the end of analyte delivery (Engstrom *et al* 1988; Sabeti *et al* 2002). Diffusional distortion also limits the amount of analyte that reaches the detection electrode. Analytes ejected from a point source diffuses spherically into the surrounding tissue, exponentially decreasing in concentration (Bard and Faulkner 2001). In order to obtain a specific concentration of analyte some distance away from the point source, a significantly larger concentration is required at the source. In the above example a 200 µM concentration was delivered into the extracellular space 200 to 300 µm away from the detection electrode in order to obtain a 1 µM DA concentration at the electrode surface (Sabeti *et al* 2002). The effects of this supra-physiological concentration of DA could alter the surrounding tissue, changing DA terminal function.

The placement of the picospritzer tip at the site of the detection electrode limits diffusion such that DA is immediately detectable at the onset of the picospritzer ejection (Fig 3.5). The DA response is both rapid and linear without acceleration or overshoot. Because there is limited diffusion, the analyte concentration detected at the site of the electrode approximates the concentration of analyte ejected. Therefore, physiologically relevant concentrations of analyte and smaller volumes of buffer solution are delivered into the extracellular space.

Spherical diffusion limits the distance analytes migrate from the tip (Bard and Faulkner 2001). Low concentrations of analytes ejected or leaked from the picospritzer tip will not reach the detection electrode at a detectable concentration. For this reason experiments placing the analyte delivery and detection electrode apart from each other were unable to detect the leak (Cass *et al* 1993; Sabeti *et al* 2002; Borland and Michael 2004; Wang *et al* 2010). Once the picospritzer electrode and tip are adjacent, the leak and its physiological impact become obvious (Fig 3.2). Spherical diffusion of an analyte prevents physiologically significant concentrations of analyte reaching the extracellular space around a detection electrode that is outside of the leak's spherical diffusion radius. Therefore, the leak is not directly impacting the DA neurons in experimental setups that separate the two devices. Thus, the electrodes in these experiments are sampling from initially unaltered tissues (Cass *et al* 1993; Cragg *et al* 2001; Sabeti *et al* 2002; Borland and Michael 2004; Daws and Toney 2007; Wang *et al* 2010).

3.5.4 Background subtraction

The ionic concentration of aCSF and the extracellular fluid are not identical. Ejection of aCSF into the extracellular space at the site of the detection electrode changes the ionic concentration, altering the redox current (Fig 3.2C and 3.5). These current changes are different in each experiment and can occur at dopamine's oxidation potential (Fig 3.5). Thus, current changes at 650 mV may not be due solely to an increase in the DA concentration (Fig 3.5 inset). As non-DA current increases occur during each picospritzer ejection (Fig 3.2A), they also occur during the ejection of DA. Therefore, changes in amplitude during a picospritzer ejection are a product of DA oxidation and ionic concentration differences between the buffer solutions. The non-DA current changes can be removed by subtracting cyclic voltammograms during the initial picospritzer ejections (aCSF only) from cyclic voltammograms during DA ejection (aCSF and

DA) (Fig 3.2C and D). This background subtraction method allows for an accurate measurement of DA delivered during each picospritzer ejection.

3.5.5 Failed devise designs

We attempted several other methods to prevent picospritzer tip leakage and gain temporal control of analyte release. In one set of experiments oil was substituted for the air bubble as a means to separate the tip and analyte solutions. Because oil is not compressible, the tip and analyte solutions did not mix during picospritzer ejections. So the analyte was never in an ejectable state. Further, the oil did not prevent leaking.

Smaller diameter picospritzer tips were pulled to minimize leakage. The tighter tips required higher pressures (>30 psi) to eject solution into the extracellular space. Following these high pressure ejections evoked DA responses were suppressed or disappeared altogether, suggesting that the ejection damaged the local terminal field. This result is not surprising as high pressure picospritzer ejections are used to create fluid percussion injuries, a traumatic brain injury model (Thompson *et al* 2005; Frey *et al* 2009). Note that low pressure picospritzer ejections of solution did not alter evoked DA response (Fig 3.2B).

In another design, the analyte solution was backfilled into the picospritzer leaving a pocket of air at the picospritzer tip. This setup prevented both analyte and aCSF leakage. The initial picospritzer ejection moved the analyte solution to the tip, delivering air into the extracellular space. Latter ejections deliver the analyte. Similar to high pressure liquid ejections, evoked DA responses following the initial air ejection were suppressed or undetectable compared to pre-ejection responses, suggesting that the air bubble damaged the neuron.

3.5.6 Segmented flow and leaking

Segmented flow gains temporal control over the release of analytes into the extracellular space. However, this design does not prevent picospritzer leakage, as the baseline signal is still very unstable (Fig 3.5). Therefore, once the analyte is in the tip solution it is free to leak into the extracellular space. As the concentration of analyte leaked can be physiologically relevant, this method cannot be used to deliver multiple doses of analyte and varying concentrations. Despite this limitation the picospritzer electrode can still be used to assess changes in neuronal activity before and after the local administration of analytes.

4.0 AN INVERSE CORRELATION BETWEEN APPARENT RATE OF DOPAMINE CLEARANCE AND TONIC AUTOINHIBITION IN SUBDOMAINS OF THE RAT STRIATUM: A POSSIBLE ROLE OF TRANSPORTER-MEDIATED DOPAMINE EFFLUX

4.1 ABSTRACT

The dopaminergic terminal field in the rat striatum is compartmentalized into sub-domains that exhibit distinct dynamics of electrically evoked dopamine release. The fast striatal domains, where dopamine release is predominantly vesicular, exhibit conventional dopaminergic activity. However, vesicular dopamine release is tonically autoinhibited in the slow domains, which suggests that dopamine reaches the autoreceptors via a non-vesicular route. Hence, it appears that the domains use distinct mechanisms to regulate the basal dopamine concentration available to activate, or not, presynaptic autoinhibitory receptors. However, direct detection of local variations in tonic extracellular dopamine concentrations is not yet possible. So, the present study employed voltammetry to test the hypothesis that the apparent rate of dopamine clearance from the extracellular space should be domain-dependent. The apparent rate of dopamine clearance is equal to the difference in the rates of dopamine release and uptake that determine extracellular dopamine concentrations. This study confirms that the apparent rate of dopamine clearance is slower in the slow striatal domains where vesicular dopamine release is tonically autoinhibited. These findings support the view that the basal concentration in slow domains is maintained by a non-vesicular release process, possibly transporter-mediated efflux.

4.2 INTRODUCTION

The dopamine (DA) transporter (DAT), a chloride-dependent member of the SLC6 family of neurotransmitter:sodium symporters, intimately contributes to the regulation of extracellular DA concentrations in the brain (Iversen 1971; Amara and Kuhar 1993). Understanding DAT function is significant because it is targeted by a variety of antidepressant and psychoactive drugs (Torres *et al* 2003; Mandt and Zahniser 2010). Prior studies have established that DAT function is dynamically regulated by protein trafficking, interactions with the DA D2 receptor (D2R), protein-lipid interactions, membrane voltage, and ligand and substrate binding (Ingram *et al* 2002). DAT's primary function appears to be reuptake of DA from the extracellular space, but it also releases DA in the presence of exogenous DA-releasers, such as amphetamine (Sulzer *et al* 1993). The present study, however, contributes to an emerging body of evidence suggesting that the DAT may also release DA in the absence of amphetamine-like drugs.

In vitro studies have demonstrated that striatal terminals release DA via DAT-mediated DA efflux (DDE) (Cheramy *et al* 1986; Lonart and Zigmond 1991; Leviel 2001). In vivo studies likewise suggest that DDE is functionally relevant within certain specific subdomains of the rat striatum (Moquin and Michael 2009; Wang *et al* 2010). Voltammetric recordings show that the striatum is compartmentalized into spatial domains that yield distinct fast-type and slow-type responses during electrical stimulation of midbrain DA axons. An autoinhibitory tone on DA terminals contributes to determining whether a given recording site corresponds to a fast or slow domain. The autoinhibitory tone is minimal in fast domains (Garris *et al* 1993; Benoit-Marand *et al* 2001) but intense in slow domains (Moquin and Michael 2009; Wang *et al* 2010), which suggests that the domains operate under different basal DA concentrations. Since electrically evoked DA release, a vesicular event, is autoinhibited in the slow domains, it appears that the

DA responsible for the autoinhibition reaches the extracellular space via a non-vesicular route. This concept is supported by the finding that the striatum contains a tonic pool of extracellular DA that is both tetrodotoxin-insensitive and nomifensine-sensitive (Borland and Michael 2004), which are classic hall-marks of DDE.

This emerging evidence that DDE has a functional role in the striatum is at odds with a considerable body of literature. According to microdialysis, for example, DA release is exclusively vesicular (Westerink *et al* 1987; Santiago and Westerink 1990) except in the presence of DA releasers (Carboni *et al* 1989; Schmitz *et al* 2001). However, microdialysis is an averaging technique (Bungay *et al* 2007) that does not detect spatially localized concentration differences. At present, no technology has the demonstrated ability to directly detect localized variations of basal extracellular DA concentrations. For this reason, the present study was designed to examine this issue via an alternate route.

We tested the hypothesis that the fast and slow striatal domains should exhibit distinct values of the apparent rate of DA clearance, V_{app}, a quantity that depends on the rates of DA uptake and release that determine the extracellular DA concentration (Chen 2005; Michael *et al* 2005; Dreyer *et al* 2010). We used voltammetry to quantify V_{app} in vivo after electrically evoking the release of endogenous DA (Wu *et al* 2001) and after ejecting exogenous DA from a pipet (Cass *et al* 1993; Kiyatkin *et al* 2000; Sabeti *et al* 2002). Our findings confirm that the rat striatum exhibits the hypothesized regional variation in V_{app} and, as expected, that V_{app} is significantly slower in those striatal domains where extracellular dopamine concentrations appear to be sufficiently high to tonically autoinhibit vesicular DA release.

4.3 METHODS AND MATERIALS

4.3.1 Carbon fiber microelectrodes

Electrodes were constructed by inserting 5-μm diameter carbon fibers (T650, Cytec Carbon Fibers LLC., Piedmont, SC) into single barrel borosilicate glass capillaries (0.4 mm ID, 0.6 mm OD, A-M systems Inc., Sequim, WA), pulling the capillaries to a fine tip with a vertical micropipette puller (Narishige, Los Angeles, CA), backfilling the tubes with a low-viscosity epoxy (Spurr Epoxy, Polysciences Inc., Warrington, PA), and connecting the fiber to a hook-up wire with a droplet of mercury. The exposed fibers were cut to 400 μm and sonicated in reagent-grade isopropyl alcohol (Sigma, St. Louis, MO) containing activated carbon (Fisher Scientific, Fair Lawn, NJ) for 30 minutes (Bath *et al* 2000).

4.3.2 Fast scan cyclic voltammetry

Voltammetric recording was performed by fast scan cyclic voltammetry using an EI 400 high-speed potentiostat (originally constructed by Ensman Instruments but presently available from ESA Inc., Chelmsford, MA) and the "CV Tar Heels v4.3" software package (courtesy of Dr. Michael Heien, present address Department of Chemistry, University of Arizona, Tucson AZ, USA). The rest potential was 0 V vs Ag/AgCl and the voltammetric waveform consisted of three linear potential sweeps to +1 V, -0.5 V, and back to 0 V at a sweep rate of 400 V/s. The scans were repeated at 10 Hz. The DA oxidation current was recorded between 0.5 and 0.7 V during the first sweep. DA voltammograms were obtained by background subtraction.

4.3.3 Animals

Male Sprague-Dawley rats (250-350g) (Hilltop, Scottsdale, PA) anesthetized with isoflurane (2% by vol.) and placed in a stereotax (David Kopf Instruments, Tujunga, CA) with the incisor bar raised 5 mm above the interaural line (Pellegrino *et al* 1979). A heating blanket (Harvard Apparatus, Holliston, MA) maintained body temperature at 37^{o}C. A twisted, bipolar, stainless steel stimulating electrode was placed over the medial forebrain bundle (from bregma: 1.6 mm lateral, 2.2 mm posterior, 8.0 mm below dura) (Pellegrino *et al* 1979). A carbon fiber microelectrode was placed in the ipsilateral striatum (from bregma: 2.5 mm lateral, 2.5 mm anterior, initially 4.5 mm below dura) (Pellegrino *et al* 1979). The final position of the stimulating electrode was determined by lowering it until evoked DA release was observed in the striatum: this is a well-established protocol for identifying effective midbrain stimulus sites (Ewing *et al* 1983; Kuhr *et al* 1984; Heien *et al* 2005). As appropriate, the striatal recording location was optimized to permit detection of hybrid evoked responses (explained further in the Results section): the optimization procedure involved lowering the carbon fiber electrode deeper into the striatum until a hybrid stimulus response was observed.

4.3.4 Stimulation

Electrical stimulation was delivered as an optically isolated, constant-current, biphasic waveform (frequency 60 Hz, pulse height 270 μA, pulse width 2 ms). The stimulus duration was 200 ms (12 pulses) during experiments involving fast-type responses, 3 s during experiments involving slow-type responses, and 3-5 s during experiments involving hybrid responses.

4.3.5 Picospritzer system

Pressure-ejection of exogenous substances (raclopride and dopamine) into the extracellular space of the striatum was by means of a double-barreled micropipet: one barrel contained a carbon fiber microelectrode and the other was used for pressure-ejection (Fig 3.1). The open barrel was pre-loaded with either 25 mM DA or 2 mM raclopride dissolved in artificial cerebral spinal fluid (1.2mM Ca^{2+}, 152mM Cl^{-}, 2.7mM K^{+}, 1.0mM Mg^{2+}, 145mM Na^{+}, pH 7.4). The solution was pressure ejected (~20 psi) with a Picospritzer III (Parker Hannifin, Fairfield, NY). In the case of experiments involving exogenous DA, the ejection time was adjusted between 0.1 and 0.5 s so that the amplitude of the voltammetric response to exogenous DA matched the amplitude of the electrically evoked response at the same recording location (see Results section for further details). In the case of experiments involving the pressure-ejection of raclopride, the ejection lasted for 2 s and occurred 5 min prior to the next electrical stimulus.

4.3.6 Electrode calibration

Microelectrode DA calibration was performed after the microelectrodes were removed from brain tissues and mounted into a gravity-fed flow-through cell. Conversion of in vivo oxidation currents to DA concentrations was based on post-calibration results. Standard solutions were prepared by dissolving DA in artificial cerebrospinal fluid.

4.3.7 Drugs

Drugs were dissolved in phosphate buffered saline (155mM Na^{+}, 155mM Cl^{-}, 100mM phosphate, pH 7.4). Nomifensine maleate (Sigma Aldrich, St. Louis, MO) was administered at a dose of 20 mg/kg i.p. Raclopride tartrate (Sigma Aldrich, St. Louis, MO) was administered at a dose of 2 mg/kg i.p.

4.3.8 Modeling and statistics

DA clearance profiles were constructed as follows: The time of the first voltammetric measurement after the termination of an electrical stimulus or pressure ejection was defined as t = 0 (x-axis). The time required for the completion of DA clearance after electrical stimulation or pressure ejection was identified by using an Excel spreadsheet to determine the linear regression slope of sequential 5-point line segments on the clearance profile. The midpoint of the first line segment with a slope below -0.1μM/s was taken as a measure of a) the extracellular lifetime of DA and b) the zero-point of the change in DA concentration (y-axis): this procedure eliminated contributions from occasional small baseline shifts that occurred between the onset of the stimulus and the completion of DA clearance.

The DA clearance profiles for each group were averaged together (n=4) and compared using two-way ANOVA (1^{st} factor – group; 2^{nd} factor – time point) and a Tukey post hoc test. Extracellular DA lifetimes were averaged together (n=4 per group) and compared using one-way ANOVA and a Tukey post hoc test. Throughout this study, the intensity of the stimulus was sufficient to cause the initial segment of the clearance profile to be linear (r^2>0.96): the initial linear clearance rates were averaged (n=4 per group) and compared using one-way ANOVA and a Tukey post hoc test. In all figures, the error bars indicate s.e.m.

4.4 RESULTS

4.4.1 Voltammetric identification of fast and slow DA domains

Voltammetric recordings of electrically evoked DA release in the rat striatum yield distinct responses, classified as fast-type and slow-type according to previously explained criteria (Moquin and Michael 2009). The slow-type responses are characterized by a delay in the onset

of evoked release when the stimulus begins and short-term facilitation of release with continued stimulation (Fig 4.1A). Systemic administration of raclopride, a selective D2-antagonist, abolishes the delay in the onset of evoked release (Fig 4.1A), confirming that the slow-type response is a consequence of an autoinhibitory tone on DA terminals. This tone is established prior to the onset of the stimulus, indicating that it derives from non-evoked DA release.

The position of the voltammetric electrode can be optimized to locate recording sites that yield hybrid responses (Fig 4.1B) with a fast-type initial component and a subsequent slow-type component. The fast-type responses are characterized by evoked release that starts without delay and then exhibits short-term depression, which sometimes produces a 'dip' between the fast and slow components of the hybrid response (Fig 4.1B). The short-term depression is attributable to the rapid onset of autoinhibition caused by the evoked DA release (Dugast *et al* 1997; Benoit-Marand *et al* 2001; Phillips *et al* 2002). The initial component sometimes appears as a leading shoulder on the response (Fig 4.1C), rather than a stand-alone peak (Fig 4.1B), because different hybrid sites have different fast and slow contributions. Pressure-ejection of raclopride from a pipet adjacent to the microelectrode (Fig 3.1) had no effect on the amplitude of the initial fast component but significantly increased the amplitude of the subsequent slow component (Fig 4.1C and 2d: see figure legend for ANOVA results). Because the fast component was refractory to raclopride, it appears to derive from DA terminals that are not autoinhibited prior to the stimulus. This finding is consistent with previous reports of fast evoked signals refractory to D2R antagonists (Garris *et al* 1994). These results, which show that autoinhibitory D2Rs are present and functional in both fast and slow domains, point to the tonic DA concentration present in the extracellular space prior to the stimulus as a principle determinant of the autoinhibitory tone.

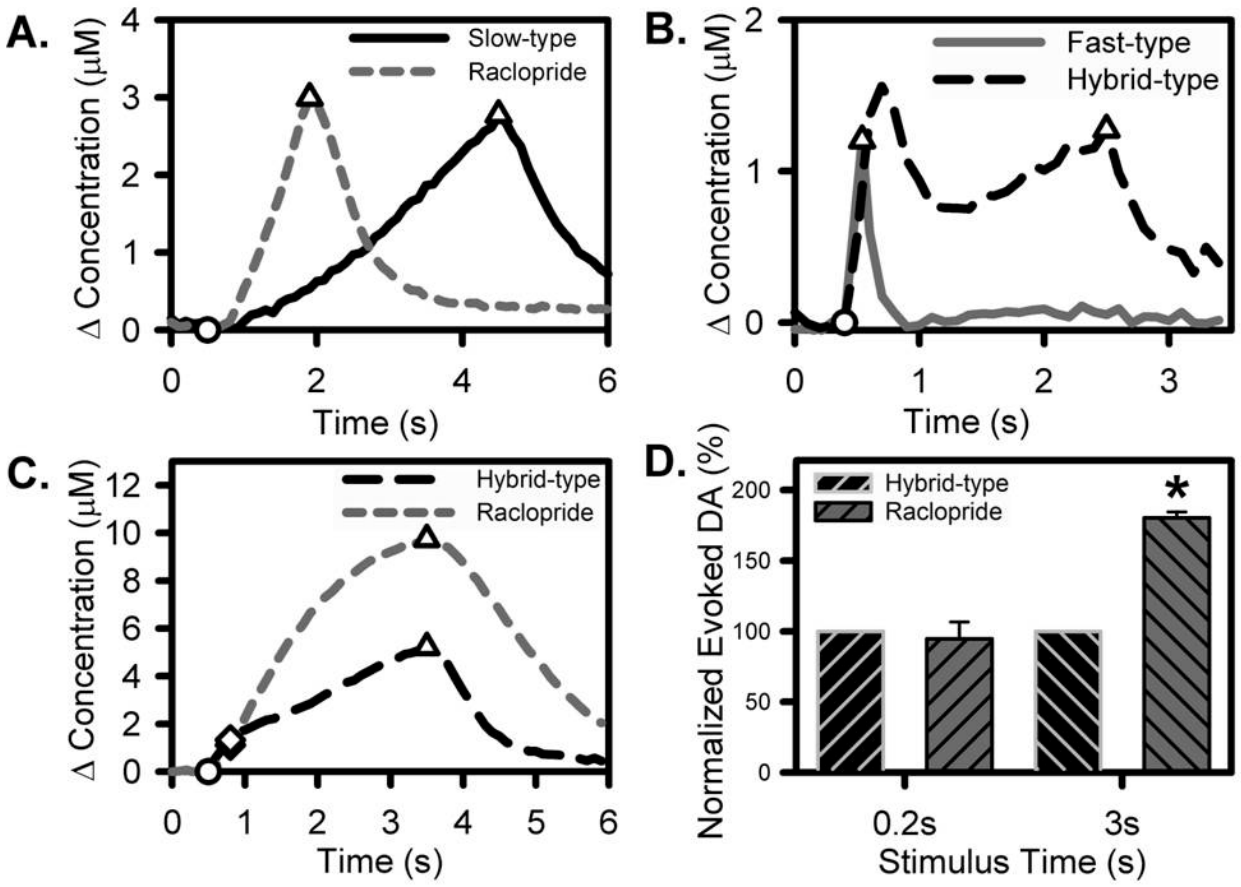

Figure 4.1 Fast and slow domains revealed by voltammetric recordings of evoked DA release.

(A) In slow domains, evoked DA release is delayed and exhibits facilitation as the stimulus proceeds. Raclopride (2 mg/kg i.p.) abolishes the delay, confirming the role of autoinhibition. (B) When the recording electrode straddles both fast and slow domains, hybrid responses are obtained. The initial component exhibits no delay in evoked release: a robust DA signal is detected on the first voltammetric measurement, which occurs 100 ms after the onset of the stimulus. The initial component exhibits depression as the stimulus continues, which is attributable to the onset of autoinhibition in the fast domain caused by the evoked rise in DA concentration. The fast component is isolated by limiting the stimulus duration to 200 ms (gray line). (C) Local picospritzer ejections of raclopride confirm the role of autoinhibition on the hybrid-type responses curve profile. (D) In hybrid-type responses, raclopride did not alter the initial amplitude of evoked DA following the first 0.2s of stimulation (n=4, One-way ANOVA, $F_{(1,6)}$=0.202, p=0.67), but significantly increased the amplitude following 3s of stimulation (n=4, One-way ANOVA, $F_{(1,6)}$=353.1, † p<0.0001).

4.4.2 Apparent DA clearance rates in fast and slow striatal domains

During the remainder of this study, fast-type responses were obtained by optimizing the electrode position to find hybrid sites and then shortening the stimulus to 200 ms (12 pulses). The difference between V_{app} within fast and slow domains of the striatum of an individual rat is readily apparent even from the illustrative responses in Fig 4.2A. DA was cleared from the fast domain within 0.5 s, whereas clearance from the slow domain required more than 2 s. To obtain Fig 4.2A, the duration of the stimuli was adjusted to obtain similar response amplitudes at the two recording sites: the time needed to clear the same DA concentration from each site is obviously different. The remainder of this study is devoted to a quantitative evaluation of the DA clearance profiles in fast and slow striatal domains.

The clearance profiles obtained in fast and slow domains are significantly different (Fig 4.2B, see figure legends for ANOVA results). The clearance profiles in slow domains persist for a longer duration and exhibit a slower initial slope. Fig 4.2C reproduces the data of Fig 4.2B but, for clarity, omits the error bars and includes the linear regression lines that best fit the initial linear segment of each clearance profile. In generating Fig 4.2C, responses were only included in the data set if at least three data points on the descending phase of the response produced a straight line with $r^2>0.96$. All slow-type clearance profiles met this criterion, whereas only 4 of the 7 fast-type profiles did so. At the other 3 fast sites, DA returned to baseline within 200 ms and was thus too fast to quantify by our method. It is likely that omitting these 'very fast' profiles leads to an underestimate of the apparent clearance rate in fast domains. Nevertheless, the initial clearance slope (Fig 4.2D) in fast and slow domains, 4.8 ± 1.2 μM/s and 1.4 ± 0.46 μM/s, respectively, are significantly different (see the figure legend for ANOVA details).

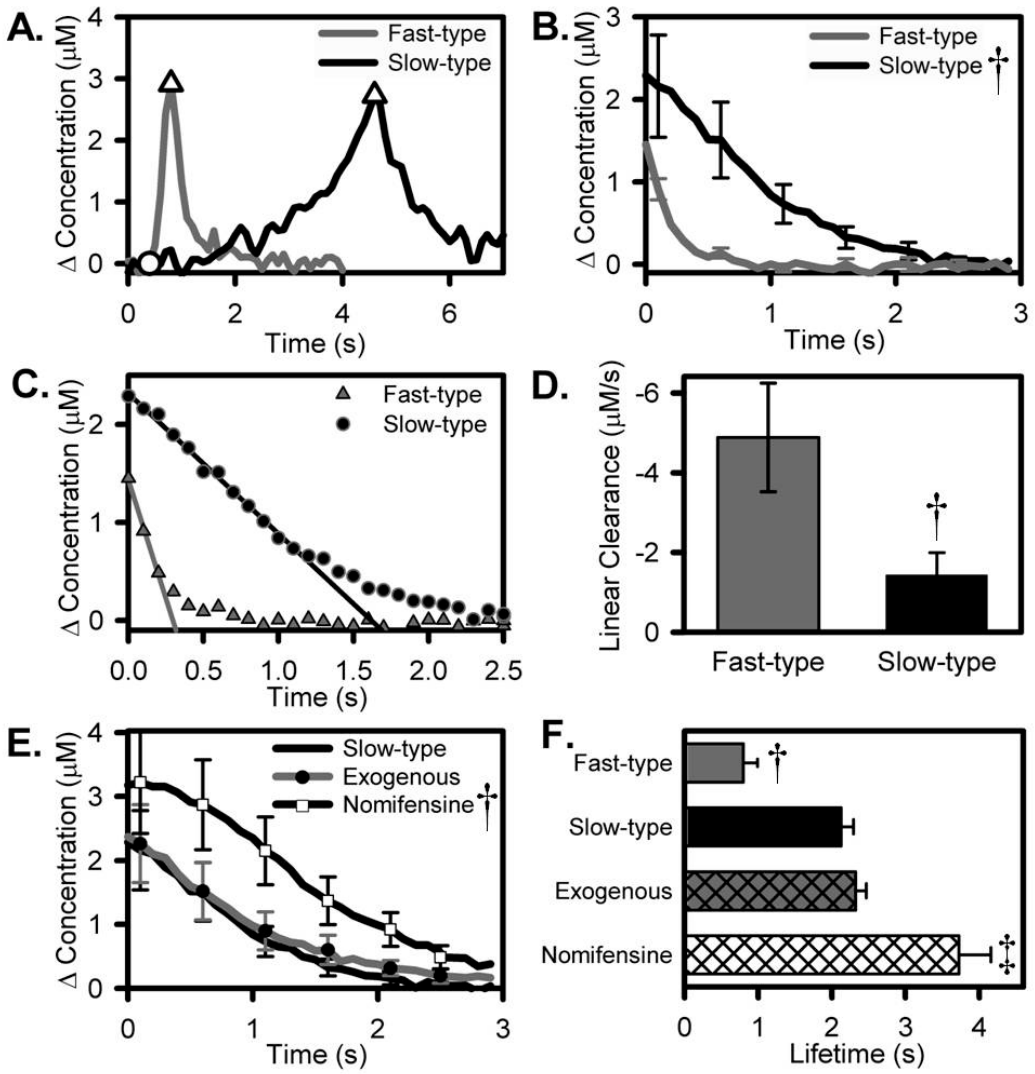

Figure 4.2 Fast-type and slow-type responses in the rat striatum.

(A) Evoked responses (stimulus start - circle, stimulus end –triangles) from two recording sites in one rat. Fast-type responses exhibit immediate DA release when the stimulus begins. Due to autoinhibition, slow-type responses exhibit a delayed onset of evoked release and short-term facilitation. (B) Fast- and slow-type responses exhibit differential apparent DA clearance rates (n=4, Two-way ANOVA, $F_{(1,180)}$=118.9, † p<0.00001). (C) Linear regression lines fit to the averaged clearance curves in panal (B) exhibit distinct slopes. (D) The clearance slopes observed in fast and slow domains are significantly different (n=4, One-way ANOVA, $F_{(1,6)}$=6.93, † p=0.039), with slow domains exhibiting the slower apparent rate of DA clearance. (E) Slow-type apparent DA clearance is identical to the apparent clearance of exogenous DA and is DAT-dependent (nomifensine-sensitive) (n=4, Two-way ANOVA – Tukey post-hoc, $F_{(2,270)}$=56.18, † p<0.00001). (F) The extracellular lifetime of DA in fast and slow domains is significantly different; in slow domains, the lifetime of DA is identical to the lifetime of exogenous DA and is DAT-dependent (n=4, One-way ANOVA – Tukey post-hoc, $F_{(3,12)}$=20.70, †‡ p=0.00005).

We compared DA clearance profiles obtained from evoked responses in slow domains with those obtained after pressure ejection in the same recording location. We adjusted the duration of the pressure ejection so that the initial amplitude of the profiles obtained after evoked release and pressure ejection were similar. The clearance profiles after evoked release and pressure ejection are essentially identical (Fig 4.2E). The evoked responses in slow domains are sensitive to the DAT-inhibitor, nomifensine, which confirms the DAT is active within slow domains (Fig 4.2E). The extracellular DA lifetime (Fig 4.2F) is shortest after fast-type evoked release (0.8 s). The lifetime is longer after slow-type evoked release (2.1 s), similar to that observed after pressure-ejection (2.3 s), and further extended after nomifensine administration (3.7 s).

4.4.3 Effect of evoked DA concentration on clearance

The clearance profiles of Fig 4.2C are re-plotted in Fig 4.3A normalized with respect to the initial DA amplitude. The normalized initial clearance slopes in the two domains are significantly different (Fig 4.3B), which further confirms that the difference in slope is not dependent on the initial DA amplitude. The regression lines that give the best fit to the initial linear segments of the clearance profiles from 8 individual experiments, 4 from fast domains and 4 from slow domains (Fig 4.3C), allow examination of the time at which the regression lines intersect the x-axis (i.e. the time at which they reach $\Delta[DA] = 0\ \mu M$): in fast domains the x-intercepts are all less than 0.5 s, while in slow domains they are all more than 1.2 s. The x-intercept times are significantly shorter in the fast domains compared to slow domains (Fig 4.3D: see the figure legend for ANOVA details). Fig 4.3 confirms that apparent DA clearance is domain-dependent.

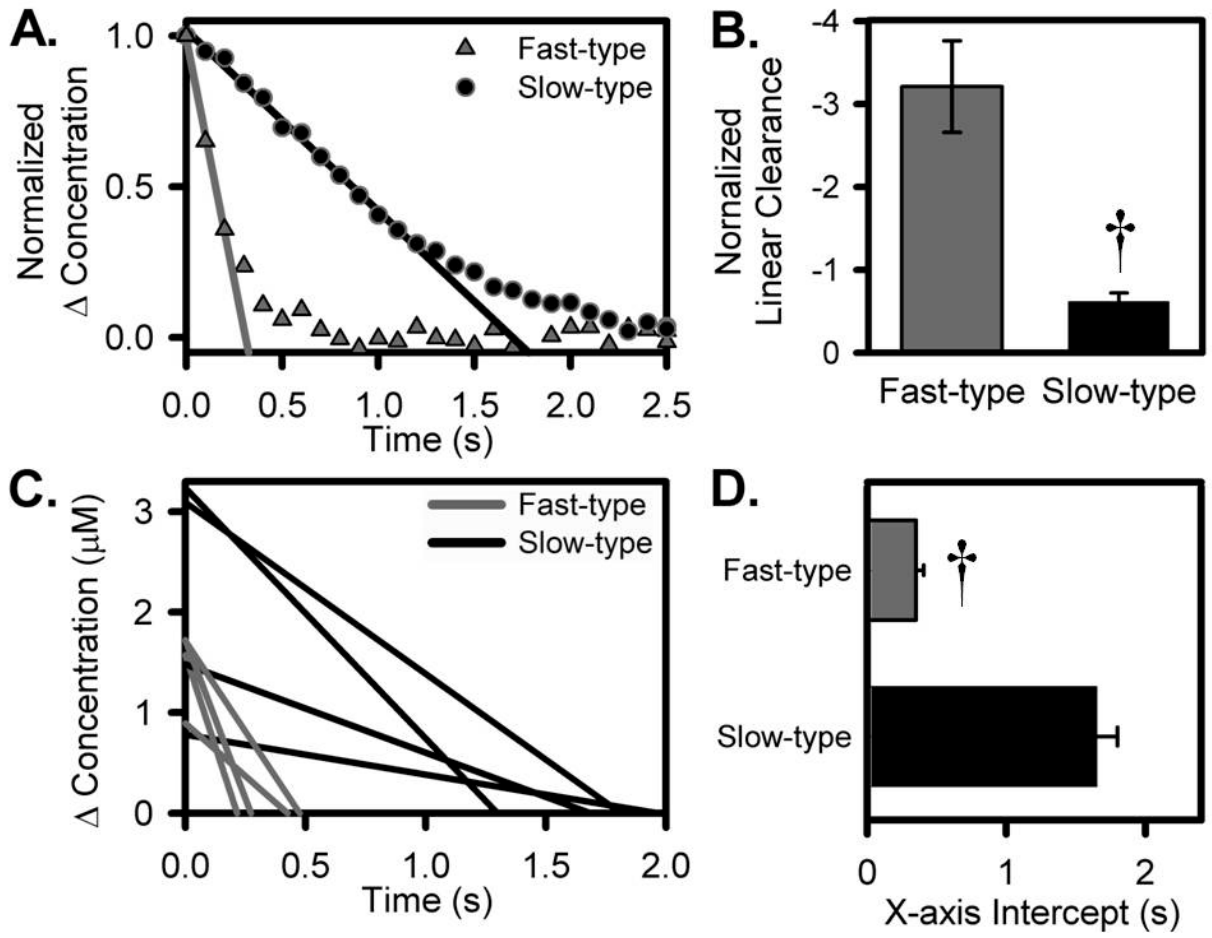

Figure 4.3 Fast and slow striatal domains exhibit significantly different rates of DA clearance.

(A and B) Normalized clearance profiles exhibit significantly different apparent DA clearance rates (n=4, One-way ANOVA, $F_{(1,6)}$=28.38, † p=0.0018). (C) Individual regression lines for the data set used to construct figure (4.2C) demonstrate that the distinction in apparent DA clearance rates is independent of the initial amplitude. The categorization of a response as fast-type or slow-type is not based on the amplitude of the evoked response but rather its temporal profile, as explained by Fig 4.1. Thus, fast-type and slow-type evoked responses often have similar amplitudes (Fig 4.1B, 4.2A). Even when the amplitudes are similar, the distinction in apparent clearance rate is maintained. (D) The fast-type regression lines intersect the x-axis significantly faster than the slow-type regression lines independent of initial evoked amplitude (n=4, One-way ANOVA – Tukey post-hoc, $F_{(1,6)}$=64.17, † p=0.0002).

4.5 DISCUSSION

The present study extends our on-going efforts to characterize the fast and slow domains of the striatal DA terminal field. It is well-known that the striatum is heterogeneous with respect to DA (May and Wightman 1989b; Kawagoe *et al* 1992; Garris and Wightman 1995; Wightman *et al* 2007). However, the compartmentalization of DA terminals into distinctive domains is a relatively recent concept (Moquin and Michael 2009; Wang *et al* 2010). Our prior studies demonstrated that the domains are distinguished by the autoinhibition-dependent dynamics of evoked DA release. The autoinhibition of evoked DA release (Fig 4.1), an accepted index of vesicular release, suggests that DA reaches the extracellular space of slow domains via a non-vesicular mechanism. So, the domains apparently exhibit different basal DA concentrations as a consequence of different rates and mechanisms of DA release. Much as we would like to, thus far we have not been able to examine this implication by directly measuring basal DA concentrations in the two domains. So, we have examined instead the related prediction that the domains should exhibit different apparent rates of DA clearance.

4.5.1 Different basal DA concentrations in the two domains

The raclopride-sensitivity of the initial delay in the onset of evoked DA release (Fig 4.1A) indicates that DA terminals within slow domains are tonically autoinhibited, while the raclopride-insensitivity of the fast-type evoked release (Fig 4.1C and 4.1D) indicates that the terminals are not tonically autoinhibition. However, the fast domains exhibit autoreceptor function in the form of short-term depression of evoked release (Fig 4.1B) and sensitivity to quinpirole, a D2R agonist (Wang *et al* 2010). Since autoreceptors are functional in both

domains, it appears that the domain difference in autoinhibitory tone derives from a difference in the basal DA concentration available to activate, or not, the D2Rs.

4.5.2 Prospects for direct detection of basal DA in striatal domains

Voltammetry measures extracellular DA with sufficient spatial and temporal resolution (May and Wightman 1989b; Kawagoe *et al* 1992; Garris *et al* 1994; Peters and Michael 2000; Greco and Garris 2003) to, for instance, expose the fast and slow striatal domains. But, it is poorly suited to determining steady-state DA concentrations (e.g. Heien *et al.* 2005). Although this limitation might eventually be resolved, voltammetry in its present form does not have the demonstrated ability to measure basal DA concentrations. Microdialysis is widely adopted for basal measurements but does not have the necessary spatial resolution to selectively sample DA from one domain or the other. So, the present study takes advantage of votlammetry's ability to quantify DA clearance, which reflects the balance in the rates of DA uptake and release that is ultimately responsible for the extracellular DA concentration.

The two striatal domains exhibit significant differences in both apparent clearance rate, deduced from the slope of the initial linear segments of the clearance profiles, and the extracellular DA lifetime (Fig 4.2 and 4.3). The DAT is saturable, so a difference in the rate of clearance could arise if the DAT were saturated during some measurements but not others. All the clearance profiles, however, exhibited an initial linear segment, which shows that clearance was zero-order in all cases, so the DAT was saturated in all cases. Differences in clearance time could be due to differences in the initial amplitude, i.e. it might take longer to clear DA after large-amplitude evoked responses simply because there is more of it to clear. This does not seem to be the main source of differences in lifetime: the lifetimes were clearly distinct in the two domains (Fig 4.2A), even though there was considerable overlap in the initial amplitude (Fig

4.3C and 4.3D). Differences in the apparent rate of DA clearance could also arise from D2R activation (Cass and Gerhardt 1994; Dickinson *et al* 1999; Wu *et al* 2002). However, these studies demonstrate that D2R activation accelerates the apparent rate of DA clearance, which is not what we observed: we found slower clearance in the presence of tonic autoinhibition. Although DA clearance is known to be heterogeneous in the striatum (Garris *et al* 1993), this is the first study to show significant differences in DA clearance between sites associated with fast-type and slow-type evoked responses.

4.5.3 Defining the apparent rate of DA clearance

The apparent rate of DA clearance is measured with voltammetry as the extracellular DA concentration returns to its basal level following a transient increase induced either by electrically evoking the release of endogenous DA (Wu *et al* 2001) or by ejecting exogenous DA into the extracellular space via a pipet (Cass *et al* 1993; Sabeti *et al* 2002). The apparent rate of clearance is the net rate at which DA is delivered to, and removed from, the recording electrode (Chen 2005; Michael *et al* 2005). Since clearance occurs after the electrical stimulus or pressure-ejection, the delivery process of interest is the spontaneous (i.e. non-evoked) release of endogenous DA. DA removal occurs by uptake and diffusion (Wightman *et al* 1988; Venton *et al* 2002; John and Jones 2007). However, the linearity of the initial segment of the clearance profiles (Fig 4.2C and 4.3A) indicates zero-order rate processes. So we can conclude that diffusion, which is not a zero-order rate process (Hrabetova and Nicholson 2007), does not contribute substantially to the initial linear stage of clearance.

Thus, during the initial linear stage of clearance, the apparent rate of DA clearance, V_{app}^{o}, is the difference between the rate of DA uptake, V_{u}^{o}, and the rate of DA release, V_{r}^{o} (Michael *et al* 2005):

Equation 2:

$$V_{app}^{0} = V_{u}^{0} - V_{r}^{0}$$

where the superscripts "o" indicate zero-order rates. In some cases, V_{u}^{o} might correspond to the V_{max} of uptake from the Michaelis-Menton model (Wu *et al* 2001; Montague *et al* 2004; Kita *et al* 2007), i.e. the maximal possible rate of uptake when the extracellular concentration of DA is sufficient to saturate the DAT and all of the DAT protein is available to participate in uptake. But, if DDE occurs, then some of the DAT protein would not be available for uptake and the zero-order uptake rate would be less than V_{max}. To leave open this possibility, we have used V_{u}^{o} rather than V_{max} to denote the intrinsic zero-order uptake rate in Equation 2.

Equation 3 explains how basal DA concentrations depend upon the rates of release and uptake (Chen 2005; Michael *et al* 2005):

Equation 3:

$$C^{*} = \frac{V_{r}^{0} K_{M}}{V_{u}^{0} - V_{r}^{0}}$$

where C* represents the basal DA concentration, K_m is the DAT's Michaelis constant, and the other terms were defined earlier. As explained above, we have replaced $V_{max}$with V_{u}^{o} to leave open the possibility that some DAT proteins are not available for uptake. Since the denominator of Equation 3 is V_{app}^{o}, it predicts an inverse relationship between V_{app}^{o} and C*.

4.5.4 The inverse relationship between C* and V_{app}^{o}

The absence of tonic autoinhibition in the fast domains might be due to a low basal DA concentration. According to Equation 3, a low C* would derive from slow release (the numerator) and/or fast apparent clearance (the denominator). When release is slow, the apparent clearance rate should approach the maximal intrinsic rate, V_{max}, i.e. $V_{app}^{o} \approx V_{u}^{o}$ and $V_{u}^{o} \approx V_{max}$. In a less-likely scenario, a low C* could derive from fast release if V_{app}^{o} were correspondingly even faster (this scenario is unlikely because it implies a high expenditure of energy for no apparent reason). In either case, rapid clearance implies a low concentration. Therefore, fast DA clearance in fast domains supports the hypothesis that tonic autoinhibition is absent because the basal DA concentration is low, presumably too low to activate D2Rs.

Tonic autoinhibition in slow domains might be due to a high basal DA concentration. According to Equation 3, a high C* would derive from fast release and/or slow apparent clearance. When release is fast, apparent clearance should be slow, because $V_{app}^{o} = V_{u}^{o} - V_{r}^{o}$ (Equation 2). As explained above, basal release in slow domains is likely non-vesicular. If this were to involve DDE, then $V_{u}^{o} \ll V_{max}$ and apparent clearance would be slowed further. So, slow apparent clearance implies a high concentration, supporting the hypothesis that the autoinhibitory tone on DA terminals in slow domains is a consequence of a high basal DA concentration, presumably high enough to tonically activate D2Rs.

4.5.5 Does DDE contribute to release in slow domains?

Equation 3 allows the alternate scenario that a high C* could derive from slow release if clearance were correspondingly even slower (note, however, there must be some release or C* goes to zero). Slow release and slow clearance might derive from a striatal location with a low

density of DA terminals. In this scenario, again, the apparent clearance rate would approach the maximal intrinsic uptake rate, V_{max}, i.e. $V_{app}^{o} \approx V_{u}^{o}$ and $V_{u}^{o} \approx V_{max}$, but V_{max} would be small because there are few DATs. This scenario, in which slow clearance still implies a high C*, upholds our hypothesis that the autoinhibitory tone is due to a high basal DA concentration. However, if there are so few DATs then DDE might not be possible and vesicular release, even though it is autoinhibited, would have to be sufficient to tonically activate D2Rs. As discussed next, there are several reasons to think this scenario is unlikely.

A low density of DA terminals is inconsistent with the large amplitude of evoked release once autoinhibition is alleviated with raclopride (Fig 4.1C and 4.1D). The nomifensine-sensitivity of the slow-type evoked responses (Fig 4.2E and 4.2F) shows that the slow domains contain DAT, which is expressed by DA terminals (Ciliax *et al* 1995; Nirenberg *et al* 1996). Our finding that diffusion is not a major contributor to the initial segment of clearance (Fig 4.2C and 4.2D implies the close proximity of DATs to the recording electrode. The rapid onset of DA clearance when the stimulus ends also indicates the presence of functional DATs near the electrode (Moquin and Michael 2009). Moquin and Michael (2009) thoroughly established that the slow-type responses exhibit multiple features that cannot be explained by diffusion.

Equation 3 shows that a domain difference in basal DA concentration requires a difference in the relative rates of release and uptake. Apparent clearance is approximately 5-fold slower in slow domains compared to fast (Fig 4.2C). Meanwhile, Moquin and Michael (2009: Figure 2.5C) found that raclopride increases the rate of slow-type evoked release approximately 5-fold, suggesting that autoinhibition slows vesicular release approximately 5-fold. Thus, the relative rates of clearance and vesicular release are not sufficiently different to produce different basal concentrations. So, we conclude that autoinhibited vesicular release is insufficient to drive

an increase in basal DA concentrations, which supports the hypothesis that a non-vesicular process is responsible for the autoinhibitory tone.

Ancillary observations further support a role for DDE. For example, raclopride promoted slow-domain evoked release when administered directly to the striatum (Fig 4.1C and 4.1D), which confirms that the low amplitude of slow-type evoked release stems from presynaptic events rather than a low-density of terminals. Furthermore, Borland and Michael (2004) reported a tetrodotoxin-insensitive, nomifensine-sensitive pool of extracellular DA in the striatum, while Wang et al (2010) found that this pool correlates with the domain type. Collectively, these various findings confirm that the type of domain is determined by the rate and mechanism of the processes that control the basal DA concentration, rather than the local density of DA terminals.

4.5.6 Clearance after evoked release and pressure-ejection

Several studies have discussed why DA clearance after pressure-ejection appears to be slower than after evoked release (Cass *et al* 1993; Cass and Gerhardt 1994; Kiyatkin *et al* 2000; Sabeti *et al* 2002). For example, since the DAT is electrogenic, there is a concern that the membrane depolarization associated with the use of electrical stimulation might bias the DAT kinetics. However, we obtained close agreement between clearance after evoked release and pressure-ejection (Fig 4.2E) by establishing several experimental conditions. First, clearance after evoked release and ejection were measured at the same recording site. Second, the initial amplitude of the clearance profiles after ejection and evoked release were made similar by placing the ejection pipet immediately adjacent to the recording microelectrode (Fig 3.1) and by adjusting the ejection time. Third, by placing the ejection pipet adjacent to the microelectrode, we kept the ejection time brief so that the ejection was finished prior to the clearance measurement. Fourth,

we performed the measurements in slow domains. Under these conditions, clearance after evoked release and pressure-ejection was indistinguishable (Fig 4.2E): this corroborates the slow apparent clearance rate and confirms that no bias was introduced by the use of a longer stimulus to overcome the autoinhibition of evoked release in the slow domains.

Thus, it appears that the domains may have contributed to the discrepancy between DA clearance rates after evoked release and pressure-ejection noted in prior studies. Voltammetry protocols usually involve a procedure to optimize the placement of the recording electrode. As we have shown, optimization seeks out those domains where DA clearance is inherently fast. The pressure-ejection technique does not seek out the fast domains and so likely reflect slow-domain clearance.

We have not, however, attempted to evaluate DA clearance after pressure-ejection into fast domains. Thus far, we have not been able to identify purely fast recording sites: rather the electrodes straddle fast and slow domains, giving rise to hybrid responses. We assume that pressure ejection would not permit the delivery of exogenous DA only into the fast subdomain of a hybrid site. However, we do not expect the electrogenic properties of the DAT to be a key factor in the faster DA clearance because we only stimulated the fast sites for 200 ms: thus, we evoked far less depolarization in the fast sites and, presumably, far less disruption of ion activities.

4.6 CONCLUSION

Figure 4.4 schematically summarizes the DAergic function of the fast and slow striatal domains that emerges from these studies. The fast domains operate under the control of an avid uptake process that rapidly clears DA from the extracellular space and maintains a low basal DA

concentration. The DAT primarily engages in uptake, so DDE is negligible and DA release is dominated by the vesicular mechanism. This is the conventional view of DAergic function deduced from voltammetric studies wherein the placement of the recording electrode was optimized to find fast-type DA. The fast-type responses reported here are similar to the optimized responses reported by other investigators. For example, the DA clearance rate we report in fast domains is similar to conventional values (Wu *et al* 2001; Venton *et al* 2003) and prior studies have demonstrated that short-stimulus responses at optimized recording locations are refractory to D2R antagonists (Garris *et al* 1994). On the other hand, DA clearance is 5-fold less-avid in the slow domains and this coincides with a higher basal DA concentration to tonically autoinhibit vesicular release. Autoinhibited vesicular release is insufficient to increase the extracellular DA concentration in the slow domains (Equation 3), so it appears that non-vesicular release contributes to the basal DA tone. This supports the conclusion that the DAT, even though it is conventionally viewed as a DA reuptake site, contributes to functionally relevant DA release.

There are indications that tonic firing of midbrain DA neurons drives tonal vesicular DA release (Floresco *et al* 2003; Venton *et al* 2003), but presumably this is only relevant in the fast domains where vesicular release is not autoinhibited. The slow domains, wherein DA release is dominated by non-vesicular processes, appear to operate along-side the fast domains. The physiological implications of the domain architecture remain to be fully elucidated but are a matter of on-going interest.

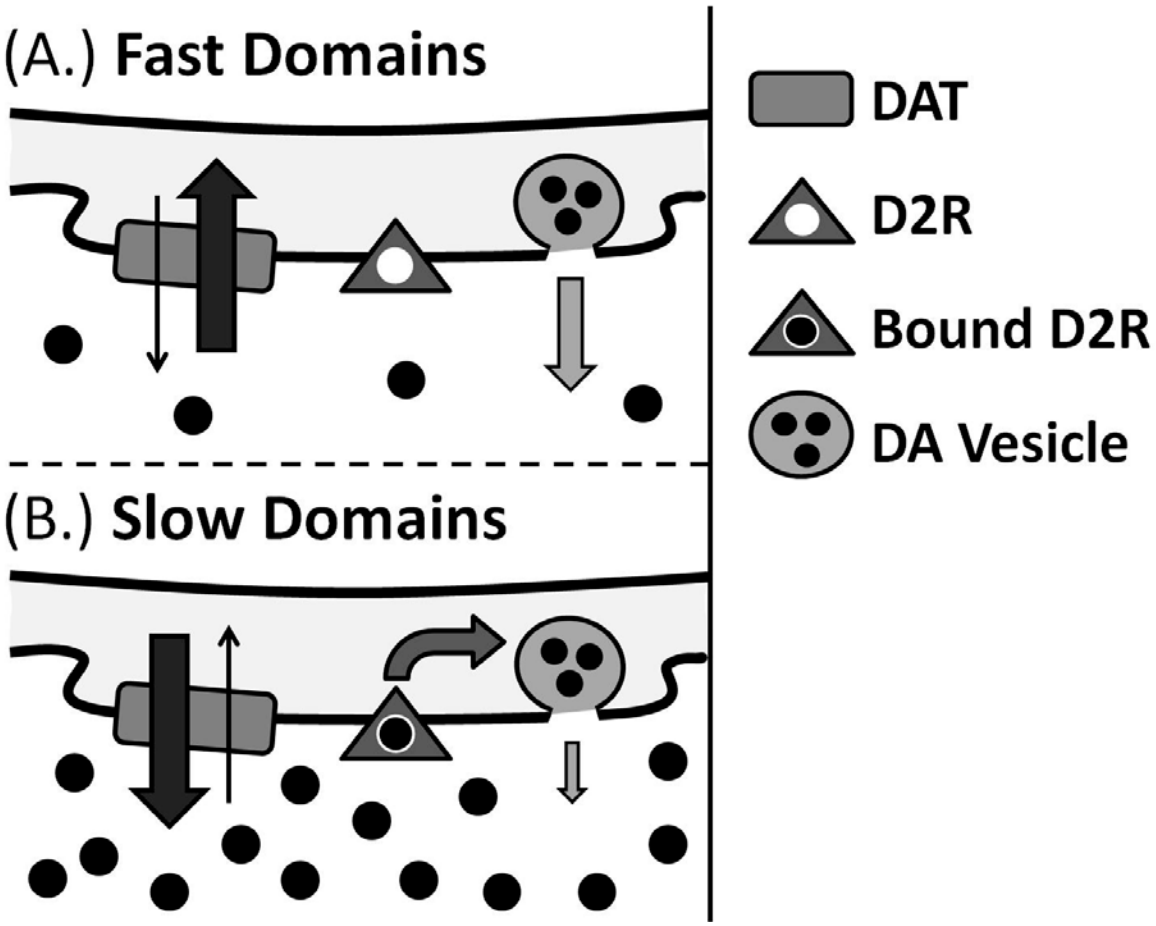

Figure 4.4 The interaction of DAT, basal DA, D2R mediated autoinhibition, and evoked DA release in fast and slow domains.

(A) In fast domains, the DAT favors DA uptake, leading to rapid evoked DA clearance. This rapid DA clearance maintains a basal DA concentration below D2R activation. Thus, tonic autoinhibition is off, enabling terminals to release DA immediately upon stimulation. (B) In slow domains the DAT favors DA efflux, leading to slowed evoked DA clearance. Constant DDE maintains a basal DA concentration large enough to activate D2Rs. Tonic D2R activation creates a constant autoinhibitory tone on these terminals, preventing evoked DA release at the onset of stimulation.

5.0 CONCLUSIONS

This dissertation concludes that the striatal DA system is comprised of two domains of neuron terminal function; the fast domain, which fits the classic model, and the previously unidentified slow domain. Further, we reveal that the slow domain is a product of DAT mediated DA efflux. Constant efflux elevates the basal DA concentration above D2R binding, causing tonic autoinhibition of evoked release. The discovery of slow-type terminal function has the potential to revolutionize our understanding DA signaling. However, there are many more questions that must be answered in order to fully characterize slow domains and their role in the nigrostriatal pathway.

For example, it is still unclear what drives different DAT function in fast and slow domains. One possibility is that anatomical differences in either the expression of DAT at the terminal surface or the density of DA terminals plays a role in setting the basal DA concentration. In order to address these possibilities we are currently probing the anatomy of fast and slow domain tissue using scanning electron microscopy. Also, intracellular processes could contribute to differences in DAT function. For example, the cytosolic DA concentration could drive the rate of DA efflux. In this proposed model, when the cytosolic DA concentration is low efflux is minimal and DAT's main function is uptake. Elevated cytosolic DA concentrations increase the rate of DA efflux, driving DA release via DAT.

Second, we must examine the effects of DA drugs in slow domains. Drug effects on the basal DA concentration and phasic DA release in fast domains has lead to a wealth of

information on terminal function (Cass and Gerhardt 1994; Garris and Wightman 1995; Sonders *et al* 1997; Dickinson *et al* 1999; Benoit-Marand *et al* 2001; Robinson *et al* 2001; Rougé-Pont *et al* 2002; Wightman and Robinson 2002; Garris *et al* 2003). However, the disparate effects of raclopride on evoked release (Moquin and Michael 2009) and kynurenate on basal DA (Wang *et al* 2010) in fast and slow domains clearly indicate that drugs can have different effects in each domain. Therefore, it is paramount to categorize drug effects in slow domains in order to understand slow domain terminal function and it's relation to fast domain activity.

For example, early reports on the effect of DAT inhibitors in slow domains shows that the DAT inhibitor, nomifensine, similarly to raclopride, converts slow-type evoked responses to fast-type (Young and Michael 1993). Thus, DAT inhibition appears to terminate autoinhibition in slow domains, which might indicates that DAT inhibition also inhibits DA efflux. This raises the possibility that the mechanism of action of drugs that inhibit the DAT might be distinct in fast and slow domains, which has interesting implications for the understanding of both the illicit and medicinal applications of such compounds.

Finally, it is necessary to understand how slow domains regulate post-synaptic GABA cell activity. While this dissertation focuses only on pre-synaptic terminals, the DA neuron's main role in the striatum is to interact with the GABA cell. Our data has shown that terminals in slow domains are under tonic autoinhibition of evoked DA release derived from pre-synaptic D2R activation. The post-synptic GABA cell expresses both D1 and D2 receptors. D1 and D2 receptors have similar binding coefficients, so it stands to reason that post-synaptic receptors are continuously activated in slow domains (Grigoriadis and Seeman 1985). Thus, we hypothesize that post-synaptic GABA cells are under a constant DAergic tone in slow domains, i.e. constant DA signaling. The existence of distinct fast and slow DA domains accords well with the concept

that DA functions on multiple time courses (Schultz 2007). Further, the slow domain adds new insights into several DA pathologies.

In Parkinson's disease there is a near complete neurodegeneration of the striatal DA system. The loss of striatal DA activation of GABA cells leads to enhanced activity of the basal ganglia, which is thought to cause the loss of motor control (Albin *et al* 1989; Maneuf *et al* 1997). However, there is a significant pre-symptomatic phase where the striatal DA terminals are significantly decreased without outward signs of the disease (Bernheimer *et al* 1973; Robinson and Whishaw 1988). Zigmond and co-workers have hypothesized that increased DA production and release by surviving DAergic terminals compensates for the decline of the DAergic system during the pre-symptomatic phase of Parkinson's disease (Zigmond *et al* 1992). They further hypothesize that DA would have a longer lifetime in the extracellular space because uptake is significantly slower due to the decreased number of uptake sites (Zigmond *et al* 1992). Therefore, they suggest that the remaining DAergic terminals are able to create a long lasting tonic DA signal that helps maintain homeostasis in the denervated striatum (Zigmond *et al* 1992). The current pharmaceutical treatments of Parkinson's disease, D2R agonists (e.g. quinpirole) or L-DOPA, also appear to alleviate Parkinson's disease symptoms through tonic activation of receptors. Administration of quinpirole alleviates akinesia the Parkinson's disease rat model by activating D2Rs (Maneuf *et al* 1997). There is no evidence that quinpirole can be packaged and released by neurons, and thus assume that it acts tonically on the receptors. Similarlly L-DOPA, which is converted into DA by aromatic L-amino acid decarboxylace, a ubiquitous enzyme that decarboxylizes all natural aromatic L-amino acids (Lovenberg *et al* 1962) increases striatal DA (Hefti *et al* 1981; Keller *et al* 1988). However, as the number of DAergic terminals has been greatly reduced it is believed that that much of the DA produced

from L-DOPA occurs in non-DAergic cells (Melamed *et al* 1980), and enters the extracellular space in a non-impulse dependent manner (Zigmond *et al* 1992). The notion that there is a homeostatic level of basal activation of post-synaptic DA receptors fits with our model of two striatal DA domains.

Schizophrenia is highlighted by both positive (e.g. delusions) and negative (e.g. anhedonia) emotional responses. One hypothesis on the duality of schizophrenic symptoms suggests that the basal DA concentration exists in a homeostatic state. Either an increase or decrease in this basal level causes an imbalance in DA signaling, triggering either positive or negative schizophrenic activity (Grace 1991). This hypothesis does not fit with the classic model of striatal DA signaling. In the classic DA model, lowering basal concentrations from nM to zero would have no effect DA receptor binding (Grigoriadis and Seeman 1985), suggesting that only increases in DA trigger disorders. The large basal DA concentration found in the slow domain resolves this discrepancy. Here, decreasing the basal DA concentration would change DA receptor binding, altering DA signaling.

In the classic ADHD model increased phasic DA signaling is the root cause of hyperactivity (Levy and Swanson 2001; Tripp and Wickens 2008). The symptoms of ADHD are successfully treated with methylphenidate, which elevates the basal DA concentration (Volkow *et al* 2001). The efficacy of methylphenidate is paradoxical in the classic model where increasing basal DA should only serve to further activate DA receptors. Slow domains provide a new hypothesis, resolving this issue. Slow domains have a large basal DA concentration that triggers tonic autoinhibition. These terminals do not release DA during physiologically relevant stimulus events (Moquin and Michael 2009). The effect of raclopride demonstrates that these terminals are capable of rapid DA release (Moquin and Michael 2009). So a decrease in basal DA in these

domains would remove the tonic autoinhibitory tone, turning slow domains into fast domains. An increase in the number of fast domains would increase phasic DA signaling. Therefore, ADHD may be caused by a decrease in the basal DA concentration that increases the ratio of fast domains compared to slow domains. In this model, methylphenidate increases basal DA converting fast domains back into slow domains, restoring the proper ratio of the two domains.

These revised models of DA pathologies highlight the significance of slow domains in the striatal DAergic pathway. Continued research into slow domain function will reveal new insights into DA signaling, enlightening our perspective on mammalian brain function, the causes of brain disorders, and potential cures.

BIBLIOGRAPHY

Abi-Dargham A, Rodenhiser J, Printz D, Zea-Ponce Y, et al. (2000) Increases baseline occupancy of D2 receptors by dopamine in schizophrenia. *PNAS* **97**, 8104-8109.

Addy NA, Daberkow DP, Ford JN, Garris PA, et al. (2010) Sensitization of rapid dopamine signaling in the nucleus accumbens core and shell after repeated cocaine in rats. *J Neurophysiol* **104**, 922-31.

Albin RL, Young AB and Penney JB (1989) The functional anatomy of basal ganglia disorders. *Trends Neurosci* **12**, 366-75.

Amara SG and Kuhar MJ (1993) Neurotransmitter transporters: recent progress. *Annu Rev Neurosci* **16**, 73-93.

Avshalumov MV and Rice ME (2003) Activation of ATP-sensitive K^+(KATP) channels by H_2O_2 underlies glutamate-dependent inhibition of striatal dopamine release. *PNAS* **100**, 11729-11734.

Bard AJ and Faulkner LR (2001) *Electrochemical methods, fundamentals and applications*. John Wiley & Sons, Inc., New York.

Bath BD, Michael DJ, Trafton BJ, Joseph JD, et al. (2000) Subsecond adsorption and desorption of dopamine at carbon-fiber microelectrodes. *Anal Chem* **72**, 5994-6002.

Benoit-Marand M, Borrelli E and Gonon F (2001) Inhibition of dopamine release via presynaptic D2 receptors: time course and functional characteristics in vivo. *J Neurosci* **21**, 9134-9141.

Benoit-Marand M, Suaud-Chagny M-F and Gonon F (2007) Presynaptic regulation of extracellular dopamine as studied by continuous amperometry in anesthetized animals. in: *Electrochemical Methods for Neuroscience*. (Michael AC and Borland LM. eds), 35-47. CRC Press, Boca Raton.

Bernheimer H, Birkmayer W, Hornykiewicz O, Jellinger K, et al. (1973) Brain dopamine and the syndromes of Parkinson and Huntington. Clinical, morphological and neurochemical correlations. *J Neurol Sci* **20**, 415-55.

Biran R, Martin DC and Tresco PA (2005) Neuronal cell loss accompanies the brain tissue response to chronically implanted silicon microelectrode arrays. *Exp Neurol* **195**, 115-26.

Borland LM and Michael AC (2004) Voltammetric study of the control of striatal dopamine release by glutamate. *J Neurochem* **91**, 220-229.

Borland LM, Shi G, Yang H and Michael AC (2005) Voltammetric study of extracellular dopamine near microdialysis probes acutely implanted in the striatum of the anesthetized rat. *J Neurosci Methods* **146**, 149-158.

Bungay PM, Morrison PF, Dedrick RL, Chefer VI, et al. (2007) Principles of quantitative microdialysis. in: *Handbook of microdialysis: methods, applications, and perspectives*. (Westerink BHC and Cremers TIFH. eds), 131-167. Elsevier, Amsterdam.

Bungay PM, Newton-Vinson P, Isele W, Garris PA, et al. (2003) Microdialysis of dopamine interpreted with quantitative model incorporating probe implantation trauma. *J Neurochem* **86**, 932-946.

Carboni E, Imperato A, Perezzani L and Di Chiara G (1989) Amphetamine, cocaine, phencyclidine and nomifensine increase extracellular dopamine concentrations preferentially in the nucleus accumbens of freely moving rats. *Neuroscience* **28**, 653-61.

Carli M, Evenden JL and Robbins TW (1985) Depletion of unilateral striatal dopamine impairs initiation of contralateral actions and not sensory attention. *Nature* **313**, 679-682.

Carr GD and White NM (1986) Anatomical dissociation of amphetamine's rewarding and aversive effects: an intracranial microinjection study. *Psychopharmacology* **89**, 340-346.

Cass WA and Gerhardt GA (1994) Direct in vivo evidence that D2 dopamine receptors can modulate dopamine uptake. *Neurosci Lett* **176**, 259-63.

Cass WA, Zahniser NR, Flach KA and Gerhardt GA (1993) Clearance of exogenous dopamine in rat dorsal striatum and nucleus accumbens: role of metabolism and effects of locally applied uptake inhibitors. *J Neurochem* **61**, 2269-78.

Cheer JF, Heien ML, Garris PA, Carelli RM, et al. (2005) Simultaneous dopamine and single-unit recordings reveal accumbens GABAergic responses: implications for intracranial self-stimulation. *PNAS* **102**, 19150-5.

Cheer JF, Wassum KM, Heien ML, Phillips PE, et al. (2004) Cannabinoids enhance subsecond dopamine release in the nucleus accumbens of awake rats. *J Neurosci* **24**, 4393-400.

Chen KC (2005) Evidence on extracellular dopamine level in rat striatum: implications for the validity of quantitative microdialysis. *J Neurochem* **92**, 46-58.

Cheramy A, Romo R, Godeheu G, Baruch P, et al. (1986) In vivo presynaptic control of dopamine release in the cat caudate nucleus--II. Facilitatory or inhibitory influence of L-glutamate. *Neuroscience* **19**, 1081-90.

Ciliax BJ, Heilman C, Demchyshyn LL, Pristupa ZB, et al. (1995) The Dopamine Transporter: lmmunochemical Characterization and Localization in Brain. *J Neurosci* **15**, 1714-1723.

Clapp-Lilly KL, Roberts RC, Duffy LK, Irons KP, et al. (1999) An ultrastructural analysis of tissue surrounding a microdialysis probe. *J Neurosci Methods* **90**, 129-142.

Clark D and White FJ (1987) Review: D1 dopamine receptor - the search for a function: A critical evaluation of the D1/D2 dopamine receptor classification and its functional implications. *Synapse* **1**, 347-388.

Cragg SJ, Nicholson C, Kume-Kick J, Tao L, et al. (2001) Dopamine-mediated volume transmission in midbrain is regulated by distinct extracellular geometry and uptake. *J Neurophysiol* **85**, 1761-71.

Cragg SJ and Rice ME (2004) DAncing past the DAT at a DA synapse. *Trends Neurosci.* **27**, 270-7.

Cserr HF, DePasquale M, Nicholson C, Patlak CS, et al. (1991) Extracellular volume decreases while cell volume is maintained by ion uptake in rat brain during acute hypernatremia. *J Physiol* **442**, 277-95.

Daws LC and Toney GM (2007) High-Speed Chronoamperometry to Study Kinetics and Mechanisms for Serotonin Clearance In Vivo. in: *Electrochemical Methods for Neuroscience*. (Michael AC and Borland LM. eds), 63-82. CRC Press, Boca Raton.

Deakin MR, Kovach PM, Stutts KJ and Wightman RM (1986) Heterogeneous mechanisms of the oxidation of catechols and ascorbic acid at carbon electrodes. *Anal Chem* **58**, 1474-80.

Delle-Donne KT, Sesack SR and Pickel VM (1997) Ultrastructural immunocytochemical localization of the dopamine D2 receptor within GABAergic neurons of the rat striatum. *Brain Research* 239-255.

Dickinson SD, Sabeti J, Larson GA, Giardina K, et al. (1999) Dopamine D2 receptor-deficient mice exhibit decreased dopamine transporter function but no changes in dopamine release in dorsal striatum. *J Neurochem* **72**, 148-56.

Doucet G, Descarries L, Audet MA, Garcia S, et al. (1988) Radioautographic method for quantifying regional monoamine innervations in the rat brain. Application to the cerebral cortex. *Brain Res* **441**, 233-59.

Dreyer JK, Herrik KF, Berg RW and Hounsgaard JD (2010) Influence of phasic and tonic dopamine release on receptor activation. *J Neurosci* **30**, 14273-83.

Dugast C, Brun P, Sotty F, Renaud B, et al. (1997) On the involvement of a tonic dopamine D2-autoinhibition in the regulation of pulse-to-pulse-evoked dopamine release in the rat striatum in vivo. *Naunyn Schmiedebergs Arch Pharmacol* **355**, 716-9.

Engstrom RC, Wightman RM and Kristense EW (1988) Diffusional Distortion in the Monitoring of Dynamic Event. *Anal Chem* **60**, 652-656.

Espana RA, Roberts DC and Jones SR (2008) Short-acting cocaine and long-acting GBR-12909 both elicit rapid dopamine uptake inhibition following intravenous delivery. *Neuroscience* **155**, 250-7.

Ewing AG, Bigelow JC and Wightman RM (1983) Direct in vivo monitoring of dopamine released from two striatal compartments in the rat. *Science* **221**, 169-171.

Falkenburger BH, Barstow KL and Mintz IM (2001) Dendrodendritic inhibition through reversal of dopamine transport. *Science* **293**, 2465-2470.

Floresco SB, West AR, Ash B, Moore H, et al. (2003) Afferent modulation of dopamine neuron firing differentially regulates tonic and phasic dopamine transmission. *Nat Neurosci* **6**, 968-73.

Frey LC, Hellier J, Unkart C, Lepkin A, et al. (2009) A novel apparatus for lateral fluid percussion injury in the rat. *J Neurosci Methods* **177**, 267-72.

Garris PA, Budygin EA, Phillips PE, Venton BJ, et al. (2003) A role for presynaptic mechanisms in the actions of nomifensine and haloperidol. *Neuroscience* **118**, 819-29.

Garris PA, Ciolkowski EL, Pastore P and Wightman RM (1994) Efflux of dopamine from the synaptic cleft in the nucleus accumbens of the rat brain. *J Neurosci* **14**, 6084-6093.

Garris PA, Collins LB, Jones SR and Wightman RM (1993) Evoked extracellular dopamine in vivo in the medial prefrontal cortex. *J Neurochem* **61**, 637-647.

Garris PA and Wightman RM (1995) Regional differences in dopamine release, uptake, and diffusion measured by fast-scan cyclic voltammetry. in: *Neuromethods: voltammertic methods in brain systems*. (Boulton A, Baker G and Adams RN. eds), **27**, 179-220. Humana, Totowa.

Gerhardt GA, Oke AF, Nagy G, Moghaddam B, et al. (1984) Nafion-coated electrodes with high selectivity for CNS electrochemistry. *Brain Res* **290**, 390-5.

Gonon F, Buda M, Cespuglio R, Jouvet M, et al. (1981) Voltammetry in the striatum of chronic freely moving rats: detection of catechols and ascorbic acid. *Brain Res* **223**, 69-80.

Gonon FG, Navarre F and Buda MJ (1984) In vivo monitoring of dopamine release in the rat brain with differential normal pulse voltammetry. *Anal Chem* **56**, 573-5.

Grace AA (1991) Phasic versus tonic dopamine release and the modulation of dopamine system responsivity : a hypothesis for the etiology of schizophrenia. *Neuroscience* **41**, 1-24.

Grace AA and Bunney BS (1984) The control of firing pattern in nigral dopamine neurons: single spike firing. *J Neurosci* **4**, 2866-2876.

Grace AA and Bunney BS (1985) Opposing effects of striatonigral feedback pathways on midbrain dopamine cell activity. *Brain Res* **333**, 271-84.

Greco PG and Garris PA (2003) In vivo interaction of cocaine with the dopamine transporter as measured by voltammetry. *Eur J Pharmacol* **479**, 117-125.

Greco PG, Meisel RL, Heidenreich BA and Garris PA (2006) Voltammetric measurement of electrically evoked dopamine levels in the striatum of the anesthetized Syrian hamster *J Neurosci Methods* **152**, 55-64.

Greengard P, Valtorta F, Czernik AJ and Benfenati F (1993) Synaptic vesicle phosphoproteins and regulation of synaptic function. *Science* **259**, 780-785.

Grigoriadis D and Seeman P (1985) Complete conversion of brain D2 dopamine receptors from the high- to the low-affinity state for dopamine agonists, using sodium ions and guanine nucleotide. *J Neurochem* **44**, 1925-1935.

Hefti F, Melamed E and Wurtman RJ (1981) The site of dopamine formation in rat striatum after L-dopa administration. *J Pharmacol Exp Ther* **217**, 189-97.

Heien MLAV, Khan AS, Ariansen JL, Cheer JF, et al. (2005) Real-time measurement of dopamine fluctuations after cocaine in the brain of behaving rats. *PNAS* **102**, 10023-10028.

Herr NR, Daniel KB, Belle AM, Carelli RM, et al. (2010) Probing presynaptic regulation of extracellular dopamine with iontophoresis. *ACS Chem Neurosci* **1**, 627-638.

Herr NR, Kile BM, Carelli RM and Wightman RM (2008) Electroosmotic flow and its contribution to iontophoretic delivery. *Anal Chem* **80**, 8635-41.

Horvitz JC (2000) Mesolimbocortical and nigrostriatal dopamine responses to salient non-reward events *Neuroscience* **96**, 651-656.

Hrabetova S and Nicholson C (2007) Biophysical properties of brain extracellular space explored with ion-selective microelectrodes, integrative optical imaging and related techniques. in: *Electrochemical Methods for Neuroscience*. (Michael AC and Borland LM. eds), 167-204. CRC Press, Boca Raton.

Hyland BI, Reynolds JNJ, Hay J, Perk CG, et al. (2002) Firing modes of midbrain dopamine cells in the freely moving rat. *Neuroscience* **114**, 475-492.

Ingram SL, Prasad BM and Amara SG (2002) Dopamine transporter-mediated conductances increase excitability of midbrain dopamine neurons. *Nat Neurosci* **5**, 971-8.

Iversen LL (1971) Role of transmitter uptake mechanisms in synaptic neurotransmission. *Br J Pharmacol* **41**, 571-91.

Izenwasser S, Werling LL and Cox BM (1990) Comparison of the effects of cocaine and other inhibitors of dopamine uptake in rat striatum, nucleus accumbens, olfactory tubercle, and medial prefrontal cortex. *Brain Res* **520**, 303-9.

Jaquins-Gerstl A and Michael AC (2009) Comparison of the brain penetration injury associated with microdialysis and voltammetry. *J Neurosci Methods* **183**, 127-35.

John CE and Jones SR (2007) Fast scan cyclic voltammetry of dopamine and serotonin in mouse brain slices. in: *Electrochemical Methods for Neuroscience*. (Michael AC and Borland LM. eds), 49-62. CRC Press, Boca Raton.

Kalivas PW (1993) Neurotransmitter regulation of dopamine neurons in the ventral tegmental area. *Brain Res Brain Res Rev* **18**, 75-113.

Kawagoe KT, Garris PA, Wiedemann DJ and Wightman RM (1992) Regulation of transient dopamine concentration gradients in the microenvironment surrouding nerve terminals in the rat striatum. *Neuroscience* **51**, 55-64.

Kehr W, Carlsson A, Lindqvist M, Magnusson T, et al. (1972) Evidence for a receptor-mediated feedback control of striatal tyrosine hydroxylase activity. *J Pharm Pharmacol* **24**, 744-7.

Keller RW, Jr., Kuhr WG, Wightman RM and Zigmond MJ (1988) The effect of L-dopa on in vivo dopamine release from nigrostriatal bundle neurons. *Brain Res* **447**, 191-4.

Kennedy RT, Jones SR and Wightman RM (1992) Dynamic Observation of Doparnine Autoreceptor Effects in Rat Striatal Slices. *J Neurochem* **59**, 449-455.

Kissinger PT, Hart JB and Adams RN (1973) Voltammetry in brain tissue--a new neurophysiological measurement. *Brain Res* **55**, 209-13.

Kita JM, Parker LE, Phillips PEM, Garris PA, et al. (2007) Paradoxical modulation of short-term facilitation of dopamine release by dopamine autoreceptors. *J Neurochem* **102**, 1115-1125.

Kiyatkin EA, Kiyatkin DE and Rebec GV (2000) Phasic inhibition of dopamine uptake in nucleus accumbens induced by intravenous cocaine in freely behaving rats. *Neuroscience* **98**, 729-41.

Kuhr WG, Ewing AG, Caudill WL and Wightman RM (1984) Monitoring the stimulated release of dopamine with in vivo voltammetry. I: characterization of the response observed in the caudate nucleus of the rat. *J Neurochem* **43**, 560-569.

Kulagina NV, Zigmond MJ and Michael AC (2001) Glutamate regulates the spontaneous and evoked release of dopamine in the rat striatum. *Neuroscience* **102**, 121-128.

Larivon E (1984) Electrochemical reactions with protonations at equilibrium: Part X. The kinetics of the p-benzoquinone/hydroquinone couple on a platinum electrode. *J Electroanal Chem Interfacial Electrochem* **164**, 213-227.

Leviel V (2001) The reverse transport of DA, what physiological significance? *Neurochem Int* **38**, 83-106.

Levy F and Swanson JM (2001) Timing, space and ADHD: the dopamine theory revisited. *Aust N Z J Psychiatry* **35**, 504-11.

Limberger N, Trou SJ, Kruk ZL and Starke K (1991) "Real time" measurement of endogenous dopamine release during short trains of pulses in slices of rat neostriatum and nucleus accumbens: role of autoinhibition. *Naunyn Schmiedebergs Arch Pharmacol* **344**, 623-629.

Lonart G and Zigmond MJ (1991) High glutamate concentration evoke Ca(++)-independent dopamine release from striatal slices: a possible role of reverse dopamine transport. *J Pharmacol Exp Ther* **256**, 1132-1138.

Lotharius J and Brundin P (2002) Pathogenesis of parkinson's disease; dopamine, vesicles nad α-synuclein. *Nature Reviews Neuroscience* **3**, 932-942.

Lovenberg W, Weissbach H and Udenfriend S (1962) Aromatic L-amino acid decarboxylase. *J Biol Chem* **237**, 89-93.

Lu Y, Peters JL and Michael AC (1998) Direct comparison of the response of voltammetry and microdialysis to electrically evoked release of striatal dopamine. *J Neurochem* **70**, 584-593.

Makos MA, Kim YC, Han KA, Heien ML, et al. (2009) In vivo electrochemical measurements of exogenously applied dopamine in Drosophila melanogaster. *Anal Chem* **81**, 1848-54.

Mandt BH and Zahniser NR (2010) Low and high cocaine locomotor responding male Sprague-Dawley rats differ in rapid cocaine-induced regulation of striatal dopamine transporter function. *Neuropharmacology* **58**, 605-12.

Maneuf YP, Crossman AR and Brotchie JM (1997) The cannabinoid receptor agonist WIN 55,212-2 reduces D2, but not D1, dopamine receptor-mediated alleviation of akinesia in the reserpine-treated rat model of Parkinson's disease. *Exp Neurol* **148**, 265-70.

May LJ and Wightman RM (1989a) Effects of D-2 antagonists on frequency-dependent stimulated dopamine overflow in nucleus accumbens and caudate-putamen. *J Neurochem* **53**, 898-906.

May LJ and Wightman RM (1989b) Heterogeneity of stimulated dopamine overflow within rat striatum as observed with in vivo voltammetry. *Brain Res* **487**, 311-320.

Melamed E, Hefti F and Wurtman RJ (1980) Nonaminergic striatal neurons convert exogenous L-dopa to dopamine in parkinsonism. *Ann Neurol* **8**, 558-63.

Michael AC, Borland LM, Mitala JJ, Jr., Willoughby BM, et al. (2005) Theory for the impact of basal turnover on dopamine clearance kinetics in the rat striatum after medial forebrain bundle stimulation and pressure ejection. *J Neurochem* **94**, 1202-11.

Mitala CM, Wang Y, Borland LM, Jung M, et al. (2008) Impact of microdialysis probes on vasculature and dopamine in the rat striatum: A combined fluorescence and voltammetric study. *J Neurosci Methods* **174**, 177-185.

Monsma FJ, Mahan LC, Mcvittie LD, GERFEN CR, et al. (1990) Molecular cloning and expression of a D1 dopamine receptor linked to adenylyl cyclase activation. *Proceedings of the National Academy of Science* **87**, 6723-6727.

Montague PR, McClure SM, Baldwin PR, Phillips PEM, et al. (2004) Dynamic gain control of dopamine delivery in freely moving animals. *J Neurosci* **24**, 1754-1759.

Montgomery AJ, Asselin MC, Farde L and Grasby PM (2007) Measurement of methylphenidate-induced change in extrastriatal dopamine concentration using [11C]FLB 457 PET. *J Cereb Blood Flow Metab* **27**, 369-77.

Moquin KF and Michael AC (2009) Tonic autoinhibition contributes to the heterogeneity of evoked dopamine release in the rat striatum. *J Neurochem* **110**, 1491-501.

Moquin KF and Michael AC (2011) An inverse correlation between the apparent rate of dopamine clearance and tonic autoinhibition in subdomains of the rat striatum: a possible role of transporter-mediated dopamine efflux. *J Neurochem* **117**, 133-42.

Nagy Z, Peters H and Huttner I (1984) Fracture faces of cell junctions in cerebral endothelium during normal and hyperosmotic conditions. *Lab Invest* **50**, 313-22.

Nicholson C (1995) Interaction between diffusion and Michaelis-Menten uptake of dopamine after iontophoresis in striatum. *Biophys J* **68**, 1699-715.

Nicholson C and Rice ME (1991) Diffusion of ions and transmitters in the brain cell microenvironment. in: *Volume Transmission in the Brain*. (Fuxe K and Agnati LF. eds), 279–294. Raven Press, New York.

Nirenberg MJ, Vaughan RA, Uhl GR, Kuhar MJ, et al. (1996) The Dopamine Transporter Is Localized to Dendritic and Axonal Plasma Membranes of Nigrostriatal Dopaminergic Neurons. *J Neurosci* **76**, 436-447.

Pellegrino LJ, Pellegrino AS and Cushman AJ (1979) *A stereotaxic atlas of the rat brain*. Plenum Press, New York.

Peters JL and Michael AC (2000) Changes in the kinetics of dopamine release and uptake have differential effects on the spatial distribution of extracellular dopamine concentration in rat striatum. *J Neurochem* **74**, 1563-1573.

Peters JL, Miner LH, Michael AC and Sesack SR (2004) Ultrastructure at carbon fiber microelectrode implantation sites after acute voltammetric measurements in the striatum of anesthetized rats. *J Neurosci Methods* **137**, 9-23.

Peters JL, Yang H and Michael AC (2000) Quantitative aspects of brain microdialysis *Anal Chem Acta* **412**, 1-12.

Phillips PE, Hancock PJ and Stamford JA (2002) Time window of autoreceptor-mediated inhibition of limbic and striatal dopamine release. *Synapse* **44**, 15-22.

Phillips PE, Robinson DL, Stuber GD, Carelli RM, et al. (2003a) Real-time measurements of phasic changes in extracellular dopamine concentration in freely moving rats by fast-scan cyclic voltammetry. *Methods Mol Med* **79**, 443-64.

Phillips PEM, Stuber GD, Heien MLAV, Wightman RM, et al. (2003b) Subsecond dopamine release promotes cocaine seeking. *Nature* **422**, 614-618.

Reese TS and Karnovsky MJ (1967) Fine structural localization of a blood-brain barrier to exogenous peroxidase. *J Cell Biol* **34**, 207-17.

Rice ME, Gerhardt GA, Hierl PM, Nagy G, et al. (1985) Diffusion coefficients of neurotransmitters and their metabolites in brain extracellular fluid space. *Neuroscience* **15**, 891-902.

Robinson DL, Phillips PE, Budygin EA, Trafton BJ, et al. (2001) Sub-second changes in accumbal dopamine during sexual behavior in male rats. *Neuroreport* **12**, 2549-52.

Robinson DL, Venton BJ, Heien ML and Wightman RM (2003) Detecting subsecond dopamine release with fast-scan cyclic voltammetry in vivo. *Clin Chem* **49**, 1763-73.

Robinson TE and Whishaw IQ (1988) Normalization of extracellular dopamine in striatum following recovery from a partial unilateral 6-OHDA lesion of the substantia nigra: a microdialysis study in freely moving rats. *Brain Res* **450**, 209-24.

Roitman MF, Stuber GD, Phillips PEM, Wightman RM, et al. (2004) Dopamine operates as a subsecond modulator of food seeking *J Neurosci* **24**, 1265-1271.

Rougé-Pont F, Usiello A, Benoit-Marand M, Gonon F, et al. (2002) Changes in extracellular dopamine induced by morphine and cocaine: crucial control by D2 receptors. *J Neurosci* **22**, 3293-3301.

Rousche PJ and Normann RA (1998) Chronic recording capability of the Utah Intracortical Electrode Array in cat sensory cortex. *J Neurosci Methods* **82**, 1-15.

Sabeti J, Adams CE, Burmeister J, Gerhardt GA, et al. (2002) Kinetic analysis of striatal clearance of exogenous dopamine recorded by chronoamperometry in freely-moving rats. *J Neurosci Methods* **121**, 41-52.

Salahpour A, Ramsey AJ, Medvedev IO, Kile B, et al. (2008) Increase amphetamine-induced hyperactivity and reward in mice overexpressing the dopamine transporter. *PNAS* **105**, 4405-4410.

Santiago M and Westerink BH (1990) Characterization of the in vivo release of dopamine as recorded by different types of intracerebral microdialysis probes. *Naunyn Schmiedebergs Arch Pharmacol* **342**, 407-14.

Schinelli S, Paolillo M and Corona GL (2004) Opposing actions of D1- and D2-dopamine receptors on arachidonic acid release and cyclic AMP production in striatal neurons. *Journal of Neurochemistry* **62**, 944-949.

Schmitz Y, Lee CJ, Schmauss C, Gonon F, et al. (2001) Amphetamine distorts stimulation-dependent dopamine overflow: effects on D2 autoreceptors, transporters, and synaptic vesicle stores. *J Neurosci* **21**, 5916-24.

Schultz W (1998) Predictive reward signal of dopamine neurons. *J Neurophysiol* **80**, 1-27.

Schultz W (2007) Multiple dopamine functions at different time courses. *Annu Rev Neurosci* **30**, 259-288.

Sesack SR, Aoki C and Pickel VM (1994) Ultrastructural Localization of D, Receptor-like lmmunoreactivity in Midbrain Dopamine Neurons and Their Striatal Targets. *Journal of Neuroscience* **14**, 88-106.

Sevak RJ, Owens WA, Koek W, Galli A, et al. (2007) Evidence for D2 receptor mediation of amphetamine-induced normalization of locomotion and dopamine transporter function in hypoinsulinemic rats. *J Neurochem* **101**, 151-9.

Sombers LA, Beyene M, Carelli RM and Wightman RM (2009) Synaptic overflow of dopamine in the nucleus accumbens arises from neuronal activity in the ventral tegmental area. *J Neurosci* **29**, 1735-42.

Sonders MS, Zhu SJ, Zahniser NR, Kavanaugh MP, et al. (1997) Multiple ionic conductances of the human dopamine transporter: the actions of dopamine and psychostimulants. *J Neurosci* **17**, 960-74.

Stuber GD, Roitman MF, Phillips PEM, Carelli RM, et al. (2005) Rapid dopamine signaling in the nucleus accumbens during contingent and noncontingent cocaine administration. *Neuropsychopharmacology* **30**, 853-863.

Sulzer D, Chen TK, Lau YY, Kristensen H, et al. (1995) Amphetamine Redistributes Dopamine from Synaptic Vesicles to the Cytosol and Promotes Reverse Transport. *Journal of Neuroscience* **15**, 4102-4108.

Sulzer D, Maidment NT and Rayport S (1993) Amphetamine and other weak bases act to promote reverse transport of dopamine in ventral midbrain neurons. *J Neurochem* **60**, 527-35.

Swanson JM, Flodman P, Kennedy J, Spence MA, et al. (2000) Dopamine genes and ADHD. *Neuroscience and Behavior Reviews* **24**, 21-25.

Szarowski DH, Andersen MD, Retterer S, Spence AJ, et al. (2003) Brain responses to micro-machined silicon devices. *Brain Res* **983**, 23-35.

Thompson HJ, Lifshitz J, Marklund N, Grady MS, et al. (2005) Lateral fluid percussion brain injury: a 15-year review and evaluation. *J Neurotrauma* **22**, 42-75.

Torres GE, Gainetdinov RR and Caron MG (2003) Plasma membrane monoamine transporters: structure, regulation and function. *Nat Rev Neurosci* **4**, 13-25.

Tripp G and Wickens JR (2008) Research review: dopamine transfer deficit: a neurobiological theory of altered reinforcement mechanisms in ADHD. *J Child Psychol Psychiatry* **49**, 691-704.

Usiello A, Baik J-H, Rougé-Pont F, Picetti R, et al. (2000) Distinct functions of the two isoforms of dopamine D2 receptors. *Nature* **408**, 199-203.

Venton BJ, Troyer KP and Wightman RM (2002) Response times of carbon fiber microelectrodes to dynamic changes in catecholamine concentration. *Anal Chem* **74**, 539-46.

Venton BJ, Zhang H, Garris PA, Phillips PE, et al. (2003) Real-time decoding of dopamine concentration changes in the caudate-putamen during tonic and phasic firing. *J Neurochem* **87**, 1284-1295.

Volkow ND, Wang G-J, Fowler JS, Logan J, et al. (2001) Therapeutic Doses of Oral Methylphenidate Significantly Increase Extracellular Dopamine in the Human Brain. *Journal of Neuroscience* **21**, RC121.

Wang Y, Moquin KF and Michael AC (2010) Evidence for coupling between steady-state and dynamic extracellular dopamine concentrations in the rat striatum. *J Neurochem* **114**, 150-159.

Westerink BH, Tuntler J, Damsma G, Rollema H, et al. (1987) The use of tetrodotoxin for the characterization of drug-enhanced dopamine release in conscious rats studied by brain dialysis. *Naunyn Schmiedebergs Arch Pharmacol* **336**, 502-7.

Wightman RM, Amatore C, Engstrom RC, Hale PD, et al. (1988) Real-time characterization of dopamine overflow and uptake in the rat striatum. *Neuroscience* **25**, 513-523.

Wightman RM, Heien ML, Wassum KM, Sombers LA, et al. (2007) Dopamine release is heterogeneous within microenvironments of the rat nucleus accumbens. *Eur J Neurosci* **26**, 2046-54.

Wightman RM and Robinson DL (2002) Transient changes in mesolimbic dopamine and their association with 'reward'. *J Neurochem* **82**, 721-735.

Wightman RM, Strope E, Plotsky P and Adams RN (1978) In vivo voltammetry: monitoring of dopamine metabolites in CSF following release by electrical stimulation. *Brain Res* **159**, 55-68.

Wipf DO, Wehmeyer KR and Wightman RM (1986) Disproportionation of Quinone Radical Anions in Protic Solvents at High PH. *J Org Chem* **51**, 4760-4764.

Wu Q, Reith ME, Walker QD, Kuhn CM, et al. (2002) Concurrent autoreceptor-mediated control of dopamine release and uptake during neurotransmission: an in vivo voltammetric study. *J Neurosci* **22**, 6272-81.

Wu Q, Reith MEA, Wightman RM, Kawagoe KT, et al. (2001) Determination of release and uptake parameters from electrically evoked dopamine dynamics measured by real-time voltammetry. *J Neurosci Methods* **112**, 119-133.

Yang H, Peters JL and Michael AC (1998) Coupled effects of mass transfer and uptake kinetics on in vivo microdialysis of dopamine. *J Neurochem* **71**, 684-92.

Young SD and Michael AC (1993) Voltammetry of extracellular dopamine in rat striatum during ICSS-like electrical stimulation of the medial forebrain bundle. *Brain Res* **600**, 305-7.

Zachek MK, Takmakov P, Park J, Wightman RM, et al. (2010) Simultaneous monitoring of dopamine concentration at spatially different brain locations in vivo. *Biosens Bioelectron* **25**, 1179-85.

Zigmond MJ, Hastings TG and Abercrombie ED (1992) Neurochemical responses to 6-hydroxydopamine and L-dopa therapy: implications for Parkinson's disease. *Ann N.Y. Acad Sci* **648**, 71-86.